PROTON MAGNETIC RELAXATION IN AQUEOUS COLLOIDAL SILICA

By

RICHARD RAYMOND SLATER, JR.

Bachelor of Science

Rose Polytechnic Institute

Terre Haute, Indiana

1960

Submitted to the Faculty of the Graduate College
of the Oklahoma State University
in partial fulfillment of the requirements
for the Degree of
DOCTOR OF PHILOSOPHY
May, 1972

PROTON MAGNETIC RELAXATION IN

AQUEOUS COLLOIDAL SILICA

Thesis Approved:

Herbert A. Pohl
Thesis Adviser

Leonard M. Raff

Bennett Basore

Dean of the Graduate College

ACKNOWLEDGEMENTS

For inspiration, support and for helping the author through a difficult period (which must necessarily remain private) at the end of his association with Oklahoma State University, he wishes to publicly extend his deep gratitude to his wife, Barbara. He would be remiss if he did not also mention the fact that large corporations can indeed treat their new employees with exceptional kindness and consideration, and for that reason he wishes to thank the Gulf Research and Development Company for (1) extending him unlimited use of its computing facilities for his own personal use when he decided that the last chapter of this thesis was unsatisfactory, (2) for performing chemical analyses reported in this thesis, and (3) for offering to reproduce this thesis at no cost to him (the offer was declined).

The author is specifically indebted to Dr. John G. Larson, Professor H. E. Harrington, and Professor W. A. Sibley for the strong moral support offered by each. Among his former contemporaries, he is pleased to have been associated with Dr. B. F. Melton and Dr. C. E. Manley, both of whom were fellow graduate students.

He especially wishes to thank the Lew Wentz Foundation of Oklahoma State University for providing him with funds during one particularly lean year when the Federal Government suddenly reduced its support for research. The most unfortunate aspect of this acknowledgement, however, is the fact that the author cannot list the many citizens of Stillwater,

Oklahoma whose personal warmth and kindness left him with a very high regard for the community within which he resided.

TABLE OF CONTENTS

LIST OF TABLES

LIST OF FIGURES

CHAPTER I

INTRODUCTION

In this thesis we report the application of proton magnetic resonance (PMR) techniques to the study of an aqueous colloidal silica. The quantities usually measured in such a study are the longitudinal relaxation time, T_1, and the transverse relaxation time, T_2, both of which may be sensitive to a wide variety of system variables. If one were to characterize in a functional form the dependence of T_1 and T_2 upon these variables, he could write the equation in the following manner:

$$T_{1,2} = f(a_1, a_2, \ldots, a_j)$$

where the a's represent measurable system parameters which affect the value of T_1 or T_2. Typically, these variables might include the sample pH, the ionic strength I, the molar concentration of the species giving rise to the relaxation, the applied magnetic field (H), and the sample temperature (T). In addition, T_1 and T_2 may change when special chemical agents are added to the system (e.g., a chelating agent such as EDTA) or when the system undergoes a rearrangement (phase changes, gelling, etc.).

An examination of T_1 and/or T_2 as a function of one or more of the system variables then yields information concerning the system itself. The problem of choosing an appropriate variable for study is often simplified by the fact that T_1 and T_2 are known to be sensitive to only one

or two of these variables so that the others may be ignored during the initial experiments. If, for example, it is known that T_1 is very sensitive to the sample temperature but is relatively insensitive to other parameters, it is common practice to initiate a detailed study of T_1 as a function of temperature only and to extract from these data certain constants appropriate to the interaction(s) which control T_1. Unfortunately, similar information was not available for the system under study, and it was therefore not possible to eliminate any of the system variables from consideration. This, in turn, implied that the effect of each of these variables upon T_1 and T_2 had to be examined and that, by virtue of the large area to be covered, the examination itself could not be extremely detailed. For example, an examination of the effect of pH upon T_1 would ideally be undertaken by holding all of the other system variables constant while varying the pH in small steps. In our case, this particular experiment was performed by varying the pH in integer pH-units rather than fractional pH-units in order to cover as rapidly as possible the complete pH range while at the same time obtaining the general (but not detailed) variation of T_1 with pH. A similar technique was employed in the investigation of T_1 and T_2 as a function of the other system variables, and this was in keeping with the objective of finding a theory which explained the gross behavior of T_1 and T_2 as a function of all the known variables. It is to be expected, therefore that the theory proposed will account for the general behavior of the system but may overlook some of the details which would have been uncovered by a more extensive examination of each of the system parameters. However, the study undertaken does delineate the major contributions to T_1 and T_2 and hence indicates the proper areas for further

study of the subject system.

The apparatus used during these studies was constructed by the author and is commonly known as an earth's-field, free-precession (EFFP) device. The motivation for constructing an EFFP apparatus lay in the fact that it allowed the author to work at very low fields (the earth's field itself represented the lower working limit) where he could examine very weak interactions which are not always visible to a commercial apparatus. Since surface effects in particular constitute such a class of weak interactions, it was expected that the device would be especially suited to the study of an aqueous system in contact with a large specific surface area, e.g., an aqueous colloidal silica.

Organization of Thesis

We have chosen to organize the following material so that it is appropriate to the devices which were used during the study. For that reason, the second chapter is concerned with a mathematical description of the various situations which apply to the remaining material in the thesis, and these descriptions are provided jointly because they all arise from the same set of phenomenological equations. Unless otherwise stated, the mathematical "manipulations" are the author's.

In the third chapter, we specifically consider the problems which must be overcome when one uses an EFFP device (e.g., sensitivity, data reduction techniques, etc.) but we again restrict ourselves to an essentially mathematical set of arguments, although we do introduce a few experimental results at this point. The reason that the EFFP device is not explicitly described therein lies in the fact that one of the author's co-workers has already provided this information (54), and

further, that the material of Chapter Three is not collected elsewhere, even though some of the calculations are generally known to workers in the field. The consideration of data reduction techniques represents our own efforts, whereas the remainder of the material represents the "uncollected" work of which we have just spoken.

In Chapter Four (and the remaining material), we proceed to a discussion of the specific system under study, and we present experimental measurements of our own which support our contention that the available literature data are applicable to the samples we employed. We then present our most important experimental results and offer a preliminary interpretation of them. We conclude by arguing that it is not possible to proceed further, because the necessary chemical information is not available in the literature, and further, because it was beyond the scope of this study to obtain these data ourselves.

CHAPTER II

PRELIMINARY DISCUSSION

Since the general features of NMR techniques have been covered adequately in the literature, we give here only a brief and semi-quantitative review of the basic principles.

Spin-Lattice Relaxation

If a uniform magnetic field $\overline{B}$ is applied to a sample containing N nuclear spins per unit volume, the equilibrium value of the induced (nuclear) magnitization is given by the Curie Law (1):

$$\overline{M}_{\infty} = N \frac{I + 1}{I} \cdot \frac{|\overline{\mu}|^2}{3kT} \cdot \overline{B} \quad (\overline{\mu} \cdot \overline{B} << kT) \tag{1}$$

where $\overline{M}_{\infty}$ is the induced magnetic moment per unit volume, $\overline{\mu}$ is the magnetic dipole-moment of an individual spin, k is Boltzmann's constant, T is the temperature in degrees Kelvin, and I is the spin quantum number (I = 1/2 for a proton). In order to produce the foregoing value of $\overline{M}_{\infty}$ an excess of spins must be aligned with the field, and the average value of $-(\overline{\mu} \cdot \overline{B})$ thereby decreased. Thus, energy must be removed from the spin system in order that $\overline{M}_{\infty}$ may be reached. This energy is transferred to the surrounding medium (the lattice) and the transfer requires a finite amount of time. If the field $\overline{B}$ is applied suddenly at t = 0, the "growth" of $\overline{M}$ with time can often be described in terms of the following exponential equation:

$$M(t) = M_{\infty}(1 - e^{\frac{-t}{T_1}}) \tag{2}$$

where T_1 is the so-called "spin-lattice relaxation time" (also called the longitudinal relaxation time). Obviously, the value of T_1 is a function of the degree of coupling between the spin system and the lattice system and a measurement of T_1 provides a means of examining this coupling.

Motion of $\overline{M}$ in the Presence of $\overline{B}$

The torque $\overline{\tau}$ exerted on a rotating nucleus having angular momentum $\overline{L}$ is given classically by

$$\overline{\tau} = \frac{d\overline{L}}{dt} = \frac{1}{\gamma}\frac{d\overline{\mu}}{dt} \tag{3}$$

where γ is the magnetogyric ratio of the nucleus ($\gamma/2\pi$ = 4.26 KHz/G for protons). But

$$\overline{\tau} = \overline{\mu} \times \overline{B} \tag{4}$$

so that the differential equation governing the motion of $\overline{\mu}$ becomes

$$\frac{d\overline{\mu}}{dt} = \gamma(\overline{\mu} \times \overline{B}) \quad . \tag{5}$$

The magnitization $\overline{M}$ is assumed to obey the same equation; i.e.,

$$\frac{d\overline{M}}{dt} = \gamma(\overline{M} \times \overline{B}) \quad . \tag{6}$$

However, Equation 6 implies that

$$\overline{M} \cdot \frac{d\overline{M}}{dt} = \frac{1}{2}\frac{d}{dt}(\overline{M} \cdot \overline{M}) = 0 \tag{7}$$

and $|\overline{M}|$ does not change with time.[1] Thus, spin-lattice relaxation is not included in Equation 6.

Before discussing this difficulty further, it is of interest to examine the solution to Equation 6 under the assumption that a static magnetic field $\overline{B}_z$ lies along the z-axis of a fixed Cartesian coordinate system. In this case, the solutions for the x, y, and z-components of $\overline{M}$ are given by

$$\begin{aligned} M_x(t) &= M_x(0)\ \cos\gamma B_z t \\ M_y(t) &= M_y(0)\ \sin\gamma B_z t \\ M_z(t) &= M_z(0) \end{aligned} \qquad (8)$$

Thus, the vector $\overline{M}$ precesses about the z-axis at an angular frequency given by

$$\omega_o = \gamma B_z \qquad (9)$$

where ω_o is the Larmour precession frequency.

If the field B_z is not constant with time at a particular nucleus,[2] but fluctuates by an amount ΔB_{loc} due to magnetic "noise" generated by surrounding nuclei, one expects a corresponding shift in ω at that nucleus given by

$$\Delta\omega = \gamma \Delta B_{loc} \qquad (10)$$

---

[1] We use the vector identity $\overline{A} \cdot (\overline{A} \times \overline{B}) = 0$.

[2] The assumption that the d.c. field at every nucleus is B_z is not always valid. However, we defer this complication to the discussion in the next section.

If the variation in B_{loc} is slow compared to the precession period,[3] the nucleus in question will lose phase coherence with the other precessing nuclei, and the magnitude of $\overline{M}$ will be decreased. This decrease can often be described in terms of the equation

$$|\overline{M}(t)| = |\overline{M}(o)| \exp\left(\frac{-t}{T_2}\right) \tag{11}$$

where T_2 is the transverse relaxation time (sometimes called the "phase memory time").

The Bloch Equations

There are two relaxation modes appropriate to $\overline{M}$ (characterized by T_1 and T_2) which are not included in Equation 6. In attempting to remedy this situation, F. Bloch (2) noted that Equation 2 is the solution to the differential equation

$$\frac{dM}{dt} = \frac{M_\infty - M}{T_1} \tag{12}$$

whereas Equation 11 is the solution of

$$\frac{dM}{dt} = \frac{-M}{T_2} \quad . \tag{13}$$

This led Bloch to write Equation 6 in component form and to add to it terms similar to those of Equations 12 and 13 in order to include relaxation effects. The so-called "phenomonological Bloch equations" are written as follows:[4]

---

[3] Actually, B_{loc} fluctuates randomly, and it is the low frequency Fourier components of this fluctuation which are the "slow" variations of importance.

[4] These equations require that any static field which is present be taken to lie along the z-axis.

$$\dot{M}_x(t) = \gamma(M_y B_z - M_z B_y) - \frac{M_x}{T_2}$$

$$\dot{M}_y(t) = \gamma(M_z B_x - M_x B_z) - \frac{M_y}{T_2} \qquad (14)$$

$$\dot{M}_z(t) = \gamma(M_x B_y - M_y B_x) + \frac{(M_\infty - M_z)}{T_1} \quad .$$

Although simple in concept, these equations have successfully described many experimental situations, and they have therefore become quite important in the interpretation of experimental data.

In the interest of continuity, we proceed immediately to a discussion of the solutions obtainable from Equation 14 under various sets of initial conditions. These initial conditions will be chosen in such a manner that they will apply to several experimental situations of interest to the author. The solutions so obtained will be used in the material of later chapters, and therefore the reader may defer examination of these solutions until the specific experimental situation has been discussed.

Solution Applicable to EFFP Apparatus

Consider the following initial conditions at t = 0:

$$B_z = B_y = 0; \qquad B_x = B_p; \qquad M_z = M_y = 0; \qquad M_x = M_o \quad . \qquad (15)$$

With these initial conditions, Equation 14 yields the solutions

$$M_x(t) = [M_\infty - M_o][1 - \exp(\frac{-t}{T_1})] + M_o \qquad (16a)$$

$$M_z(t) = M_y(t) = 0 \quad . \qquad (16b)$$

Assume that at time t', we have the following initial conditions:

$$B_z = B_o; \qquad B_x = B_y = 0; \tag{17}$$

$$M_x = M_x(t'); \qquad M_y = M_z = 0 \quad . \tag{18}$$

A reapplication of Equation 14, with the preceeding taken as initial conditions, yields the solution (for $t \geq t'$)

$$\begin{aligned} M_x(t) &= M_x(t') \cos[\gamma B_o(t - t')] \exp\left[\frac{-(t - t')}{T_2}\right] \\ M_y(t) &= -M_x(t') \sin[\gamma B_o(t - t')] \exp\left[\frac{-(t - t')}{T_2}\right] \end{aligned} \tag{19}$$

i.e., the magnitization vector precesses about the field B_o with angular frequency

$$\omega_o = \gamma B_o \tag{20}$$

and decays toward zero with time-constant T_2. Figure 1 summarizes graphically the variation of M_x with time under the assumption that, at $t \leq t'$, its behavior follows an expression similar to Equation 16a. This is the result observed during one cycle of the EFFP apparatus.

Solution Applicable to CW (Continuous-Wave) Experiments

We consider the application of a large, static field $\overline{B}_o$ along the z-axis of a Cartesian coordinate system and the simultaneous application of a field $\overline{B}_1$ which rotates in the x-y plane at angular frequency ω. The direction of rotation is such that the field $\overline{B}_1$ rotates about $\overline{B}_o$ in the same direction that one would expect the vector $\overline{M}$ to process in the absence of field $\overline{B}$ (see Equation 8). The boundary conditions therefore become

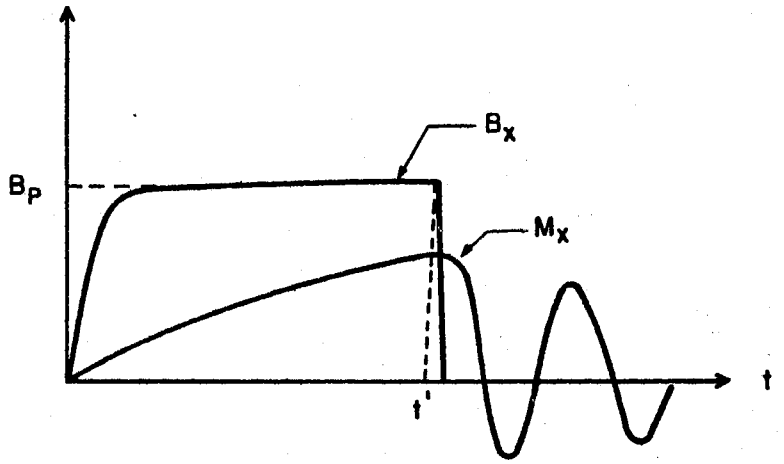

Figure 1. Variation of B_x and M_x With Time

$$B_x = B_1 \cos \omega t;$$

$$B_y = -B_1 \sin \omega t; \qquad (21)$$

$$B_z = B_o \quad .$$

Note that the field $\overline{B}_1$ rotates an angular frequency which is not necessarily the same as the Larmour precession frequency given by Equation 9. The steady-state solutions to Equation 14 are of interest in this case, and these solutions are most easily obtained by transforming the Bloch equations into a rotating set of coordinates, x', y', and z'.

B_o is taken to be parallel to the z'-axis in the rotating frame, while the x' and y' axes rotate at angular frequency ω in such a manner that the field $\overline{B}_1$ appears to lie along the x'-axis at all times. Under these conditions, the Bloch equations corresponding to Equation 14 become

$$\begin{aligned} \dot{M}_{x'} &= (\gamma B_o - \omega) M_{y'} - \frac{M_{x'}}{T_2} \\ \dot{M}_{y'} &= (\gamma B_o - \omega) M_{x'} + \gamma B_1 M_{z'} - \frac{M_{y'}}{T_2} \qquad (22) \\ \dot{M}_{z'} &= -\gamma B_1 M_{y'} + \frac{(M_o - M_{z'})}{T_1} \quad . \end{aligned}$$

The appropriate steady-state solutions are easily found in this frame by setting the time derivatives of Equation 22 equal to zero and solving for the individual components of $\overline{M}$. In this case, the solution for $M_{x'}$ will represent the component of $\overline{M}$ in phase with the rotating field B_1; $M_{y'}$ will represent the "out-of-phase" component, and $M_{z'}$ will, as in the previous case, be the component parallel to the static field $\overline{B}_o$. One obtains the following solutions for the steady-state condition:

$$M_{x'} = \frac{\gamma M_o B_1 T_2^2 (\omega_o - \omega)}{1 + T_2^2 (\omega_o - \omega)^2 + \gamma^2 B_1^2 T_1 T_2}$$

$$M_{y'} = \frac{\gamma M_o B_1 T_2}{1 + T_2^2 (\omega_o - \omega)^2 + \gamma^2 B_1^2 T_1 T_2} \qquad (23)$$

$$M_{z'} = \frac{1 + T_2^2 (\omega_o - \omega)^2}{1 + T_2^2 (\omega_o - \omega)^2 + \gamma^2 B_1^2 T_1 T_2} \cdot M_o \quad .$$

Figure 2 illustrates the variation of $M_{x'}$ and $M_{y'}$ with angular frequency ω. Note that the component $M_{x'}$ goes through zero at $\omega = \omega_o$. The components $M_{x'}$ and $M_{y'}$ are termed the dispersion and absorption components, respectively.

Under the condition $\gamma B_1^2 T_1 T_2 << 1$,[5] the half-width at half-maximum of the absorption component $M_{y'}$ is related to T_2 through the equation:

$$\Delta\omega_{\frac{1}{2}} = \frac{1}{T_2} \quad . \qquad (24)$$

The resonance behavior exhibited under these conditions has led to the term "nuclear magnetic-resonance" (NMR).

The Modified Bloch Equations

Implicit in the foregoing discussion is the assumption that each magnetic moment $\bar{\mu}$ experiences the same interaction with its surroundings. This was the reason that the magnitization vector $\bar{M}$ was assumed to obey an equation identical to Equation 5, prior to the introduction of relaxation terms. When multiple magnetic environments are present,

---

[5] If this condition is not satisfied, saturation is beginning to set in, and the absorption and dispersion components are less intense. In this situation, the dispersion component is preferred because it disappears last.

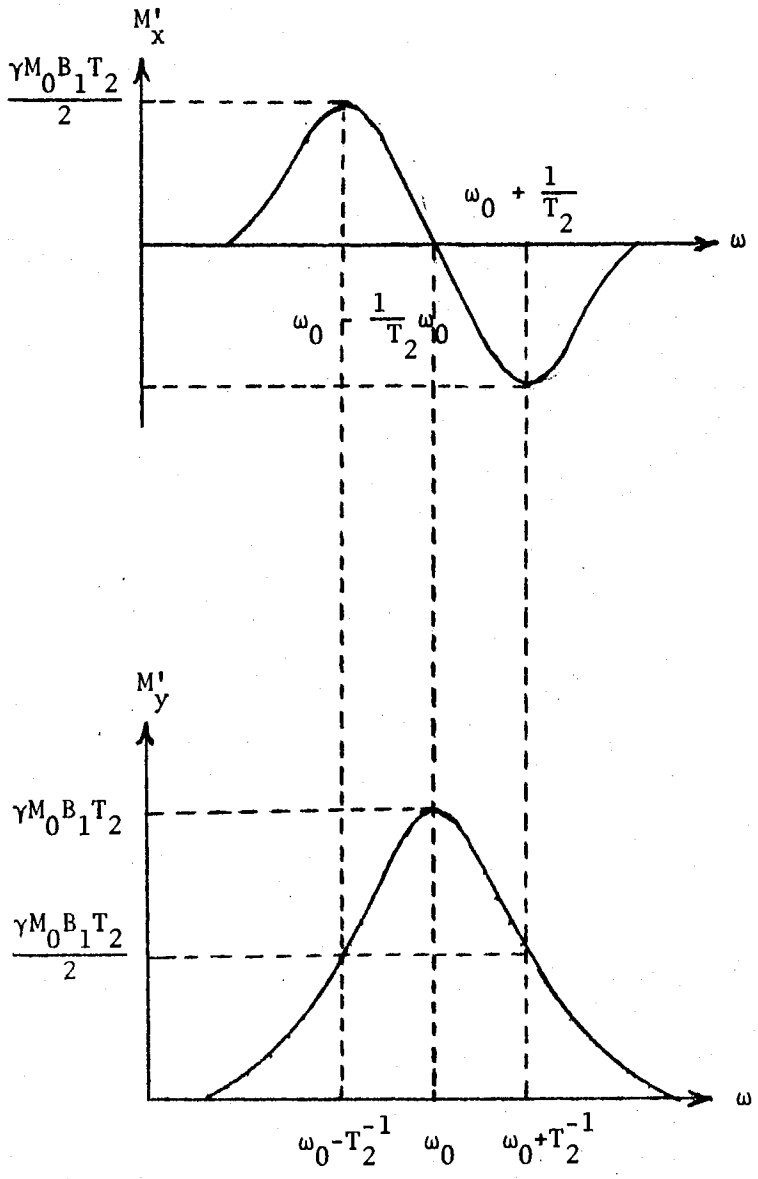

Figure 2. Variation of Equation 23 With Respect to ω

it is therefore not to be expected that Equation 14 will correctly describe the motion of $\overline{M}$.

It may be suspected that one could focus his attention on the magnetization vector $\overline{M}_i$, due to spins in a particular environment, "i", and apply Equation 14 to environment "i" to determine the time-dependence of $\overline{M}_i$. The total magnetization, $\overline{M}$, would then be the vector sum of the individual contributions; i.e.,

$$\overline{M} = \sum_i \overline{M}_i \tag{25}$$

However, the Bloch equations neglect the fact that magnetic moments may migrate among the various environments, so that $\overline{M}_i$ may change due to effects other than spin-lattice relaxation or dephasing. McConnell (3) recognized that the effect of migration could be included in Equation 14 by adding simple terms similar to the relaxation terms added by Bloch, and when these terms (which involve the mean lifetime in each environment) have been added to the Bloch equations, one may then use Equation 25 to compute $\overline{M}$.

With two exchanging environments, "a" and "b", McConnell has proposed that the following equations be used to describe the components of $\overline{M}$:

1. General relations -

$$\begin{aligned} M_x &= M_{xa} + M_{xb} \\ M_y &= M_{ya} + M_{yb} \\ M_z &= M_{za} + M_{zb} \quad ; \end{aligned} \tag{26}$$

2. Equations governing environment "a" -

$$\dot{M}_{xa} = \gamma(M_{ya}B_{za} - M_{za}B_{ya}) - \left(\frac{M_{xa}}{T_{2a}}\right) - \left(\frac{M_{xa}}{\tau_a}\right) + \left(\frac{M_{xb}}{\tau_b}\right)$$

$$\dot{M}_{ya} = \gamma(M_{za}B_{xa} - M_{xa}B_{za}) - \left(\frac{M_{za}}{T_{2a}}\right) - \left(\frac{M_{za}}{\tau_a}\right) + \left(\frac{M_{yb}}{\tau_b}\right) \qquad (27)$$

$$\dot{M}_{za} = \gamma(M_{xa}B_{ya} - M_{ya}B_{xa}) + \left(\frac{M - M_{za}}{T_{1a}}\right) - \left(\frac{M_{za}}{\tau_a}\right) + \left(\frac{M_{zb}}{\tau_b}\right);$$

3. Equations governing environment "b" -

(These are similar to Equation 27 and may be obtained from them by interchanging the indices a and b).

In the preceeding equations, τ_a and τ_b are the lifetimes in environments a and b, and all other symbols have their usual meaning.

The above equations are not actually those given by McConnell in his original article, although they may easily be reduced to his equations. McConnell's equations include some boundary conditions appropriate to CW experiments and are written in a rotating frame of reference (3). We prefer to use the laboratory frame of reference in order to facilitate easy comparison to Equation 14 (the Bloch equations), and we also wish to omit boundary conditions in order to preserve generality.

Even this simple system involves the solution of six coupled differential equations, and it may be seen that consideration of three or more environments involves a procedure which rapidly becomes so complicated that its usefulness may be doubtful. Nevertheless, these equations have been extended to three or more exchanging environments although, as may be expected, this usually involves the use of simplifying assumptions and a subsequent loss of generality. We do not consider more than two exchanging environments in this thesis, and the reader is

referred to the literature for the discussion of other cases (4).

Solutions Applicable to EFFP Apparatus

We introduce the following initial conditions:

$$B_{ya} = B_{xa} = B_{yb} = B_{xb} = 0; \qquad B_{za} = B_{zb} = B_1 \quad . \tag{28}$$

Note that we have assumed that nuclei in environments a and b see the same static field. This is not necessarily the case when one takes shielding effects into account, but at the low fields employed with the EFFP apparatus this is probably a valid assumption in the majority of cases. Under the preceeding conditions, the equations governing the growth of the z-component of the magnetization become

$$\dot{M}_{za} = \frac{(M_\infty^{(a)} - M_{za})}{T_{1a}} - \frac{M_{za}}{\tau_a} + \frac{M_{zb}}{\tau_b} \tag{29}$$

$$\dot{M}_{zb} = \frac{(M_\infty^{(b)} - M_{zb})}{T_{1b}} - \frac{M_{zb}}{\tau_b} + \frac{M_{za}}{\tau_a} \tag{30}$$

A slight simplification of the Bloch-McConnell equations may be achieved by introducing the following definitions:

$$\begin{aligned} \tau_{1a}^{-1} &\equiv T_{1a}^{-1} + \tau_a^{-1} \quad , \\ \tau_{1b}^{-1} &\equiv T_{1b}^{-1} + \tau_b^{-1} \quad . \end{aligned} \tag{31}$$

We can therefore trace the growth of the z-component of magnetization with Equations 29 and 30. Applying the LaPlace operator to them and inserting 28 and 31 into the resulting expressions, one obtains

$$M_{za}(S)(S + \tau_{1a}^{-1}) + M_{zb}(S)(-\tau_b^{-1}) = \frac{M_\infty^{(a)}}{ST_{1a}} \tag{32}$$

$$M_{za}(S)(-\tau_a^{-1}) + M_{zb}(S)(S + \tau_{1b}^{-1}) = \frac{M_\infty^{(b)}}{ST_{1b}} \quad . \tag{33}$$

At this point, we note that an interchange of indices a and b will convert Equation 32 to Equation 33 so that one may find $M_{za}(t)$ and then interchange indices in that solution to obtain the solution for $M_{zb}(t)$. After applying standard LaPlace methods to Equations 32 and 33, it becomes apparent that it is necessary to define two constants γ_1 and γ_2, such that

$$\gamma_{1,2} = -\frac{1}{2}(\tau_{1a}^{-1} + \tau_{1b}^{-1}) \pm \frac{1}{2}\sqrt{(\tau_{1a}^{-1} - \tau_{1b}^{-1})^2 + \frac{4}{\tau_a\tau_b}} \quad . \tag{34}$$

The solution to 32 and 33 may then be written in the following way:

$$M_{za}(t) = M_\infty^{(a)}(e^{\gamma_1 t} - e^{\gamma_2 t})(\gamma_1 - \gamma_2)^{-1}T_{1a}^{-1} + M_\infty^{(a)}(\gamma_1 - \gamma_2 + \gamma_2 e^{\gamma_1 t}) \cdot$$

$$[\tau_{1b}\, T_{1a} \cdot \gamma_1\gamma_2(\gamma_1 - \gamma_2)]^{-1} + M_\infty^{(b)}(\gamma_1 - \gamma_2 + \gamma_2 e^{\gamma_1 t} - {}_1e^{\gamma_2 t}) \cdot$$

$$[T_{1b}\tau_b\gamma_1\gamma_2(\gamma_1 - \gamma_2)]^{-1} \quad . \tag{35}$$

If the indices a and b are interchanged, one obtains the solution for $M_{zb}(t)$.

The last equation given is valid only under the condition $\gamma_1 \neq \gamma_2$. However, it is generally not to be expected that $\gamma_1 = \gamma_2$, for if this were true, one would have (from 34)

$$(\tau_{1a}^{-1} - \tau_{1b}^{-1})^2 = \frac{-4}{\tau_a\tau_b} \quad . \tag{36}$$

Since all of the above are real, positive quantities, Equation 36 cannot hold, and $\gamma_1 \neq \gamma_2$.

As may be seen by inspection of Equation 35 (and also by consideration of the counterpart to Equation 35 which is obtained by interchanging indices a and b), the resulting expressions for $M_{za}(t)$ and $M_{zb}(t)$ are quite complicated, and it is extremely doubtful that they would be useful in their present form. It is therefore necessary to introduce some sort of simplifying assumption at this point in order to obtain a more useful set of solutions.

The experimental situation of interest in this thesis is that which is obtained when the lifetimes τ_a and τ_b are much shorter than T_{1a} and T_{1b} respectively, and we consider this limiting condition next.

It is not sufficient to equate τ_{1a} and τ_{1b} to τ_a and τ_b, since the resulting expressions for γ_1 and γ_2 become

$$\gamma_1 = 0; \qquad \gamma_2 = -(\tau_a^{-1} + \tau_b^{-1}) \tag{37}$$

and spin-lattice relaxation is completely neglected. Equation 34 may be written so that the radicand approaches unity as these limits are taken. We therefore express $\gamma_{1,2}$ in the following manner:

$$\gamma_{1,2} = -\frac{1}{2}(\tau_{1a}^{-1} + \tau_{1b}^{-1}) \pm \frac{1}{2}(\tau_{1a}^{-1} + \tau_{1b}^{-1}) \sqrt{1 - \frac{\frac{4}{\tau_{1a}\tau_{1b}} - \frac{4}{\tau_a\tau_b}}{(\frac{1}{\tau_{1a}} + \frac{1}{\tau_{1b}})^2}} \; . \tag{38}$$

The following definitions introduce dimensionless parameters which are useful in a Taylor's expansion of (38)

$$\alpha \equiv \frac{\tau_a}{T_{1a}}; \qquad \beta \equiv \frac{\tau_b}{T_{1b}} \; . \tag{39}$$

As a consequence of Equation 39, Equation 31 becomes

$$\tau_{1a}^{-1} = \tau_a^{-1}\,(\alpha + 1); \qquad \tau_{1b}^{-1} = \tau_b^{-1}\,(\beta + 1) \tag{40}$$

with the product $(\tau_{1a}\tau_{1b})^{-1}$ being given to a good approximation by the expression

$$(\tau_{1a}\tau_{1b})^{-1} = (\tau_a\tau_b)^{-1}\,(\alpha + \beta + 1) \tag{41}$$

where second-order terms in α and β have been neglected. Examining for the moment only the radicand of Equation 38, and substituting Equations 40 and 41, it follows that

$$1 - 4[(\tau_{1a}\tau_{1b})^{-1} - (\tau_a\tau_b)^{-1}][\tau_{1a}^{-1} + \tau_{1b}^{-1}]^{-2} \approx$$

$$1 - \frac{4(\alpha + \beta)}{(\alpha + \beta + 1)\left(\frac{2 + \tau_{1b}}{\tau_{1a}} + \frac{\tau_{1a}}{\tau_{1b}}\right)} \qquad . \tag{42}$$

We next introduce the occupation probabilities P_a and P_b associated with each environment, and take

$$\frac{P_a}{P_b} = \frac{\tau_a}{\tau_b}\,; \qquad P_a + P_b = 1 \qquad . \tag{43}$$

The radicand becomes

$$1 - 4(\alpha + \beta)P_aP_b \qquad . \tag{44}$$

Equation 44 allows expansion of the radical in Equation 38 in a Taylor's series in α and β. Retention of only the linear terms leads to the following expression for γ_1:

$$\gamma_1 = -\frac{1}{2}\,(\tau_{1a}^{-1} + \tau_{1b}^{-1}) + \frac{1}{2}\,(\tau_{1a}^{-1} + \tau_{1b}^{-1})[1 - 2(\alpha + \beta)P_aP_b] \qquad . \tag{45}$$

Before considering this expression further, we note that the following identities are useful:

$$\frac{\alpha + \beta}{\tau_{1a}} \equiv \frac{(\alpha + 1)}{T_{1a}} + \frac{P_b(\alpha + 1)}{T_{1b} P_a}; \qquad \frac{\alpha + \beta}{T_{1b}} \equiv \frac{(\beta + 1)P_a}{T_{1a} P_b} + \frac{(\beta + 1)}{T_{1b}} \quad . (46)$$

One may rewrite Equation 45 (by the use of Equation 46) so that it is possible to allow both α and β to go completely to zero, thereby yielding the limit under the condition of "rapid exchange"; i.e.,

$$\gamma_1 = - \left(\frac{P_a}{T_{1a}} + \frac{P_b}{T_{1b}}\right) \quad . \qquad (47)$$

By a similar process, one can obtain

$$\gamma_2 = -\gamma_1 - (\tau_a^{-1} + \tau_b^{-1}) \quad . \qquad (48)$$

It may be observed that γ_2 is an extremely large negative exponent and that the terms of Equation 35 which contain γ_2 rapidly disappear with increasing time. Thus γ_1 controls the observed "growth" of $\overline{M}$, and that growth is exponential with time-constant $T_{1(obs)}$ given by

$$\frac{1}{T_{1(obs)}} = \frac{P_a}{T_{1a}} + \frac{P_b}{T_{1b}} \qquad (49)$$

in good agreement with results obtained by Zimmerman and Brittin (5) who did not use the Bloch-McConnell equations in deriving this result. The growth of the total z-component of the magnetization (i.e., the component given by Equation 26) may therefore be expressed in the following manner (6):

$$M_z(t) = M_{eq}\left[1 - e^{\frac{-t}{T_{1(obs)}}}\right] \qquad (50)$$

where M_{eq} is the equilibrium value of the magnetization, and $T_{1(obs)}$ is given by Equation 49.

Transverse component. In examining the motion of the transverse component of $\overline{M}$, we are interested in the equations governing $M_x(t)$ and $M_y(t)$. We choose to consider the following initial conditions:

$$B_{xa} = B_{xb} = B_{yb} = B_{ya} = 0; \qquad B_{za} = B_{1a}; \qquad B_{zb} = B_{1b}$$
$$M_{xa} = M_{oa}; \qquad M_{xb} = M_{ob}; \qquad M_{ya} = M_{za} = M_{yb} = M_{zb} = 0 \quad . \tag{51}$$

It is also useful to introduce the following definitions:

$$\omega_{oa} = \gamma B_{1a}; \qquad \omega_{ob} = \gamma B_{1b};$$
$$\tau_{2a}^{-1} = T_{2a}^{-1} + \tau_a^{-1}; \qquad \tau_{2b}^{-1} = T_{2b}^{-1} + \tau_b^{-1};$$
$$G_a(t) = M_{xa}(t) + i\, M_{ya}(t); \qquad \eta = -(i\, \omega_{oa} + \tau_{2a}^{-1}) \tag{52}$$
$$G_b(t) = M_{xb}(t) + i\, M_{yb}(t); \qquad \rho = -(i\, \omega_{oa} + \tau_{2b}^{-1}) \quad .$$

Use of the preceeding initial conditions and definitions, reduces the Bloch-McConnell equations which must be solved to the following pair:

$$\dot{G}_a(t) = \eta G_a(t) + \tau_b^{-1} G_b(t) \tag{53}$$

$$\dot{G}_b(t) = \rho G_b(t) + \tau_a^{-1} G_a(t) \quad . \tag{54}$$

The solutions to Equations 53 and 54 may be obtained by LaPlace methods. The general solutions are given by

$$G_a(t) = \frac{A}{\gamma_1-\gamma_2}(\gamma_1 e^{\gamma_1 t} - \gamma_2 e^{\gamma_2 t}) - \frac{A\rho}{\gamma_1-\gamma_2}(e^{\gamma_1 t} - e^{\gamma_2 t}) + \frac{B}{\tau_b(\gamma_1-\gamma_2)}(e^{\gamma_1 t} - e^{\gamma_2 t}) \tag{55}$$

$$G_b(t) = \frac{B}{\gamma_1-\gamma_2}(\gamma_1 e^{\gamma_1 t} - \gamma_2 e^{\gamma_2 t}) - \frac{B\eta}{\gamma_1-\gamma_2}(e^{\gamma_1 t} - e^{\gamma_2 t}) + \frac{A}{\tau_a(\gamma_1-\gamma_2)}(e^{\gamma_1 t} - e^{\gamma_2 t}) \tag{56}$$

where these solutions are valid under the condition $\gamma_1 \neq \gamma_2$, and where $A = G_a(0)$, $B = G_b(0)$ and

$$\gamma_{1,2} = \frac{(\eta + \rho)}{2} \pm \frac{1}{2}\left[\eta - \rho)^2 + \frac{4}{\tau_a \tau_b}\right]^{\frac{1}{2}} \quad . \tag{57}$$

The general solutions for $\gamma_1 = \gamma_2 = \gamma$ are given by

$$G_a(t) = te^{\gamma t}\left(A\gamma + A\rho + \frac{B}{\tau_b}\right) + Ae^{\gamma t} \tag{58}$$

$$G_b(t) = te^{\gamma t}\left(B\gamma + B\eta + \frac{A}{\tau_a}\right) + Be^{\gamma t} \quad . \tag{59}$$

We state without proof that a procedure similar to that used in finding the solution for the longitudinal component of $\overline{M}$ (under the condition of rapid exchange) shows that the magnetization vector in the x-y plane precesses at an angular frequency $\omega_{o(obs)}$ given by

$$\omega_{o(obs)} = P_a\omega_{oa} + P_b\omega_{ob} \tag{60}$$

and that the appropriate decay time-constant $T_{2(obs)}$ is given by

$$T_{2(obs)}^{-1} = P_a T_{2a}^{-1} + P_b T_{2b}^{-1} \quad . \tag{61}$$

Furthermore, the decay is exponential.

Solutions Applicable to High Field Experiments

Since the majority of NMR experiments are performed at high fields, and because there is a great interest in phenomena involving chemical exchange, a rather large number of solutions have been published in the literature which have been derived from the Bloch-McConnell equations. These solutions depend upon the assumed boundary conditions, which are taken so as to approximate the existing experimental situation.

For the purposes of this thesis, we shall concern ourselves with

only one of these published solutions -- that due to Swift and Connick (7). We report the results of that derivation in the following material.

The Location of the Absorption Maximum. Swift and Connick have considered the situation in which only one absorption maximum is observed, even though several magnetic environments may be present. Arbitrarily denoting the environment giving rise to the absorption maximum as "a", it was noted that the Bloch-McConnell equations implied that the frequency corresponding to the absorption maximum, ω_a, is shifted from the value associated with pure a by an amount $\Delta\omega_a$ given by

$$\Delta\omega_a = -\sum_j \frac{\Delta\omega_j}{\tau_{aj}\,\tau_{ja}\left[\left(\frac{1}{T_{2j}}+\frac{1}{\tau_{ja}}\right)^2+(\Delta\omega_j)^2\right]} \tag{62}$$

where τ_{aj} is the lifetime of a spin which migrates from a to j, and τ_{ja} is the lifetime for the reverse process. The quantities $\Delta\omega_j$ are also defined as the difference in the (hypothetical) absorption frequency due to environment j and that due to pure a.

The Absorption Line Width. Under the conditions previously stated, the half-width at half-maximum ($1/T_2$) is given by (8)

$$T_2^{-1} = T_{2a}^{-1} + \sum_j \tau_{aj}^{-1}\,\frac{\frac{1}{T_{2j}^2}+\left(\frac{1}{T_{2j}\tau_{ja}}\right)+(\Delta\omega_j)^2}{\left(\frac{1}{T_{2j}}+\frac{1}{\tau_{ja}}\right)^2+(\Delta\omega_j)^2} \tag{63}$$

Limiting Conditions. Assume that only two environments are present -- water and one type of paramagnetic ion. Denoting the lifetime in the hydration sphere of an ion as τ_M and associating the value of T_{2a} with that of pure water, one obtains (from Equation 63)

$$T_2^{-1} = T_{2a}^{-1} = \tau_a^{-1} \frac{\frac{1}{T_{2M}^2} + \frac{1}{(T_{2M}\, m)} + (\Delta\omega_M)^2}{(\frac{1}{T_{2M}} + \frac{1}{\tau_M})^2 + (\Delta\omega_M)^2} \quad . \tag{64}$$

Under the condition of rapid exchange, $\tau_M << T_{2M}$, and

$$T_2^{-1} - T_{2a}^{-1} \doteq \tau_a^{-1} \left[\frac{\frac{\tau_M}{T_{2M}} + \tau_M^2\, \Delta\omega_M^2}{1 + \tau_M^2\, \Delta\omega_M^2} \right] .$$

Using the partial-fraction identity

$$\frac{A + X}{1 + X} \equiv A + \frac{(1 - A)X}{1 + X}$$

one may show that[6]

$$T_2^{-1} - T_{2a}^{-1} = P_M \left[\frac{\tau_M\, \Delta\omega_M^2}{1 + (\tau_M\, \Delta\omega_M)^2} + T_{2M}^{-1} \right] \tag{65}$$

where P_m is the probability of finding a spin in the hydration sphere of a paramagnetic ion. This expression yields all of the limiting cases discussed by Swift and Connick and therefore, will be used in place of their expressions.

Luz and Shulman have shown that (under these same conditions) the correct expression for $\Delta\omega_a$ is given by (9)

$$\Delta\omega_a = P_M \frac{\omega_M}{\tau_M^2 \{[(\frac{1}{T_{2M}}) + (\frac{1}{\tau_M})]^2 + \Delta\omega_M^2\}} \quad . \tag{66}$$

---

[6] In this form, the equation has similarities to that derived by Gutowsky, et al., J. Chem. Phys. 21, 279 (1953); for the case of two "resolved" lines it yields an apparent T_{2M} given by $(T'_{2M})^{-1} = T_{2M}^{-1} + \tau_M^{-1}$ in exact agreement with the result obtained by Gutowsky. Therefore it seems possible that Equation 65 may be obtainable from work preceeding that of Swift and Connick.

Equations 65 and 66 are important to the high field results which are discussed in later chapters.

T_1 Versus B_p. A typical series of experiments will include the measurement of T_1 as a function of field (B_p). The data so obtained are often describable in terms of the equation

$$T_1^{-1} = \frac{K'\tau}{1 + (\omega\tau)^2} + T_b^{-1} \tag{67}$$

where

$\omega = \gamma B_p$

T_b = high field limit of T_1

K' = adjustable constant

τ = correlation time, regarded as a second adjustable constant.

The reason that this form is chosen is that it conforms to several expressions which have been derived on a theoretical basis (see Chapter V). The constants K' and τ can be directly interpreted in terms of these theories, and it is therefore of interest to extract them from the T_1 vs B_p data.

We note that Equation 67 predicts the result that $T_1 \to T_b$ as $B_p \to \infty$. At times, it is possible to generate a large enough field B_p so that one can measure T_b directly. On the other hand we have observed cases where T_1 is still increasing at the highest field the EFFP apparatus can produce, and it would therefore be desirable to extract T_b from these data.

Therefore, a complete analysis of T_1 vs B_p data in terms of Equation 67 requires the extraction of K', τ, and T_b. One may obtain a least-squares technique which yields these three constants, and we proceed to its derivation.

Assume that in the earth's field $T_1 = T_2$ (this is usually a valid assumption), and that $\omega\tau << 1$. We therefore have

$$T_2^{-1} = K' \tau + T_b^{-1} \tag{68}$$

We re-express Equation 67 as

$$y' = \frac{K'\tau}{(1 + X^2\tau^2)} + T_b^{-1} \tag{69}$$

and we take

$$y'_o = T_2^{-1} = K' \tau + T_b^{-1} \quad . \tag{70}$$

Then

$$(y'_o - y')^{-1} = (K')^{-1} \left(\frac{1}{X^2\tau^3} + \frac{1}{\tau}\right) \quad . \tag{71}$$

This suggests a second change of variables, namely

$$y = (y'_o - y')^{-1}; \qquad K = (K')^{-1} \quad . \tag{72}$$

Equation 71 therefore becomes

$$y = K(X^{-2}\tau^{-3} + \quad ^{-1}) \quad . \tag{73}$$

Note that

$$y = \frac{T_1T_2}{(T_1-T_2)}; \qquad x = \gamma B_p \quad .$$

Given N data points (x_i, y_i), we wish to minimize the mean square deviation given by

$$\frac{1}{N}\sum_{i=1}^{N}(y - y_i)^2 = \frac{K^2}{N}\sum_i x_i^{-4}\tau^{-6} + \frac{2K^2}{N}\sum_i x_i^{-2}\tau^{-4} + K^2\tau^{-2}$$
$$- \frac{2K\tau^{-3}}{N}\sum\left(\frac{y_i}{x_i}\right) - \frac{2K\tau^{-1}}{N}\sum_i y_i + \frac{1}{N}\sum_i y_i^2 \quad . \tag{74}$$

The partial with respect to K must be zero. This condition yields the result

$$K = \frac{\tau^3\sum\left(\frac{y_i}{x_i^2}\right) + \tau^5\sum y_i}{\sum x_i^{-4} + 2\tau^2\sum x_i^{-2} + N\tau^4} \quad . \tag{75}$$

The partial with respect to τ must also be zero, and this in turn implies that τ is one of the roots of the function $f(\tau)$ given by

$$f(\tau) = \tau^5\sum y_i - KN\tau^4 + 3\tau^2\sum\left(\frac{y_i}{x_i^2}\right) - 4K\tau^2\sum x_i^{-2} - 3K\sum x_i^{-4} \quad . \tag{76}$$

Note that K may be eliminated from Equation 76 by substituting the expression given by Equation 75. Once this substitution is made, one is faced with the problem of finding the roots of an equation which contains terms in τ raised to the ninth power. Obviously, digital computer techniques are necessary if the method is to be used at all.

Before discussing the method of solving the preceeding equations, one additional comment is in order. Note that

$$y_i = \frac{T_{1(i)}T_2}{(T_{1(i)} - T_2)} \tag{77}$$

and a value of $T_{1(i)}$ which is within roughly 10% of T_2 produces a large value of y_i. Furthermore, a small error in this $T_{1(i)}$ produces a large error in y_i. This problem arises because of the coordinate selection; i.e., one would really like to minimize the sum

$$\frac{1}{N}\sum_i (T - T_{1(i)})^2 \quad . \tag{78}$$

This may be effected by including a weighting function ω_i in the original sum;

$$\frac{1}{N} \sum_i (y - y_i)^2 \omega_i \quad .$$

This is standard procedure in least squares methods, and in this case one can show that an appropriate ω_i is given by

$$\omega_i = \left[\frac{(T_{1(i)} - T_2)}{T_2}\right]^2 \quad . \tag{79}$$

Note that this function gives zero weight to those points near T_2 and therefore reduces the effect previously mentioned. When the function ω_i is included, Equations 75 and 76 become

$$K = \frac{\tau^3 \sum \left(\frac{y_i}{x_i^2}\right) \omega_i + \tau^5 \sum y_i \omega_i}{\sum x_i^{-4} \omega_i + 2\tau^2 \sum x_i^{-2} \omega_i + \tau^4 \sum \omega_i} \tag{80}$$

$$f(\tau) = \tau^5 \sum y_i \omega_i - K\tau^4 \sum \omega_i + 3\tau^3 \sum \left(\frac{y_i}{x_i^2}\right) \omega_i - 4K\tau^2 \sum x_i^{-2} \omega_i - 3K \sum x_i^{-4} \omega_i . \tag{81}$$

When $\omega_i = 1$, these equations revert to their previous form.

A digital computer program was written which requires an IBM 1620 with auxiliary disk storage for its operation (FORTRAN II-D system). In operation, it solves Equations 80 and 81 and produces a fitted curve by adjusting the value of K, τ, and T_b. Equation 81 is solved by Newton's method (an iterative procedure) and the resulting value of τ is with $\sim$ 1% of the correct root. Typical running times have been 5

minutes per set of data points.[7] The function ω_i may be altered if desired by changing one FORTRAN statement in the SUM subroutine.[8] Fits to experimental data have been obtained with $\omega_i = 1$, but the results were generally unsatisfactory. The program is summarized in Appendix A.

[7] On a faster system, such as the OS/360, the calculation is typically completed in two seconds or less.

[8] See Appendix A for full details.

CHAPTER III

INSTRUMENTATION

In the preceeding chapter, we discussed the phenomonological approach to describing the motion of the induced nuclear magnetization $\overline{M}(t)$ in the presence of a field $\overline{B}(t)$. Assuming that the correct solution of $\overline{M}(t)$ is known under a particular set of experimental conditions (determined by the imposed external field $\overline{B}(t)$), one may presumably determine both the spin-lattice relaxation time T_1 and the spin-spin relaxation time T_2 by observing the magnetiziation vector $\overline{M}(t)$ and applying the results of Chapter II to the data so obtained. We therefore consider in the present chapter the next step which must be taken in obtaining T_1 and T_2; namely, the measurement of $\overline{M}(t)$.

The EFFP Technique[1]

Fundamental Method

Consider a solonoidal coil which has been oriented in such a manner that the earth's magnetic field $\overline{B}_e$ is perpendicular to the coil axis (see Figure 3). The sample to be examined is placed inside the coil, and at $t = 0$ a large d.c. current is passed through the windings, developing a magnetic field $\overline{B}_p$ along the coil axis such that

$$|\overline{B}_p| >> |\overline{B}_e| \tag{82}$$

[1] EFFP -- earth's field, free-precession.

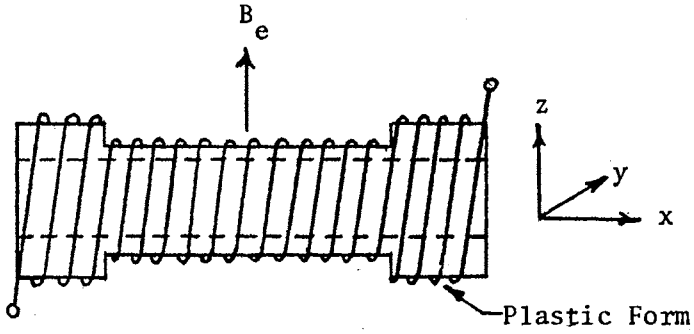

Figure 3. Sample Coil Configuration With Respect to the Earth's Field

Thus, the net field is well approximated by $\overline{B}_p$ alone. We choose a right-handed set of fixed coordinates such that the z-axis lies along $\overline{B}_e$ and the x-axis coincides with the coil axis. In this case $\overline{M}_x(t)$ is given by Equation 2 of Chapter II, i.e., assuming a true Lorentzian behavior

$$M_x(t) = |\overline{M}_\infty| \ (1 - e^{\frac{-t}{T_1}}) \tag{83}$$

where $\overline{M}_\infty$ is given by Equation 1, with $\overline{B} = \overline{B}_p$.

At $t = t'$ the field $\overline{B}_p$ is suddenly removed, (by "instantaneously" removing the d.c. current) leaving the magnetization vector $M_x(t')$ perpendicular to the field $\overline{B}_e$. We then have at $t = t'$

$$\begin{aligned} B_x &= B_y = 0; & B_z &= B_e \\ M_y &= 0; & M_x &= M_x(t') \end{aligned} \tag{84}$$

and Equation 8 of Chapter II applies. $M_x(t)$ and $M_y(t)$, therefore obey the relations

$$\begin{aligned} M_x(t) &= M_x(t') \exp\left[\frac{(t - t')}{T_2}\right] \cos \gamma B_e(t - t') \\ M_y(t) &= -M_x(t') \exp\left[\frac{(t - t')}{T_2}\right] \sin \gamma B_e(t - t') \end{aligned} \tag{85}$$

for all $t \geq t'$. The precessing vector $\overline{M}(t)$ produces a rotating dipolar field which links the coil turns. This rotating field induces a sinusoidal voltage across the coil terminals whose initial amplitude is proportional to $M_x(t')$ and whose envelope decays exponentially with time-constant T_2. Since no d.c. current is flowing through the coil at $t > t'$, one may connect it to a suitable amplifier, and by measuring the initial amplitude of the signal as a function of t', one may trace

the growth of $M_x(t)$ in the field B_p and extract the time-constant T_1. Since the envelope of the signal decays with time-constant T_2, one may extract T_2 (in the field B_e) from the free-precession signal. Note that the free-precession always takes place in the field B_e; i.e., the instrument is capable of measuring T_2 only in the field B_e, and it is not possible to measure the field-dependence of T_2.

At our location $B_e = 0.54$ G; for proton resonance this yields an f_o given by

$$f_o = \frac{\gamma B_e}{2\pi} = \left(\frac{4.26 \text{ KHz}}{\text{G}}\right)(0.54 \text{ G}) = 2.3 \text{ KHz}$$

and a conventional, low-noise audio amplifier may be used to observe the signal.

T_1 Versus Field

In principle, one can measure the field-dependence of T_1 by varying the polarizing field $\overline{B}_p$. However, in any practical experiment one has to contend with the thermal noise which is always present, and this noise becomes particularly troublesome when a small value of $\overline{B}_p$ is employed (recall that the maximum signal voltage which may be obtained under the previous conditions depends upon $\overline{B}_p$). In order to surmount the problem just outlined, we have developed an alternative technique which produces a large signal voltage, even when $\overline{B}_p$ is reduced to 1/1000 of its maximum possible value. This technique relies upon the fact that once a field $\overline{B}_p$ is established, the magnetiziation $M_x(t)$ decays toward its equilibrium value with time-constant T_1 no matter what the original value of $M_x(0)$ may have been. In the previous case, we had $M_x(0) = 0$, but this is not at all necessary.

The procedure is executed as follows: The largest field which can be generated by the coils (roughly 600 G) is applied to the sample for a time long compared to T_1 at that field. Denoting this value of M_x as M_o, one can see that if the field is suddenly reduced to an intermediate value of $\overline{B}_p$, Equation 16a of Chapter II applies, and

$$M_x(t) = (M_\infty - M_o)(1 - e^{\frac{-t}{T_1}}) + M_o \tag{86}$$

where we have taken $t = 0$ when the sudden reduction of field takes place and where M_∞ is the (new) equilibrium magnetization approached by $M_x(t)$. If at $t = t'$ the field $\overline{B}_p$ is reduced to zero, a free-precession signal is observed whose initial amplitude depends upon $M_x(t')$. Thus it is again possible to "trace out" $M_x(t)$ by varying t'. The important point here is the fact that, even where $M_\infty << M_o$, the signal observed for $t' \leq T_1$ is much larger than that which would be observed under the previous conditions, and the noise problem is minimized. The situation is shown graphically in Figure 4.

Signal-to-Noise

It is obvious that the preceeding methods will fail when the free-precession signal is masked by noise, and it is therefore necessary to attempt an analysis of this problem.

The noise at the coil terminals may be due to one or both of two sources: (1) thermal noise $e_n(t)$; and (2) induced noise $e_i(t)$ arising from stray a.c. fields which couple the sample coil (these are usually due to 60 Hz power lines in the vicinity). The total signal e(t) then becomes

$$e(t) = e_s(t) + e_n(t) + e_i(t) \tag{87}$$

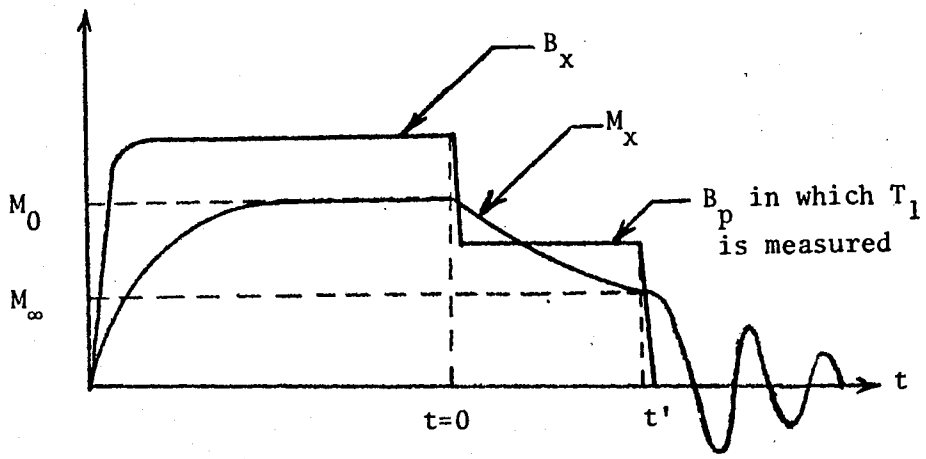

Figure 4. A Pulse Sequence Typical of That Used in a Field-Dependence Measurement. The time t is varied to trace the decay of M_x in the field $B_x=B_p$ and thereby recover T_1.

where $e_s(t)$ is the signal produced by the free-precession alone. If the fields producing $e_i(t)$ are sufficiently uniform over the space surrounding the sample coil, one may place a second coil near the sample coil whose sole purpose is to measure these fields and to subtract their effect; i.e., the second coil contains no sample and is (ideally) not magnetically coupled to the first. If the new coil is wound so as to produce a voltage $-e_i(t)$ across its terminals, then putting the two coils in series effectively eliminates $e_i(t)$ from the (summed) output. This is, in fact, the method used with the present instrument. It is worthy of note that the absence of the second coil made observation of $e_s(t)$ impossible with our apparatus.

The quantities $e_s(t)$ and $e_n(t)$ are subject to straight-forward calculation, and we consider this problem next.

Consider a sample coil of n turns and inductance L which is completely immersed in a sample of susceptability X. If a field B_p is produced by a (d.c.) current i_p and the magnetization is allowed to reach its equilibrium value, one has a magnetization $\overline{M}$ given by

$$\overline{M} = X \frac{\overline{B}_p}{\mu_o} \tag{88}$$

where

$$X = \frac{\mu_o N(I + 1)\mu^2}{3IkT} \quad . \tag{89}$$

If ϕ_p is the flux due to the field $\overline{B}_p$, then the flux due to $\overline{M}$ is given by

$$\phi_{max} = X \phi_p \quad . \tag{90}$$

After removal of the field $\overline{B}_p$, the flux coupling the coils becomes time-dependent and is given by

$$\phi = \phi_{max} \cos \gamma B_e t \quad . \tag{91}$$

The peak value of $e_s(t)$ is therefore

$$e_{pk} = -n \left(\frac{d\phi}{dt}\right)_{max} = n \gamma B_e X \phi_p \quad . \tag{92}$$

Since $Li_p = n\phi_p$

$$e_{pk} = \gamma B_e X \, Li_p \quad . \tag{93}$$

However, the sample does not completely surround the coil so that Equation 93 gives too large an estimate of e_{pk} and must be modified. We note that there are two methods whereby the energy W contained in the coil field may be computed; they are

$$W = \frac{1}{2} L i^2 \quad , \tag{94}$$

and

$$W = \frac{1}{2} \int_v \overline{B} . \overline{H} \, dv = \frac{1}{2\mu_o} \int_v B^2 \, dv \quad . \tag{95}$$

If the ratio B/i is constant over the volume of the sample (sample contained well within the uniform part of the coil field), we can calculate an "equivalent" inductance which would contain the energy of the sample alone as

$$L_{eq} = \mu_o^{-1} \int \left(\frac{B_s}{i_s}\right)^2 dv_s \tag{97}$$

where B_s is the field in the sample, i_s is the coil current giving rise to that field, and the integration is carried out over the sample. Note that, for a particular coil, B_s/i_s is a constant in the uniform part of

the field and is independent of i_s.[2] Defining this as the field-to-current ratio K, we have

$$L_{eq} = \frac{K^2 v_s}{\mu_o} \tag{98}$$

where v_s is the volume of the sample. We use L_{eq} in Equation 93 in place of L to obtain

$$e_{pk} \doteq \frac{\gamma B_o X i_p K^2 v_s}{\mu_o} \quad . \tag{99}$$

In practice, a capacitor is placed across the coil so as to bring the electrical system into parallel resonance at $\omega_o = \gamma B_o$. Therefore, for an inductor of $Q_o \geq 10$,

$$e_{pk} = \frac{Q_o \omega_o X i_p K^2 v_s}{\mu_o} \quad . \tag{100}$$

The mean-square noise voltage appearing across a parallel resonant circuit has been shown to be given by (10)

$$\overline{e_n^2} = 4kTR_p b_o \tag{101}$$

where $R_p = Q_o R_o$ (R_o = a.c. resistance of coil), and where b_o is the equivalent noise bandwidth. b_o is related to the standard 3 dB bandwidth B_o as follows (10):

$$b_o = \frac{\pi}{2} B_o \quad . \tag{102}$$

After some algebraic manipulation, one may express the rms voltage signal-to-noise ratio appearing at the terminals of the parallel-

---

[2] If, in some portions of the sample, B_s is not axial, the free-precession signal amplitude will be degraded. However, homogeneity of this field is not a critical parameter, as it is in the case of B_e.

resonant circuit as

$$\frac{e_{s(rms)}}{e_{n(rms)}} = (0.707)\ Q_o X i_p K^2 v_s (kTL)^{-\frac{1}{2}} \mu_o^{-1} \qquad (103)$$

With a 500 ml sample of pure water at 300 ^oK inserted into the apparatus, we would have $v_s = 5x10^{-4}\ M^3$; $X = 4.1x10^{-9}$; $i_p = 7$; $K = 5.9x10^{-3}$ W/M^2A; $Q_o = 25$; $L = 0.1$ Hy. We therefore obtain as a typical signal-to-noise ratio

$$\frac{e_{s(rms)}}{e_{n(rms)}} \doteq 340 \qquad . \qquad (104)$$

In practice, the induced noise $e_i(t)$ is at least one hundred times larger than $e_n(t)$ to the point where, even in the summed output

$$e_i(t) \sim e_n(t) \qquad . \qquad (105)$$

In this case, a more realistic signal-to-noise ratio is $\sim$ 200 and is in fact typical of measured values.

It is obvious from the preceeding calculations that the technique potentially yields a high signal-to-noise ratio and the precession signal should be easily detectable. Actually, the present system employs a specially wound sample coil whose Q exceeds 100 at 2.3 KHz; therefore, the theoretical signal-to-noise ratio exceeds 10^3.

The effect of amplifier noise in this situation as well as a detailed consideration of alternative input circuits has been discussed by us elsewhere (11). We, therefore, do not reproduce these results here.

Practical Considerations

Since the sample coil has a finite d.c. resistance, it is not possible to "instantaneously" apply the field $\overline{B}_p$ as had been assumed previously. After a voltage E has been applied to the coil terminals, the current (and hence the polarizing field) rises exponentially towards i_p with time-constant R/L, where R is the d.c. resistance of the coil. One may, therefore, express $B_x(t)$ as

$$B_x(t) = B_p(1 - e^{\frac{-Lt}{R}}) \tag{106}$$

and if the preceeding solutions for $M_x(t)$ are to be valid, one must have

$$\frac{R}{L} << T_1 \quad . \tag{107}$$

Since R/L is typically 10 - 15 milliseconds, this requirement is usually met in practice. Where it is not met, one may obtain a correction factor by solving the Bloch equations with Equation 106 included in the initial conditions. The result of this calculation indicates that a good first-order correction is obtained by subtracting the time constant R/L from all time measurements; i.e., if a set of data points consists of E_i vs t_i' (where E_i is the measured initial amplitude of the precession signal and t_i' is the length of time the field B_p is applied), one may replace all of the t_i' by $(t_i' - R/L)$ to obtain a first-order correction. This correction reflects the fact that a field which is applied for a time t' and which rises exponentially towards B_p with time-constant R/L may be replaced by a field B_p which rises instantaneously, but which is applied for a shorter time. This time difference is R/L.

It is also impossible to remove the field B_p instantaneously, and

one must, therefore, consider the speed with which it ought to be removed in order to leave the magnetization M_x unperturbed. If α is the angle between the resultant field $\overline{B}(t)(=\overline{B}_p(t)+\overline{B}_e)$ and the earth's field $\overline{B}_e$, consideration of the fact that M_x tends to precess about $\overline{B}(t)$ with frequency $|\gamma\overline{B}(t)|$ leads to the condition

$$\frac{d\alpha}{dt} >> |\gamma\overline{B}(t)| \tag{108}$$

That is, the resultant field $\overline{B}(t)$ must rotate into alignment with $\overline{B}_e$ at an angular frequency much greater than the rotational rate of M_x about $\overline{B}(t)$. By considering the geometry of the situation, one may express this equation in the more useful form

$$\frac{dB_p}{dt} >> \gamma B_e^2 \quad . \tag{109}$$

Inserting the values of γ and B_e, one obtains

$$\frac{dB_p}{dt} >> 6\ \frac{G}{msec} \quad . \tag{110}$$

The equipment employed is capable of removing the field B_p at a rate of $\sim$ 300 gauss per millisecond, and the preceeding condition is well satisfied (actually, rates as low as 15 Gauss per millisecond are acceptable).

In the previous chapter, mention was made of the fact that a "spread" in Larmour frequencies $\Delta\omega_o$ gave rise to an exponential decay of the free-precession signal, and that this decay was due to a loss of phase coherence. If the field in which the free-precession takes place is not uniform over the volume of the sample, a similar loss of phase coherence will occur. If one were to place in this field a sample having an infinite T_2, the observed signal would still decay towards

zero due to the inhomogeneity of the field. Where this (hypothetical) decay is exponential with time-constant T_2^*, one may include the effect of field inhomogeneity upon the observed T_2 as follows:

$$T_{2(obs)}^{-1} = T_2^{-1} + (T_2^*)^{-1} \quad . \tag{111}$$

Here, $T_{2(obs)}$ is the experimentally measured value of T_2, T_2^* is the contribution due to field inhomogeneity, and T_2 is characteristic of the sample itself. Thus, where T_2^* is known, one may obtain the sample T_2 from the relation

$$T_2 = \frac{(T_2^*)(T_{2(obs)})}{(T_2^* - T_{2(obs)})} \quad . \tag{112}$$

Note that a reliable measurement is assured when $T_2^* >> T_{2(obs)}$; i.e., the field should be as homogeneous as possible. In our case, this requirement was met by placing the sample coil well away from any structures which would distort the earth's field, and the sample coil was, therefore, located near the center of an open field. The value of T_2^* in this case was found to be 7.50 sec.[3] and represents the limiting value of $T_{2(obs)}$ which may be measured by the system. In general, where $T_{2(obs)} \leq 0.750$ sec, one may assume that $T_{2(obs)} = T_2$.

Data Reduction Techniques

The raw data obtained from the instrument are measurements of a signal voltage E at a particular time t. All of the raw data obtained

---

[3]The measurement is easily accomplished by using a sample which is known to have $T_1=T_2$ (pure water will often suffice). Then

$$T_2^* = T_{2(obs)}T_1/(T_1-T_{2(obs)}).$$

Obviously, one should also have $T_1 >> T_{2(obs)}$.

in this study may be described in terms of the equation

$$E(t) = (E_\infty - E_o)(1 - e^{\frac{-t}{T_{1(obs)}}}) + E_o \qquad (113)$$

where $T_{1(obs)}$ is the time-constant which must be extracted from the raw data. Note that this equation will fit any exponential decay, provided one selects E_o and E_∞ properly. E_∞ is proportional to M_∞, so that this voltage may be observed at $t >> T_1$. E_o may be unobservable due to time-delays in the equipment and also because of transient voltages associated with switching to the "receive" mode. However, it will be seen in the following sections that a knowledge of E_o is not required. Note also that Equation 113 may be used to describe the free-precession envelope by setting $E_\infty = 0$.

We describe two methods for extracting $T_{1(obs)}$ which shall be denoted as the "linear" and "semi-log" methods, respectively.

Linear Method

It is easily shown from Equation 113 that if one measures E(t) and follows this by a second measurement τ seconds later, E(t) is related to $E(t + \tau)$ by the equation

$$E(t + \tau) = E_\infty(1 - e^{\frac{-\tau}{T_{1(obs)}}}) + e^{\frac{-\tau}{T_{1(obs)}}}E(t) \quad . \qquad (114)$$

Therefore, if one plots (on linear paper) $E(t + \tau)$ vs E(t), he obtains a straight line of slope $\exp(-\tau/T_{1(obs)})$. This suggests that a series of measurements should be taken which are separated by a constant time interval τ, and that the resulting voltages should be plotted according to Equation 114. Then, if m is the slope of the resulting straight

line,

$$T_1 = \frac{-\tau}{\ln m} \quad . \tag{115}$$

If the straight line is fitted manually to the resulting series of points, the natural "scatter" in the data will make a range of slopes appear equally reasonable to the observer. Let this range of slopes be Δm, and assume $\Delta m << m$. In this case

$$\left| \frac{\Delta T_1}{T_1} \right| \doteq \left| \frac{1}{\ln m} \right| \cdot \left| \frac{\Delta m}{m} \right| \tag{116}$$

or

$$\left| \frac{\Delta T_1}{T_1} \right| \doteq \frac{T_1}{\tau} \left| \frac{\Delta m}{m} \right| \quad . \tag{117}$$

If one wishes to obtain a reasonable number of data points, he must choose $\tau < T_1$; therefore, the percentage error in T_1 is always larger than the percentage error in selecting the "correct" slope. In terms of the voltage measurements, one expects

$$\left| \frac{\Delta m}{m} \right| \sim \left| \frac{\Delta E}{E} \right| \quad . \tag{118}$$

This leads to the undesirable result that the error in T_1 should be larger than the error in the measured voltage, and one would hope to have available a manual procedure which yielded values of T_1 containing errors no larger than those associated with the voltage measurements. However, the method does not require a knowledge of E_o or E_∞, and this may represent an advantage in some cases.

It is also worthy of note that the x and y coordinates are interrelated, and that an error Δy_i in the y-coordinate of the ith data point causes an error $\Delta x_{i+1} = \Delta y_i$ in the x-coordinate of the $(i + 1)$st data point. This effect produces scatter in the x-direction which cannot be

minimized by a standard least-squares fit since this method operates on the y-coordinates only.

Semi-log Method

It is easily shown that Equation 113 may be recast into the form

$$\ln|E(t) - E_\infty| = \ln|E_o - E_\infty| - \frac{t}{T_1} \quad . \tag{119}$$

Thus, a plot of $|E(t) - E_\infty|$ vs t on semi-log paper will yield a straight line of slope m such that

$$T_1 = \frac{-1}{m} \quad . \tag{120}$$

It is useful to examine the effect of choosing a value of E_∞ which is not quite correct. Let the chosen value be K; then

$$\ln|K - E(t)| = \ln|E_o - E_\infty| + \ln|\beta + e^{\frac{-t}{T_1}}| \tag{121}$$

where

$$\beta = \frac{K - E_\infty}{E_o - E_\infty} \quad .$$

A Taylor's expansion yields

$$\ln|K-E(t)| \approx \ln|E_o-E_\infty| + \ln|\beta+1| + \left(\frac{1}{\beta+1}\right)\left(\frac{t}{T_1}\right) + \frac{\beta}{2(\beta+1)^2}\left(\frac{t}{T_1}\right)^2 . \tag{122}$$

If $K = E_\infty$, Equation 122 reverts to Equation 119.

One may examine the squared term in order to determine how "bad" the guess at E_∞ must be before a non-linearity in the plot becomes observable. Since measurements seldom extend beyond $t = 2T_1$, we choose this as our point of examination and require that the squared term be at least 10% as large as the linear term; i.e.,

$$\left| \frac{\beta}{2(\beta+1)^2} \left(\frac{t}{T_1}\right)^2 \right| = (0.1) \frac{t}{T_1(\beta+1)} \quad . \tag{123}$$

Inserting the value $t = 2T_1$, we find that

$$\frac{(K - E_\infty)}{E_\infty} = \pm \frac{(E_o - E_\infty)}{9E_\infty} \quad . \tag{124}$$

With our apparatus, the smallest experimental value of $E_o - E_\infty$ has $E_o = 2E_\infty$. Hence

$$\frac{(K - E_\infty)}{E_\infty} = \pm \frac{1}{9} \quad . \tag{125}$$

Therefore, K may deviate from E_∞ by approximately 10% before any deviation from linearity is noticed in the plot. Within these limits, one has

$$m = -(\beta + 1)^{-1} T_1^{-1} \tag{126}$$

and a simple calculation gives

$$\frac{\Delta T_1}{T_1} \doteq - \frac{\Delta m}{m} \doteq \frac{\Delta K}{K} \frac{E_\infty}{E_o - E_\infty} \quad . \tag{127}$$

Thus, as $E_\infty \to 0$, a poor choice of K has less and less effect upon the outcome. Note that Equation 127 works in favor of the experimenter, because at low fields, where the measurement of E_∞ is complicated by the presence of thermal noise, the influence of an error in this measurement is minimized.

It has been found that, where this method is used, the largest errors in T_1 are usually caused by a poor measurement of E_∞. As a matter of fact, the values of T_1 at the highest fields employed always show more scatter than those measured at low fields, indicating that an effect similar to that predicted by Equation 127 is responsible.

Where E_∞ is not directly measurable, due to a poor signal-to-noise ratio, one may calculate it in terms of the d.c. coil current. Let $E_\infty^{(a)}$ be a measurable value of E_∞ which corresponds to d.c. coil current $i_p^{(a)}$. If the sample remains undisturbed, and a d.c. current $i_p^{(b)}$ is passed through the coil, the (unmeasurable) value $E_\infty^{(b)}$ is given by

$$E_\infty^{(b)} = \frac{E_\infty^{(a)} i_p^{(b)}}{i_p^{(a)}} \quad . \tag{128}$$

Thus, precision metering of the coil current is required in order to obtain E_∞ at low fields. It is not necessary for the current meter to be an accurate instrument; the only requirement is that the meter indication be proportional to i_p over its entire range (precision). Meters employing a taut band suspension were used throughout because of their inherent precision, and they were calibrated periodically against a secondary standard. Table I shows a check of Equation 128 performed with a set of measurable $E_\infty^{(i)}$.

Comparison of the two Methods

Experience has led to the belief that where manual techniques are to be employed, the semi-log method is superior. An experimental comparison of the two methods (where the same raw data were analyzed in each case) is shown in Figure 5. The sample chosen was a glycerol-water mixture, known to have a field-independent T_1. The addition of glycerol to water shortens the proton T_1, and it was desired to adjust T_1 to a value near that which would be typical of a sample of colloidal silica. As may be seen in the figure, the semi-log method results in an excellent set of data points, whereas the linear method shows noticeable

TABLE I

A TEST OF EQUATION 128 WITH GLYCEROL-WATER MIXTURES[1]

Polarizing Current (Amperes)	Calculated E_∞ (Millivolts)	Measured E_∞ (Millivolts)	% Difference
7.82[2]	--	2230[2]	--
5.08	1450	1500	-3.34
2.38	680	680	0.00
1.18	337	340	-0.88
0.640	183	190	-3.68
0.381	109	105	3.81
0.180	51.4	50	2.80

[1]These figures indicate a reliability of $\pm$ 4% in the predicted E_∞. From Equation 127, we conclude that this is our expected error in T_1 at high fields.

[2]All subsequent figures based upon this value.

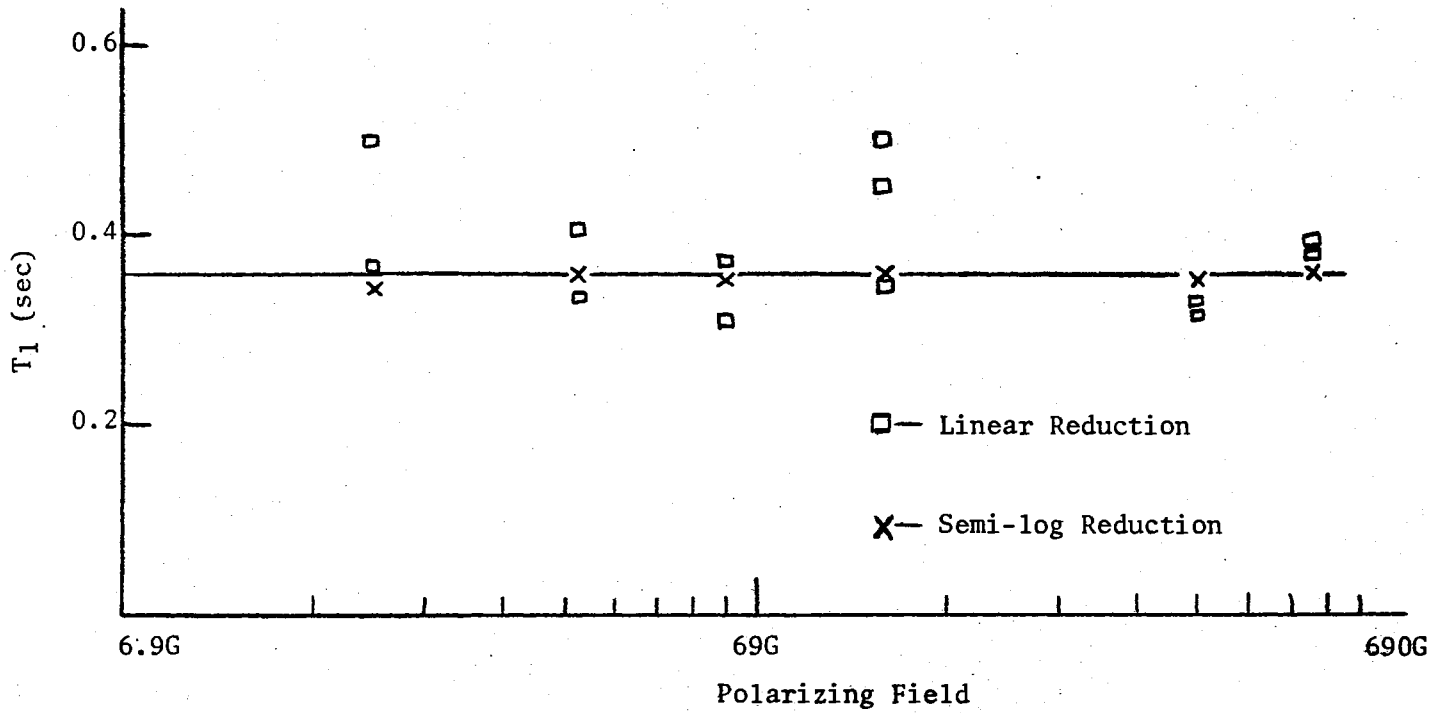

Figure 5. Comparison of a Semi-log Reduction to a Linear Reduction of T_1 Data in a Glycerol-Water Mixture. Note the superiority of the semi-log reduction.

scatter. For this reason, all data reported in this thesis have been analyzed by the semi-log method.

To speed the process (which can be quite laborious when large amounts of raw data are to be analyzed), an IBM 1620 computer was used to carry out the necessary calculations. The program was written in such a way that the computer "constructed" a semi-log plot in its memory and then used a least-squares method to obtain T_1. The input to the computer consisted of data obtained directly from the EFFP apparatus, thereby eliminating any manual calculations. The computer output was such that poor data could be detected by the operator and appropriate action taken. In some cases, the computer was capable of initiating this action automatically.

CHAPTER IV

COLLOIDAL SILICA

Some Appropriate Definitions

Colloid chemistry is defined as "the physical chemistry of two-phase systems, one of the phases being dispersed to ... colloidal dimensions within the other phase" (12). Typical colloidal dimensions lie in the range 10 - 10^3 Å, with the upper limit being set by the maximum particle size which can be tolerated by a given system; i.e., it is set by the system itself.

A colloidal silica (or silica sol) is defined as "a dispersion of silica in a liquid medium in which the particle size of the silica is within the colloidal range" (12).

Preparation of Colloidal Silica

The most common procedure employed in making a colloidal silica is to neutralize a dilute solution of sodium silicate with acid until one has reached roughly pH 9. The resulting solution contains small colloidal particles of 10 millimicron diameter or less, but, by adding acid, one has also increased the electrolyte concentration and has endangered the stability of the colloid just produced. In order to obtain concentrations exceeding 15% by weight, one must adopt an approach which avoids the electrolyte effect, and toward that end, several new procedures have been invented.

The first colloidal silicates containing SiO_2 exceeding 15% by weight were reported in a patent due to M. F. Bechtold and O. E. Snyder (U.S. Patent no. 2,574,902). Bechtold and Snyder proposed that the original solution produced (i.e., the solution containing 10 millimicron particles) be used as a so-called "heel" solution to which more of this same solution was to be added at an elevated temperature under conditions of controlled viscosity and pH. The procedure is outlined in the Bechtold and Snyder patent as follows:

> ... according to the present invention it has been found that particles in aqueous silica sols can be built up to any desired size and stable sols may thereby be produced by processes comprising forming a heel, by heating to a temperature above 60°C. an aqueous sol of silica particles of less than 10 millimicrons diameter, adding to said heel a silica sol containing particles of less than 10 millimicrons diameter, and continuing the addition and heating until at least 5 times as much silica has been added to the heel as was originally present. By such build-up processes sols may be produced which are amenable to concentration even to as high as 35% SiO_2 without gelling.

In a following patent by J. M. Rule (13), it was shown that the colloidal silica could be further stabilized by de-ionization, and that the concentration of SiO_2 could, therefore, be increased. To quote from the Rule patent:

> The aqueous sols may be concentrated to a very high silica content merely by boiling off water. Sols which are stable against gelation for extended periods of time may be readily prepared containing silica in proportions as high as 50% by weight or more.

The procedure suggested by Rule was essentially the removal of electrolytes by ion-exchange methods, followed by the addition of a small amount of NaOH to act as a stabilizing agent. Both of these patents are assigned to E. I. DuPont de Nemours and Company of Wilmington, Delaware.

Since the preparation of a stable, highly concentrated silica sol

is a difficult undertaking, the sols used in this study were of commercial manufacture produced by procedures similar to those outlined in the Rule and Bechtold-Snyder patents. These sols are marketed by DuPont under the general trade name "Ludox". There are several members of this series which are distinguished from one another by appending to the trade name a two letter designator which is intended to convey the essential character of the specific colloid. These designators are: HS (for "high sodium"); LS (low sodium); AS (ammonia stabilized); AM (alumina modified); and SM (seven millimicron - refers to particle diameter). The physical and chemical properties of these colloids are listed in Table II. Of those listed, only HS, LS, and SM will be discussed at length in this thesis.

Since Ludox HS is available in two grades (30% and 40% by weight of SiO_2), we have arbitrarily chosen to designate these two grades as 3HS and 4HS, respectively.

Before completion of this section, one more comment is in order. A water-soluble colloidal silicate powder has been developed by Wolter and has been reported in a patent assigned to E. I. DuPont Corporation. The dry powder (which is marketed under the trade name "Estersil") seldom exceeds 90% by weight of SiO_2, the remaining 10% consisting of organic additives and also of impurities.

Colloid Stability

The particles of a stable colloid carry a charge which is often established by the preferential adsorption onto the surface of ions already present in the system (peptization). Other ions of opposite charge are attracted to the surface, but because of mutual repulsion

TABLE II

PROPERTIES OF DUPONT COLLOIDAL SILICA

	4HS	LS	AS	AM	SM
% Silica as SiO_2	40.2	30.3	30	30	15
Chloride as % NaCl	0.02	0.002	0.001	0.007	0.001
% Na_2O	0.43	0.10	0.25	0.13	0.10
Viscosity at 25°C, cps.	34	9	12	10	4
pH at 25° C	9.7	8.3	9.6	9.1	8.5
Approximate Particle Diameter, Millimicrons	12	15	12	12	7
Surface Area, M^2/g	220-235	195-215	220-235	220-235	350-400
Specific Gravity at 25°C	1.303	1.209	1.206	1.209	1.093

and thermal agitation they do not form a compact charge layer; instead, they form a diffuse layer which surrounds the colloidal particles. This diffuse (or double) layer of charge has been shown by Verwey and Overbeek to be responsible for the mutual repulsion existing among the particles (14). Stability is attributed to a balance between the second-order VanDerWall-London attraction of one particle for another and the repulsion between the double layers.

When the earlier theory of Derjaguin and Landau (15) is combined with the more recent theory of Verwey and Overbeek (the combined theory is usually called "D.L.V.O. theory"), one finds that an increase in electrolyte concentration ought to lead to an eventual loss of colloid stability, followed by agglomeration of the particles. According to D.L.V.O. theory, the addition of an electrolyte decreases the "thickness"[1] of the diffuse layer, thereby allowing the particles to approach one another more closely and eventually destroying the stability of the colloid. At higher values of the surface charge, the diffuse layer is more extensive and D.L.V.O. theory predicts that a correspondingly larger amount of electrolyte will have to be added in order to destroy the stability. This prediction has been found to be correct only for univalent electrolytes and the theory apparently fails in the case of multivalent electrolytes. Levine and Bell (16) have attributed the failure to the fact that D.L.V.O. theory does not regard the ionic charge as discrete. Inclusion of the "discreteness-of-charge effect" leads to better agreement between theory and experiment.

---

[1] In this case, the thickness is taken to be the distance between the surface of the colloidal particle and the point at which the electrostatic potential has dropped to 1/e of its value at the surface. Typical thicknesses lie in the range 10^{-5} to 10^{-4} cm.

Other refinements of D.L.V.O. theory have included consideration of solvent effects (17) as well as consideration of the fact that the bulk ions possess a finite diameter (18). Since the results modify D.L.V.O. theory very slightly, it is usually taken as being essentially correct.

When D.L.V.O. theory is combined with that due to Levine and Bell, the theoretical prediction of stability against gelation may still be far different from the experimental situation. This is due to the fact that gelation requires the formation of specific chemical bonds between the colloidal particles -- a process which may involve impurity ions (12,19). Since chemical effects are not included in D.L.V.O. theory, the predicted gel point can be in error. Because the gelation of aqueous colloidal silica is influenced by such chemical effects, it is not possible to use D.L.V.O. theory to obtain an accurate prediction of the gel point (a more complete discussion of this effect will be found in a later section). However, the theory is useful in obtaining the diffuse-layer parameters and has been applied by H. Y. Li to the Ludox series of aqueous colloidal silica (20). Since these parameters will be shown to have very little effect on PMR in the colloids studied, they are not reproduced here.

The preceding comments apply only to that class of colloids known as lyophobic or "solvent fearing". Where the solvent is water, the term is often changed to "hydrophobic" for obvious reasons.

Chemical and Physical Properties

Colloidal Particles

To quote from the manufacturer's data sheet, "The silica particles in Ludox are colloidal in size, discrete and highly hydrated. They are dense, non-porous spheres of high purity SiO_2 which have no internal surface or detectable crystallinity" (21).

Although the colloidal particles are amorphous, there has been a great deal of interest in the local crystalline structure which must prevail over one or two unit cells. If this structure can be deduced, one is then in a position to gain some information about the nature of the particle surface. X-ray diffraction studies indicate that the local structure may be related to crystobalite, but the density is midway between the values obtained for crystobalite and trydimite (12) (the density values for all amophous silicas range between 2.20 and 2.35 g/cc), and the results are, therefore, open to question.

No matter which structure is chosen, one can be fairly certain that the surface is covered by a monolayer of OH-groups (generally termed "bound" or "chemically adsorbed water"). Each OH-group is assumed to complete the required valence for one of the surface silicon atoms, and, hence, surface structures of the type shown in Figure 6 have been proposed. Such diagrams tend to oversimplify the situation since the real surface structure probably involves a mixture of several ideal ones. Nevertheless, they are useful in obtaining at least a crude visualization of the particle surface, and they will have to suffice until narrow-beam LEED techniques provide a better picture.

Experimental work indicates that the OH-groups are very tightly

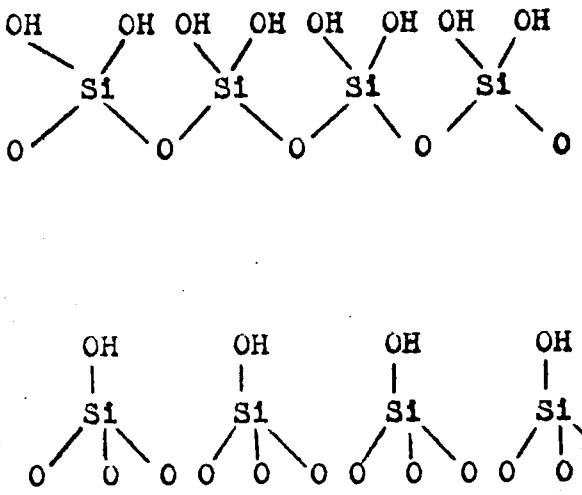

Figure 6. Two Proposed Surface Structures for Amorphous Silica. Top Structure: trydemite; Bottom Structure: crystobalite. The actual structure is unknown, but it is often assumed to be a "mixture" of the two. In this way, some silicons can hold two hydroxyl groups while others hold one, in agreement with infrared measurement.

bound to the surface, since the silica must be heated to at least 500°C. before removal of these groups is initiated (22). Secondary adsorption (or physical adsorption) of H_2O may also take place, and is usually attributed to one or both of the following possibilities (12):

1. The H_2O forms hydrogen-bonds with surface OH-groups;
2. The H_2O forms bonds with "buried" Si atoms in the surface Si-O-Si linkages.[2]

Density of OH-groups

It is of interest to discover the number of OH-groups bound per unit surface area, and the experimental work of Iler, et al. (23), as well as theoretical calculations by Iler, indicate that the probable number of OH-groups per square millimicron is 8.[3]

Density of H_2O Molecules

In vacuo, H_2O molecules seem to be adsorbed as a result of mechanism 1 above. The experimental evidence which suggests that there are eight OH-groups per square millimicron, also yields the same number of H_2O molecules per unit of surface area. Furthermore, when the number of OH-groups is reduced by heating the silica above 500°C., there is a corresponding reduction in the number of adsorbed H_2O molecules (25). When this evidence, as well as that related to surface charge (see following discussion), is considered in detail the crystobalite structure

[2]A "buried" Si atom has its valence requirements completed entirely by oxygen atoms, but is still accessable to bulk H_2O molecules.

[3]Fripiat, et al., disagree with this conclusion (24), but since their method of measurement was less direct than Iler's, the latter values have been assumed to be correct.

becomes favored and is, in fact, the local structure most often assumed for amorphous silica.

Surface Charge

In aqueous media, there is the second possibility that the "buried" Si atoms may link with OH-groups or with H_2O molecules. Any "extra" OH-groups which are adsorbed by this mechanism must give rise to a negative surface charge (12). Since this surface charge is responsible for the stability of the colloid, it is important to be able to estimate the maximum charge density attainable. Experimental work by W. M. Heston, Jr., et al. indicates that a maximum of 3.5 negative charges may be adsorbed by each square millimicron of surface area, and that the prevailing surface charge is a function of both the Na-ion concentration and the pH (26).

A rough calculation of the surface charge may be made with an equation given by Iler which neglects the sodium-ion effect (12). Let "a" be the number of ionized surface sites (in gram-moles/liter) and let "b" be the number of uncharged sites. Then, according to Iler, the ratio of a to b is given by

$$\frac{a}{b} = 10^{pH-9.8} \tag{129}$$

at $30^{o}C.$, where the facts that (1) the surface charge depends upon the sodium-ion concentration, and (2) that the surface charge may reverse its sign, have been neglected.

Later work by Heston has shown that a better empirical equation would be

$$\frac{a}{b} = 10^{0.3\,(pH-11)} \tag{130}$$

for a sodium-ion concentration between 10^{-3} normal and 10^{-2} normal (26). This equation correctly gives the surface charge of Ludox aqueous colloidal silica as 50% of its maximum possible value at pH 11.

All available experimental evidence strongly supports the hypothesis that the surface charge density is independent of the particle diameter (12,26,27).

The Suspension Effect

During the course of his surface charge measurements, Bolt was able to demonstrate the fact that an ordinary pH meter cannot always accurately determine the true pH of the liquid phase of the colloid (27). This so-called "suspension effect" is present because the charged colloidal particles interfere with the normal diffusion of potassium chloride across the calomel electrode; the electrode potential is, therefore, disturbed, and the pH indication is erroneous. If Bolt's interpretation is correct, one must exercise extreme caution in those experiments where a pH measurement is required. There is some evidence, however, that Bolt may have over-estimated the importance of the suspension effect. Since he used a semi-permeable membrane (actually, an agar bridge) to separate the colloid under test from the calomel electrode, the possibility arises that the Donnan equilibrium may have "driven" OH-ions into the region of this same electrode, thereby producing a "corrected" reading which was actually too high. A numerical estimate of the Donnan effect (which is usually observed under the conditions of Bolt's experiment) cannot be made without a knowledge of the sample volumes involved, and we can only state that, if it did have an influence, it would be expected to produce observations similar to those

recorded by Bolt.

Heston and co-workers, although aware of Bolt's work, did not incorporate his correction into their measurements of surface charge. Nevertheless, they were able to incorporate the Bolt data into their results and show that there was good agreement even at pH 10 with a 10^{-3} normal NaCl concentration in the bulk (Bolt found a maximum error in the pH reading under these conditions). According to Bolt, Heston's true pH at this point should have been close to pH 11, and this should have produced an order-of-magnitude error in Heston's calculation of the OH-ion concentration. Presumably, such an error would have markedly affected the surface charge calculated by Heston, and his excellent agreement with Bolt's data would be unexpected at the very least. We note, however, that Bolt added OH-ions both to the colloid under study and to the solution near the calomel electrode. It is conceivable that his pH differences were, as a result, accurate whereas his absolute measurements were not. If such is the case, the measurements of both groups of workers can be reconciled although the status of the suspension effect cannot (Bolt's arguments in its favor are quite compelling).

The present author's measurements of pH as a function of SiO_2 concentration seem to be readily explainable in terms of the suspension effect. A direct measurement of colloid pH produced the interesting result that the sample pH appeared to increase as distilled water was added (see Figure 7). Heston has remarked that the suspension effect should disappear at infinite dilution (26), and the pH increase (which for Ludox LS amounted to nearly 1 pH-unit) could be very nicely explained in terms of the disappearance of Bolt's suspension effect. An alternative explanation could invoke the desorption of OH-ions from the

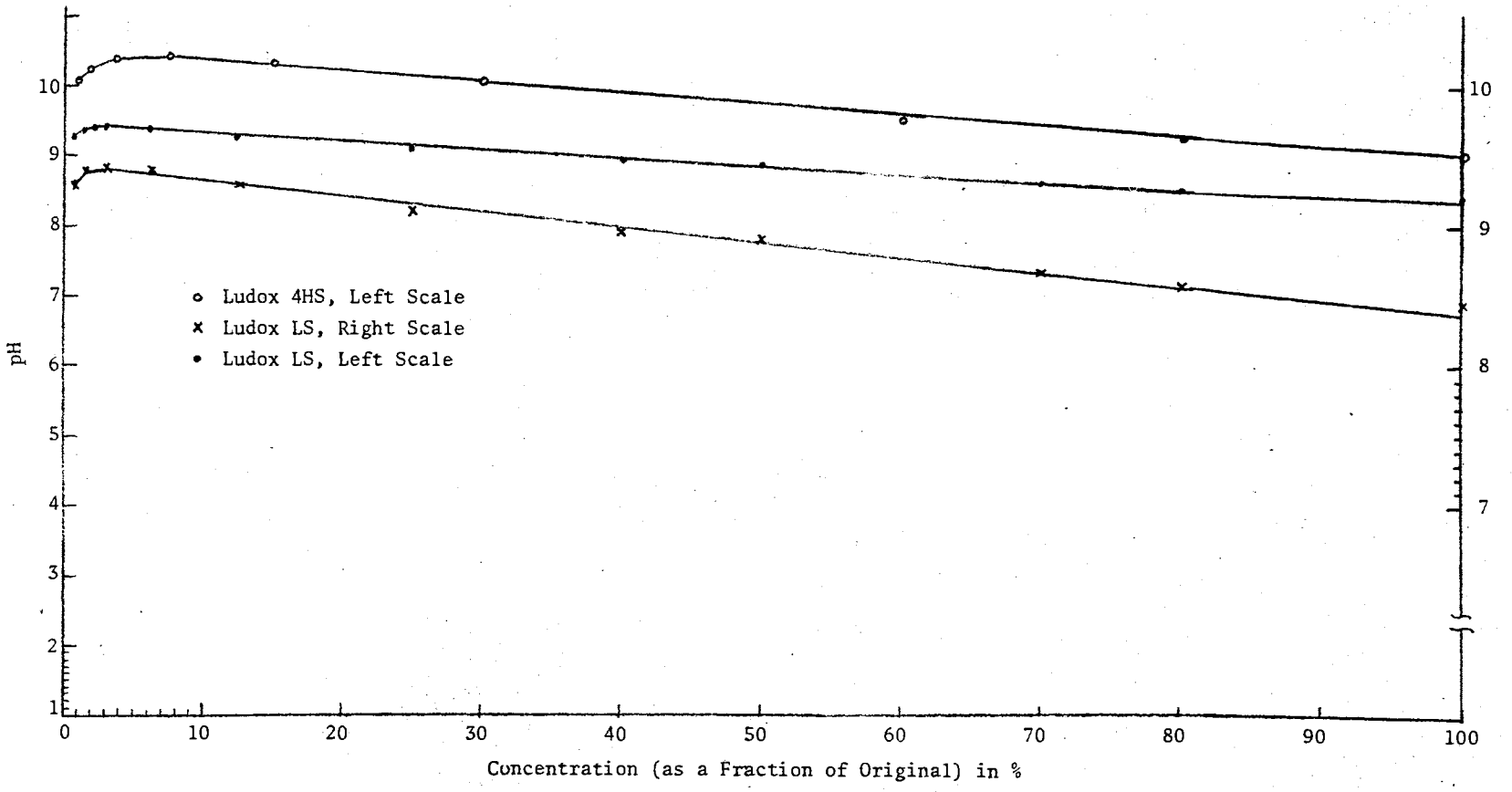

Figure 7. Indicated pH as a Function of the Original Concentration for Both Ludox LS and Ludox 4HS at 25°C

particle surface as the colloid is diluted. It has been remarked that the specific surface charge is weakly dependent upon the sodium-ion concentration and that a reduction of this concentration by an order of magnitude will reduce the surface charge by ca 10%. However, it seems unlikely that the majority of the pH increase can be attributed to a reduction in sodium-ion concentration, and a suspension effect still seems most plausible.

The results of later chapters will show that the NMR relaxation time T_2 is a function of the hydrogen-ion concentration. A real change of 1 pH unit with dilution could have caused the relaxation rate ($1/T_2$) to vary in a non-linear manner when plotted against particle concentration. Fortunately, these experiments were performed in a region where a unit change in pH had little influence on T_2, and linear dilution plots were obtained. If the suspension effect does not account for the observed pH increase, then one may be able to repeat this experiment at pH6 - pH7 and obtain non-linearities in the results.

Titration of Ludox LS

The colloids used in the Bolt and Heston experiments had been passed over ion-exchange resins and hence, did not have the same chemical composition as the colloids employed in our experiments. In the material to follow, it will be argued that the rate of change of specific surface charge with pH is such that one can eliminate any surface charge effect from the interpretation of the NMR results. It was, therefore, necessary to experimentally confirm the expectation that Heston's measurements would apply equally well to the "Ludox" series of

colloids.[4]

It was less important to obtain the absolute magnitude of the surface charge than to obtain its rate of change with pH. Furthermore, it was only necessary to show that the experimental results were consistent with Heston's, and for that reason the following (simplified) procedure was used in performing the titration:

1. The sample pH was initially reduced to 7, and it was assumed that the surface charge given by Heston for this pH applied to our situation;[5]
2. Using the surface charge at pH 7 as a base, the titration was performed, and the surface charge calculated for higher pH values;
3. The resulting data were taken to be consistent with those of Heston, since, at higher pH, both sets of data still agreed. This could not have occurred if the rate of change of specific charge were drastically different in our case.

In the next several paragraphs we report the experimental procedure in detail.

A sample of Ludox LS was diluted with distilled water until the SiO_2 concentration was approximately 8% by weight. (At this concentration, there was enough SiO_2 in the sample that a titration could be successfully completed, yet the concentration was not high enough to

---

[4]Heston's sol had had mostly indifferent ions removed, and, except for a weak ionic-strength effect, the surface charge should have been undisturbed.

[5]Ideally, one would start at pH 3.5 -- the point of zero surface charge. However, maximum sensitivity requires a high colloid concentration, and in this situation, the sample pH must be kept above $\sim$ 6.5 to avoid gelling.

produce difficulties with the glass electrodes of a pH-meter.) The pH was then reduced to 6.90 with reagent grade HCl. It was assumed at that point that the surface was essentially uncharged, (Heston's results indicate the surface charge to be 2% of its maximum possible value) and the presence of any titratable surface OH-ions was neglected. Known amounts of Banco 1 N standardized NaOH were then added to the sample, and the number of OH-ions sorbed by the colloidal particles was obtained by combining these data with the direct pH measurements.

After Heston (26), let

a = concentration of base, expressed as equivalents per liter of water and electrolytes, excluding colloid;

a_s = difference between the known concentration a and the measured concentration of bulk OH-ions, as "seen" by a standard pH-meter.

Then, if W is the volume of water and electrolytes in 100 ml. of colloid, one has

$$W = 100 - 0.438C \tag{131}$$

where C is the concentration of SiO_2 in grams per 100 ml. of sol. For the case under discussion, the concentration of silica was 9.05 g/100 ml. sol prior to the addition of NaOH. When the dilution of the sample by the addition of reagent is taken into account, one obtains for a 200 ml. sample

$$C \doteq 9.05\ (1\text{-}M/200)\ \text{g/100 ml} \tag{132}$$

where M is the number of ml. of NaOH added to the sample and where it has been assumed that $M \leq 20$ ml. By combining the preceding formulas,

one can obtain the more useful form

$$W \doteq 96.0 + 1.98 \times 10^{-2} M \quad \text{ml } H_2O/100 \text{ ml sol} \quad . \quad (133)$$

The total surface area, S, is given by

$$S = 10^3 \, CA/W \quad (134)$$

where A is the surface area per gram of solid SiO_2 suspended in the sample. Assuming that there are 3.5 sites per square millimicron available to the OH-ions, one gets the fraction of sites charged, f, from the formula

$$f = \frac{a_s}{5.80 \times 10^{-6} . S} \quad . \quad (135)$$

With A = 200 M^2/g, we have obtained the values listed in Table III; they are in reasonable agreement with those reported by Heston. We have, therefore, concluded that the Heston experiments apply to Ludox LS, at least insofar as the rate of change of charge is concerned. Since Ludox HS, and SM are formed from the same "heel" solution as Ludox LS, and further, since the known impurity ions are not expected to have any great influence on the specific surface charge, we have assumed without test that they apply as well to these other colloids (Ludox AM must be excluded from these considerations since its surface charge is not simply related to pH).

Gelation

It is believed by Iler and others that a colloidal silica does not gel simply by virtue of the fact that the electrostatic repulsion between the colloidal particles is destroyed (12,19,28), and a rather

TABLE III

10/20/69 TITRATION OF LUDOX LS

pH	$a = \frac{[OH]}{1H_2O}$	ml 1N NaOH added	10^{pH-14}	$a_s = a - 10^{pH-14}$	f_1[1]	f_2[2]	f_3[3]
6.90	---	0	---	---	---	0.018	---
8.35	5.20×10^{-3}	1	2.24×10^{-6}	5.20 x 10-6	0.048	0.045	0.035
9.10	1.04×10^{-2}	2	1.26×10^{-5}	1.04×10^{-2}	0.096	0.080	0.080
9.58	1.56×10^{-2}	3	3.80×10^{-5}	1.56×10^{-2}	0.145	0.110	0.130
9.89	2.08×10^{-2}	4	7.70×10^{-5}	2.08×10^{-2}	0.195	0.160	0.200
10.10	2.60×10^{-2}	5	1.26×10^{-4}	2.06×10^{-2}	0.243	0.190	0.240
10.30	3.12×10^{-2}	6	2.00×10^{-4}	3.10×10^{-2}	0.294		0.260
10.50	3.64×10^{-2}	7	3.16×10^{-4}	3.61×10^{-2}	0.344		0.300
10.63	4.16×10^{-2}	8	4.60×10^{-4}	4.11×10^{-2}	0.393		0.390
10.79	4.68×10^{-2}	9	4.77×10^{-4}	4.63×10^{-2}	0.445		0.450
10.91	5.20×10^{-2}	10	4.90×10^{-4}	5.15×10^{-2}	0.495		0.500

[1] f_1 -- value calculated from preceding data.

[2] f_2 -- Heston's value at 10^{-3}N NaCl concentration.

[3] f_3 -- Heston's value at 10^{-2}N NaCl concentration.

simple experiment can confirm this belief. If NaCl (an indifferent electrolyte) is added to Ludox LS at pH 9, the double-layer thickness is reduced, and a gel forms at once. However, if the pH is reduced to 3.5 -- where there is no surface charge and, hence, no double-layer -- one can add excessively large amounts of NaCl without producing any effect at all. On the other hand, very small amounts of NaF can be added at this pH to produce almost instantaneous gelling; obviously, double-layer effects are of small importance at this pH, and the different effect obtained with NaF must involve the chemical properties of the fluorine ion.

It is also observed that the point of minimum stability does not occur at pH 3.5, where the surface charge is absent, but occurs instead in the range pH 5-6 (21). It is Iler's contention that these observations can be explained on the basis that the following conditions must be satisfied if a gel is to form:

1. The mutual repulsion between particles must be low;
2. There must be a sufficient number of "catalyst" ions present to promote the formation of interparticle Si-O-Si linkages.

In the normal situation, OH-ions satisfy (2) by acting as the catalytic agent, and, therefore, the point of minimum stability is shifted toward a (higher) pH where there are more OH-ions available. It has been postulated that the F^- ion can also act as a catalyst (12).

We should also point out the fact that an unstable sample can be gelled at an elevated temperature, apparently because the number of particle collisions per unit time is increased.

Unfortunately, the mechanism by which a colloid gels is not as simple as that proposed by Iler, since there are at least two

recognizably different types of gel observed experimentally. Furthermore, Ludox colloids have a stability which can be directly related to the concentration of iron (III) impurity in the sample.

Stumm and O'Melia have found that, in the case of Ludox colloids, one can obtain (1) a "sweep floc" in which the colloidal particles are enmeshed in a three-dimensional network of polynuclear iron complexes, or (2) a true gel, in which sorption of $Fe(OH)_n$ plays the dominant role in determining the double-layer interaction (28). The precise behavior is difficult to predict and may be a function of the iron concentration, the pH, and the surface area of the dispersed phase. Furthermore, an initially unstable colloid may be restabilized by the addition of very small amounts of positively charged iron complexes such as $Fe_2(OH)_2^{4+}$ (below pH 3, stability may be entirely due to the presence of such species).

The situation is further complicated by the fact that the iron species equilibrate very slowly after a change in pH. In some cases, it has been observed that gradual changes can occur for up to 200 hours and that these changes can be accelerated by applying heat to the sample (29). At a later point in this thesis, we shall relate the NMR of gelled colloids to such behavior.

Recent articles by Stumm and Matijevic have revealed the fact that the gel mechanism can be very complicated and can be strongly influenced many ions other than iron, via a direct chemical interaction (19,30). r these reasons, it is not possible to say which mechanism was domiant in our experiments, although we strongly suspect that the presence of iron impurities was the single most important factor.

Impurities on the Colloidal Surface

Metallic impurities apparently attach themselves to the colloidal surface via one or both of the following two mechanisms (31):

1. The surface hydroxyl groups fill the coordination sphere of the metal ion, or
2. The metal ion replaces a Si atom in the crystal lattice.

The second mechanism is favorable for Al^{3+} and Fe^{3+}, whereas mechanism (1) is assumed to dominate for most other metal ions. Those metal ions which are precipitated as hydroxides below pH 4 and which are also strongly acidic have been found to adsorb strongly on silica at low pH and to form Brönstead acid sites. Iron forms moderately strong ferrisilicic acid and aluminum behaves in a similar manner; both ions leave the surface negatively charged. Chromium, barium, lanthanium, and copper, on the other hand, do not form acid groups when adsorbed on the surface (31).

The acidic impurities which are present in the Ludox series of colloidal silicates are apparently responsible for the shift of the isoelectric pH away from its theoretical value of 6.5 to 7.0 (12). It is the present author's belief that Fe (III) is largely responsible for the observed shift.

In order to test the assumption of a significant iron concentration, Ludox LS and Ludox HS were both subjected to a specific analysis for iron.[6] The results of that analysis (which will be discussed in more detail at a later point) showed that the total iron concentration

---

[6]Analysis performed through the courtesy of the Analytical Services Division of Gulf Research and Development Company at Harmarville, Pa.

was indeed significant, being as high as 45 ppm for Ludox LS and 128 ppm for Ludox 4HS. At this impurity level, it is to be expected that some of the colloidal properties can be related to the chemical behavior of iron (28).

Proton Diffusion Rates in Silica Gel

Becase the colloids under discussion are directly related to an important class of catalytic materials, namely, the zeolites, a great deal of effort has been expended in determining the role that (proton) diffusion plays in controlling reactions which take place near the surface of an amorphous silica. It has been found by J. J. Fripiat and others that the activation energy associated with proton diffusion through an Si-O-Si "mesh" is roughly 4 Kcal/mole (32) -- a value which is also characteristic of the NMR temperature measurements to be discussed in a later chapter.

Measurements Revealing the Presence of Impurities

Direct Chemical Analysis

Two samples of Ludox colloidal silica, types HS and 4LS, were subjected to the following steps, prior to a chemical analysis:

1. Unmodified samples were held at an elevated temperature until they appeared to be completely dry.
2. The solid powder which remained was soaked in concentrated hydrochloric acid (37% by weight HCl) for 24 hours; the acid was separated from the solids, and the solids were rinsed with dilute hydrochloric acid and distilled water.
3. The liquid portions were combined and saved as a separate

sample.

4. Both the solid and the liquid samples were subjected to a specific analysis for iron.
5. In addition, a "blank" sample was subjected to the preceding steps in order to insure that the amount of iron introduced during the laboratory procedure was minimal.

Since any iron not intimately associated with the colloidal particles themselves should have been removed during step two, the analysis of the resulting liquid sample provided us with a means of estimating a maximum amount of iron which could be expected to be in the liquid phase of the colloid under test. We proceed next to a calculation of the appropriate concentrations from the data given in Table IV.

TABLE IV

RESULTS OF Fe ANALYSIS

Sample	Weight	Volume	ppm Iron
LS solids	11.20 gm	---	45.3
LS liquid	94 gm	94 ml	1.5
HS solids	16.45 gm	---	128.2
HS liquid	78 gm	78 ml	9.5
Solid blank[1]	90 gm	90 ml	< 0.1
Liquid blank	87 gm	87 ml	< 0.1

[1]The "solid blank" was subjected to the same treatment with HF acid that was used to destroy the solid samples.

If the dried solids weigh W_{SiO_2} grams, it is possible to obtain the original volume of sol (V_{LS} or V_{HS}) from the formulas

$$V_{LS} = 2.71\ W_{SiO_2} \qquad \text{(for LS solids)} \qquad (136)$$

and

$$V_{HS} = 1.90\ W_{SiO_2} \qquad \text{(for 4HS solids)} \quad . \qquad (137)$$

The original liquid volume, excluding suspensate, is obtained from Heston's formula as

$$V'_{LS} = 0.84\ V_{LS} \qquad \text{(Ludox LS)} \qquad (138)$$

or

$$V'_{HS} = 0.77\ V_{HS} \qquad \text{(for Ludox 4HS)} \quad . \qquad (139)$$

Therefore, one can use these formulas to obtain the maximum concentration of iron available to the bulk liquid, provided it is assumed that all of this iron was extracted when the solids were washed in HCl. Table V summarizes results of such a calculation.

TABLE V

IRON CONTENT IN THE LIQUID PHASE OF TWO UNMODIFIED SOLS, CALCULATED FROM THE DATA OF THE PRECEDING TABLE

Colloid Type	W_{SiO_2}	V'	Total Iron Extracted	Liquid Phase Iron Content
4HS	16.45 gm	24.2 ml	7.41×10^{-4} gm	3.30×10^{17} ion/ml H_2O
LS	11.20 gm	25.5 ml	1.41×10^{-4} gm	5.96×10^{16} ion/ml H_2O

In a later chapter, we will show that the concentrations given in Table V are in keeping with the assumption that iron impurities control the proton T_1, but at the present time we wish to consider the SiO_2 impurities.

Assume that the iron in the colloidal particles is distributed uniformly and that it replaces Si in the crystal lattice of SiO_2. According to Iler, there are 8 Si atoms per square millimicron of surface area, and, according to our assumption, the fraction of these atoms which is replaced by iron, α, is identical to the fraction within the bulk of a colloidal particle. A sample calculation for unmodified Ludox LS should make the situation clear, and it is included in the following paragraphs.

The total number of Si atoms in 100 ml of unmodified Ludox LS is easily found to be

$$N_{Si} = 0.614\ N_a \text{ per 100 ml} \tag{140}$$

where N_a is Avogadro's number. From the data of Table IV, one finds that the number of Fe atoms is given by

$$N_{Fe} = 2.99 \times 10^{-5}\ N_a \text{ per 100 ml} \tag{141}$$

so that α, the fraction of iron atoms, is given by

$$\alpha = \frac{N_{Fe}}{N_{Si}} = 4.87 \times 10^{-5} \quad . \tag{142}$$

The surface area in 100 ml of sol is given by

$$S \doteq \left(\frac{36.9 \text{ g } SiO_2}{100 \text{ ml sol}}\right) \times \left(\frac{200\ M^2}{1 \text{ g } SiO_2}\right)$$

or

$$S \doteq 7.38 \times 10^{21} \ (m\mu)^2 \text{ per } 100 \text{ ml} \quad . \tag{143}$$

The number of "exposed" Si atoms $N_{Si}^{(e)}$ is, by Iler's contention

$$N_{Si}^{(e)} = \frac{8}{(m\mu)^2} \cdot S = 5.90 \times 10^{21} \text{ per } 100 \text{ ml} \tag{144}$$

so that the number of exposed Fe ions is given by

$$N_{Fe}^{(e)} = \alpha N_{Si}^{(e)} = 2.88 \times 10^{18} \text{ ion/100 ml} \quad . \tag{145}$$

Thus, since there are 84 ml of water in 100 ml of sol, the concentration of exposed iron per ml of bulk H_2O, $C_{Fe}^{(e)}$, is given by

$$C_{Fe}^{(e)} = \frac{N_{Fe}^{(e)}}{84 \text{ ml}} = 3.43 \times 10^{16} \text{ ion/ml} \quad . \tag{146}$$

By a similar process, one can find that C_{Fe} for unmodified Ludox HS ought to be 1.69×10^{17} ion/ml. At a later point in this thesis, it will be shown that the concentrations just calculated can produce a value of T_1 in each colloid which is remarkably close to that measured experimentally, although the agreement is probably fortituious.

CHAPTER V

PROTON RELAXATION IN COLLOIDAL SILICA

Some Preliminary Experiments

Colloidal silica seems to be an ideal medium in which to observe surface effects. A typical sample employed by the EFFP apparatus would have a volume of 500 ml and contain a total surface area of SiO_2 exceeding 10^4 M^2. If protons on or near the colloidal surface relax more strongly than their counterparts in the bulk, the very large surface area involved should make observation of the effect more probable.

It is obvious from the material of preceeding chapters that Ludox colloidal silicates do indeed exhibit a shorter proton T_1 than would be expected in pure water. It remains to be seen, however, whether this shorter proton T_1 can be attributed to a true surface effect or if it is due instead to some other property, such as an impurity in the bulk. It is also necessary to be able to estimate the influence of particle geometry upon the observed relaxation.

The preliminary questions to be answered are the following:

1. Is the effect -- or any part of the effect -- attributable to the particle surface?
2. Does the surface geometry play an important role in determining the details of the PMR signal?

It will be our task in this chapter to answer the foregoing questions in reverse order. In Chapters VI and VII we shall consider the specific

interactions in greater detail.

Influence of Particle Geometry

Diffusion Calculations

Consider a situation in which water protons, initially aligned with an external magnetic field $\overline{B}_p$, diffuse toward a colloidal surface and then relax (lose alignment with the original direction of $\overline{B}_p$). In the most general situation, we should expect that the induced nuclear magnetization per unit volume $\overline{M}$ will be a function of the coordinate position and the time. Furthermore, it will be necessary to integrate $\overline{M}$ over the sample volume in order to determine the magnitude of the free-precession signal at any given instant. In an unpublished derivation, V. L. Pollak has considered this problem and has reached the important conclusion that, if the surface of the colloids studied in any way controls T_1, the free-precession signal must be independent of surface geometry and can depend only upon the specific surface area (33). The details of that derivation are presented next.

Since the (initially aligned) protons diffuse across hydrogen bonds toward the colloidal surface before relaxing, there is a current density $\overline{j}$ in the magnetization $\overline{M}$ given by Fick's law, i.e.,

$$\overline{j} = -D \text{ grad } |\overline{M}| \tag{147}$$

where D is the isotropic coefficient of diffusion. At points where there are no sources or sinks of $\overline{M}$, the continuity equation

$$\overline{\nabla} \cdot \overline{j} = \frac{\partial |\overline{M}|}{\partial t} \tag{148}$$

must apply. When this is combined with 147, the diffusion equation

$$\frac{\partial |\overline{M}|}{\partial t} = D \nabla^2 |\overline{M}| \tag{149}$$

is obtained. It has been suggested by Pollak that the right-hand side of Equation 149 could be included as an additional term in the phenomenological Bloch equation in order to obtain the time rate of change of $\overline{M}$. Because the statistical approach is an alternative means of solving the problem, we did not have to introduce this method while obtaining the equations of Chapter II.

Relaxation at the surface is included in Equation 149 by assuming that the outward current density at the relaxing surface is proportional to the magnetization, $\overline{M}_s$, near the surface. If $\overline{n}$ is a unit vector normal to the surface, one may then write the equation

$$(\vec{j} \cdot \vec{n})_s = -D(\vec{n} \cdot \nabla M)_s = \alpha M_s \quad . \tag{150}$$

If the surface is non-relaxing, one takes $\alpha = 0$; if the surface is "perfectly" relaxing, one takes $\alpha \to \infty$. In the latter case, one must also have

$$M_s = 0 \tag{151}$$

in order to keep the current finite.

The precession signal $e_s(t)$ is proportional to the total magnetic moment in the sample $\int \overline{M} dV$, where the integration is carried out over the sample volume.

Fick's law and the boundary conditions give

$$\int (\vec{j} \cdot \vec{n}) ds = -D \int (\vec{n} \cdot \nabla M) ds = \alpha \int M ds \quad . \tag{152}$$

The divergence theorem and the continuity equation gives

$$\int (\vec{j} \cdot \vec{n}) ds = \int \nabla \cdot \vec{j}\, dV = - \frac{\partial}{\partial t} \int M dV \quad . \tag{153}$$

Therefore,

$$\alpha \int M ds = - \frac{\partial}{\partial t} \int M dV \tag{154}$$

i.e., the parameter α controls the rate of signal decay. The assumption that the surface is weakly relaxing gives an approximately uniform $\overline{M}$ over the sample volume, so that the last equation becomes

$$\frac{\partial \overline{M}}{\partial t} + \alpha \frac{S}{V} \overline{M} = 0 \tag{155}$$

from which

$$\overline{M} = \overline{M}_0 \, e^{-\alpha \frac{S}{V} t} \quad . \tag{156}$$

This result applies if α, D and the surface geometry are such that a typical proton gets a sampling of all possible environments before relaxing.

Consider the case of suspended spherical particles of radius r_0 having perfectly relaxing surfaces. Each particle is taken to be associated with a surrounding sphere whose radius, a, is equal to half the mean particle separation. On the surface of this sphere, $\overline{M}$ is taken to have a maximum, and the boundary conditions are therefore as follows:

$$\begin{aligned} &\overline{M}(r_0, t) = 0 \\ &\frac{\partial \overline{M}}{\partial r} (a, t) = 0 \quad . \end{aligned} \tag{157}$$

The general solution to the diffusion equation in spherical-polar coordinates is of the form (34)

$$M(r,t) = \sum_n \left(A_n \frac{\sin K_n r}{K_n r} + B_n \frac{\cos K_n r}{K_n r}\right) e^{-DK_n^2 t} \qquad (158)$$

where the K_n are solutions of

$$K_n a = \tan K_n (a - r_0)$$

and

$$K_1 a \approx \left(\frac{3r_0}{a}\right)^{\frac{1}{2}} \text{ for } r_0 << a \quad .$$

The boundary conditions previously quoted give the result that, after a sufficient time, the first term of 158 dominates and one obtains a relaxation rate given by

$$\frac{1}{T_1} \approx \frac{3D}{a^2} \cdot \frac{r_0}{a} \qquad (r_0 << a) \quad . \qquad (159)$$

In terms of the particle concentration N, this becomes

$$\frac{1}{T_1} = 4\pi N r_0 D \quad . \qquad (160)$$

It is possible to use Equation 160 to estimate the relaxation time T_1 for a suspension of "perfectly relaxing" SiO_2 spheres typical of a Ludox colloidal silica. Inserting the values, $N = 3 \times 10^{18} ml^{-1}$ $r_0 = 12$ millimicron, $D \doteq 10^{-5} M^2$ sec, one obtains $T_1 = 10^{-10}$ sec for unmodified 4HS. Obviously the surface is weakly relaxing and Equation 156 applies. The parameter α in Equation 156 must be on the order of 10^{-7} m/sec in order to reproduce the experimentally measured T_1.

The chief utility of this derivation lies in the fact that, in our case, we can take

$$\frac{1}{T_1} = \alpha \frac{S}{V} \quad . \qquad (161)$$

If relaxation due to other mechanisms in the bulk is included in this expression, we would then have $T_{1(obs)}$ given by

$$\frac{1}{T_{1(obs)}} = \alpha \frac{S}{V} + \frac{1}{T_b} \tag{162}$$

where T_b^{-1} is the relaxation rate of protons in the bulk medium alone. It should be obvious that Equation 49 of Chapter II will apply and is equivalent to the above expression with $P_b \approx 1$; $P_a = S\,\Delta/V$ and $1/T_a = \alpha/\Delta$, where Δ is the "thickness" of the surface layer ($S\Delta$ is therefore a surface volume).

We have thus answered the second question, and the answer is that the surface geometry does not play an important role in determining the decay of $\overline{M}$, at least in the case of the colloids under examination. We have not shown, however, that the particle surface has any influence on T_1, but have merely shown that where such an influence is assumed to be important, the foregoing answer applies. We therefore must proceed to the next problem, that problem being to answer the first question posed at the beginning of the chapter.

Influence of the Particle Surface

Several experiments have been performed which relate directly to the surface influence, but unfortunately no single experiment gives an unequivocal answer to the question posed. We will state at the beginning of this section that our conclusion is that the majority of the effect is directly attributable to the influence of the particle surface, and we will support this statement by exhibiting a series of experiments which are most easily explained in terms of this assumption.

Dilution Experiment

If the relaxation which is responsible for the observed effect in Ludox colloidal silica takes place primarily at the particle surface, it should be possible to demonstrate a linear dependence of $1/T_1$ upon the specific surface area available to the sample protons. This may be expressed alternatively as a dependence on N, the number of particles per unit volume of sol, since the ratio S/V is obviously proportional to this quantity. Both Ludox HS and LS were diluted with distilled water and the relaxation rate per unit surface area and per unit volume was plotted as a function of SiO_2 concentration. As may be seen from Figure 8, the relaxation rate $(1/T_{1,2})$ per unit surface area and volume appears to be independent of concentration. Since this is the case, some of the data to be reported in the following material are presented in these terms. This effectively eliminates the necessity of including the concentration of SiO_2 as one of the parameters mentioned in the introduction.

The experiment was not a conclusive demonstration that the observed effect is directly attributable to the surface. It is equally possible that paramagnetic impurities are present in the bulk liquid, in which case an analogous behavior is expected. However, it is undoubtedly true that if the surface is weakly relaxing and if the surface is also the controlling factor, the dilution behavior must be identical to that observed. In short, the condition is necessary but not sufficient to prove the presence of a true surface effect.

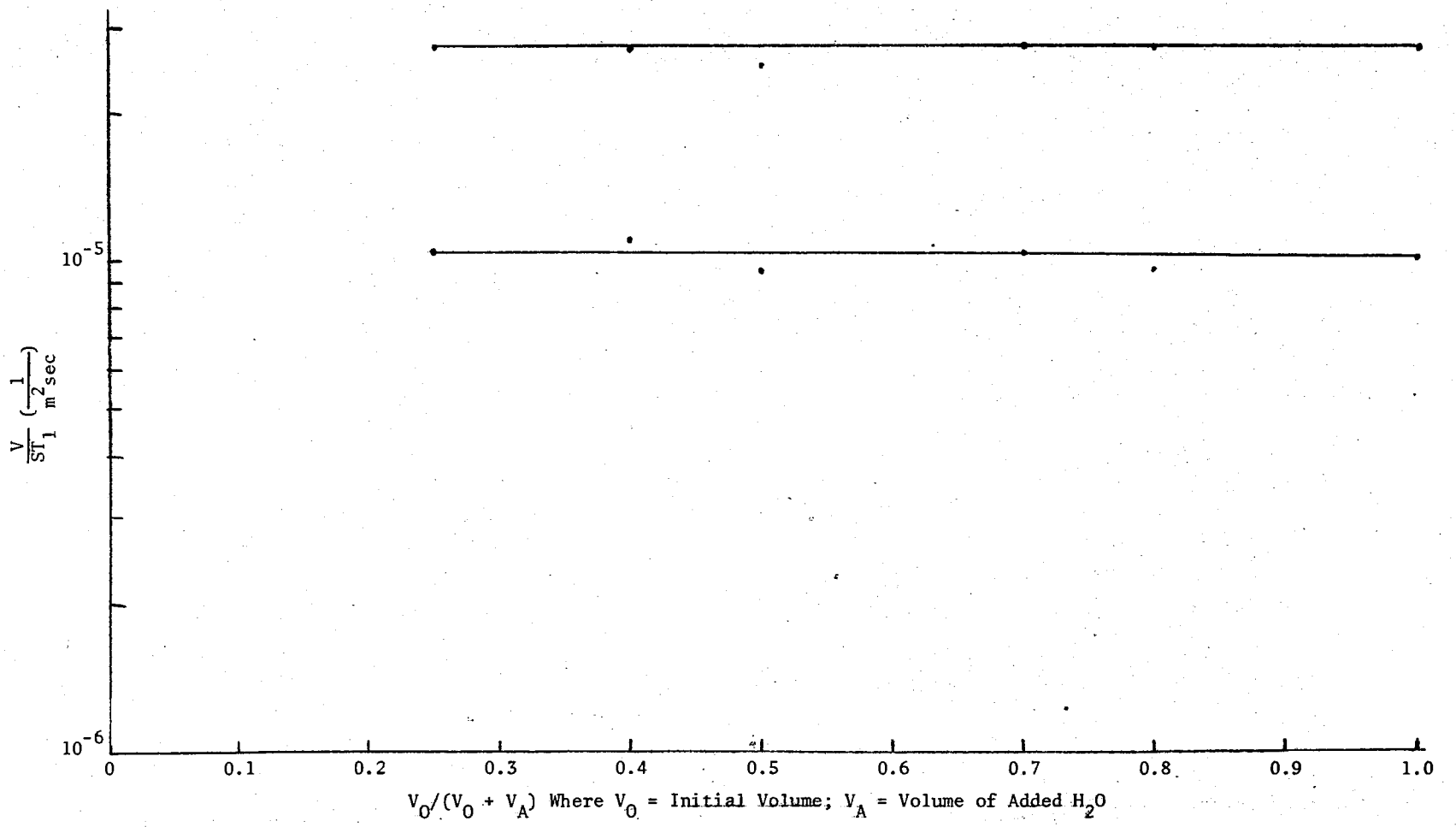

Figure 8. Reduced Relaxation Rate for 30% Ludox LS as a Function of the Original Concentration. Upper curve taken at 1 G; lower curve at 320 G. Temperature 40°C.

Washing Experiment

A sample of Ludox LS was dried at an elevated temperature (100°C), and the solids were "washed" with 5N hydrochloric acid by allowing them to stand in the acid for one hour and then filtering the remaining solution. The filtrate was diluted with distilled H_2O until the original sample volume was restored, and a control sample of pure H_2O was subjected to the same procedure. Since most paramagnetic ions are extremely soluble below pH 2, the procedure should have resulted in the extraction of any ions not intimately associated with the colloidal particles themselves. The control sample served as a check upon the presence of paramagnetic ions in the reagents themselves, and demonstrated that the procedure introduced no significant impurity, since the control sample T_1 was that of pure H_2O (including dissolved atmospheric O_2). Table VI shows the experimentally observed value of T_1 for these samples and also shows the values obtained with the original Ludox LS sample.

TABLE VI

WASHING EXPERIMENT SAMPLES, ALL AT 30° C

	T_1 at 580 Gauss	T_2 at 0.54 Gauss
Pure H_2O	2.76 sec.	2.76 sec.
Washings From LS Solids[1]	1.97 sec.	1.97 sec.
Ludox LS[2]	1.90 sec.	1.07 sec.

[1] pH 1.30 and at 30° C.

[2] 8% by weight SiO_2 at 30° C, pH 9.

The long T_2 obtained at 0.54 G with the "wash" sample, as well as the absence of any field-dependence, would seem to indicate that, although T_1 may be slightly reduced by the presence of some bulk impurities (compare the 580 G values) the difference at 0.54 G among the samples seems to be characteristic of a surface effect. Furthermore, the field-dependence seems to be characteristic of the surface, since the absence of a "surface" also leads to the absence of this effect. Note that the value of T_1 at 580 G observed in 8% Ludox LS was also observed in the "wash" sample. This may indicate that the high field limit of T_1 is controlled by paramagnetic impurities either loosely bound to the surface or actually dissolved in the bulk liquid. Iler has noted the strong adsorptive properties of the silica surface towards Fe^{3+} ions (among others) above pH 3, and it therefore seems likely that so-called "bulk" impurities may actually be loosely bound to the surface above this pH (12).

In the previous chapter, we reported the results of a specific analysis for iron -- an analysis for which the sample preparation was nearly identical to that reported here. It therefore seems appropriate to calculate the typical T_1 to be expected in the presence of the iron impurities revealed by chemical analysis. In our apparatus, the measured T_1 of H_2O (including dissolved O_2) was 2.20 seconds at 22°C, and this information must be included in the calculation.

Hausser and Laukien have found that a concentration of 2.6×10^{19} Fe^{3+} ions/ml will produce a water proton T_1 of 10^{-3} seconds (35). Thus, by proportionality, the "extractable iron" content given by Table V should produce, for unmodified Ludox LS

$$T_{1(LS)} = 0.44 \text{ seconds} \quad . \qquad (163)$$

If pure LS is diluted until its volume is increased by a factor of four, the extractable iron concentration is reduced by a factor of 0.218. Thus, if iron were solely responsible for the observed proton T_1, one should expect

$$T_{1(LS)} = 2.00 \text{ seconds} \quad . \tag{164}$$

If the intrinsic relaxation time of pure water, including dissolved O_2, is incorporated into the preceding estimate, one has

$$T_{1(LS)} = \frac{(2.00)(2.20)}{2.20 + 2.00} \text{ seconds} = 1.05 \text{ seconds} \quad . \tag{165}$$

This agrees with experiment at 600 G as well as with the data of Table VI.

Up to this point, the iron which was found to be non-extractable (and therefore presumed to be contained in the colloidal particles) has been neglected. By assuming that the "exposed" Fe^{3+} produces a proton T_1 identical to that of free Fe^{3+} (an assumption contrary to the one which will be made later, but nevertheless useful for the present purpose), one can use the data of Hausser and Laukien to estimate that the contribution due to exposed Fe^{3+} alone, $T_{1(LS)}^{(e)}$, would be

$$T_{1(LS)}^{(e)} = 0.76 \text{ seconds} \quad . \tag{166}$$

If the effects of (a) diluting the sample until its volume is quadrupled, of (b) the water relaxation, and of (c) the extractable iron are all included, one obtains as a final estimate

$$T_{1(LS)} = 0.83 \text{ seconds} \quad .$$

This agrees with the 600 G data for Ludox LS at pH 9 and at 22°C. The

results of the preceding calculations, as well as of a similar set for HS-40, are summarized in Table VII. The value of T_1 estimated for 12% HS-40 agrees with data obtained at 1 G and at pH 1.2.

TABLE VII

CALCULATED PROTON T_1 DUE TO THE PRESENCE OF IRON IMPURITIES

Sample Type	T_1 Due to Extractable Iron	T_1 Due to Exposed Iron[1]	Estimated T_1
Unmodified LS	0.44 sec	0.76 sec	0.24 sec
Unmodified HS-40	0.079 sec	0.15 sec	0.051 sec
8% LS[2]	2.00 sec	3.48 sec	0.83 sec
12% HS-40	0.39 sec	0.76 sec	0.23 sec

[1]Note the 2:1 ratio between this and the preceding column.

[2]By weight of SiO_2.

ESR Experiments

Samples of Ludox LS and Ludox SM were dried and subjected to a standard ESR measurement of g. Both samples exhibited resonances at g = 2, 4.2 and 6. According to T. Castner, Jr., et al. (36), such resonances are typical of iron in the crystal lattice of SiO_2 and

cannot occur unless Fe^{+++} occupies the silicon lattice sites.[1]

We might also note that, after the present author's experiments were performed, D. Geschke reached a nearly identical conclusion in his experiments with a colloidal silica of German manufacture. To quote from his paper (37), "A line with a g-value of approximately 4.3 points to a strong crystoelectric field of low symmetry. One such crystal field is probably associated with the layer especially near to the paramagnetic centers. ..."[2] In other words, it is quite reasonable to explain the ESR measurements as arising from iron which has been substituted for silicon in an environment of such low symmetry that one can take the sample to be an essentially amorphous compound. It is also reasonable to assume that the broad background in the ESR spectrum is due to interstitial iron, but that its solubility is such that the lattice iron must predominate (iron is soluble in silicon to a level of approximately 10^{16} atoms/cc, whereas in the colloids studied we found $\sim 10^{18}$ iron atoms/cc).

Relaxation in H_2O-D_2O Mixtures

The first PMR measurements related to water sorbed on SiO_2 were undertaken by Zimmerman, who demonstrated that the T_2 observed for a monolayer coverage on silica gel could be described in terms of two distinct environments (5). The exchange of water protons between these two environments was apparently slow enough that two values of T_2 could

---

[1] In considering this result, one must remember that surface Fe^{3+} is ordinarily not visible to ESR. Due to the large electric field gradients expected near the surface, the level splitting becomes too large to observe.

[2] Present author's translation.

be measured, one for each environment. Zimmerman estimated the environmental lifetime of a typical proton as 10^{-3} sec, and both the intra and inter-molecular dipole-dipole interactions were considered to be dominant. One of the major difficulties encountered in the Zimmerman interpretation was the fact that the temperature dependence of T_1 and T_2 in one of the (assumed) environments was not consistent with a simple dipole-dipole interaction.

In a later extension of Zimmerman's work, D. E. Woessner attempted to resolve the problem on the basis that isotropic tumbling of the adsorbed molecules was not to be expected (38); he therefore developed a model which allowed the inclusion of the effects of anisotropic rotation into the dipole-dipole interaction, and found that the effect of the anisotropy was nearly identical to the one to be expected in the presence of multiple environments. His model seemed to resolve the entire difficulty and was temporarily adopted as the "correct" one.

Recently, D. Michel suggested that the preceding authors may have overlooked the very important possibility of the presence of paramagnetic impurities (39). If such impurities were in fact present, the experimental results may be explainable without the use of Woessner's rather complicated model. As a matter of fact, Michel has shown, through a series of D_2O dilution experiments, that in a number of colloidal silicates of German manufacture the relaxation is almost completely due to paramagnetic impurities. Since Zimmerman dna Woessner mentioned no tests for paramagnetic centers, one can only assume that the possibility was overlooked. In view of the fact that O'Reilly had previously demonstrated the importance of paramagnetic centers in a similar situation (40), this seems to be an unfortunate omission.

The present author has also been able to demonstrate the dominance of paramagnetic impurities in Ludox colloidal silica. This work, depending essentially upon D_2O dilution, was performed at the same time Michel was carrying out his experiments and is discussed in the following paragraphs.

Let an H_2O-D_2O mixture be characterized by a "dilution parameter" α, defined as follows:

$$\alpha = \frac{V_{H_2O}}{(V_{H_2O} + V_{D_2O})} \tag{167}$$

where V_{H_2O} and V_{D_2O} represent the volumes of ordinary and heavy water, respectively. Abragam (1) states without proof that, in an H_2O-D_2O mixture, the observed proton T_1 is given by the formula

$$\frac{1}{T_{1(obs)}} = \alpha \cdot (1 - R) \cdot \frac{1}{T_{1(H_2O)}} + R \frac{1}{T_{1(H_2O)}} \tag{168}$$

where $R = 0.042$ and where $T_{1(H_2O)}$ is the value of T_1 obtained in pure water. Because the proof of this result is not readily available, it is included in Appendix B.

Where H-H and H-D couplings are the only ones present, it is to be expected that there will be a linear dependence of $1/T_{1(obs)}$ upon α. Conversely, if this linear dependence is not in evidence, one has an indication that other relaxation mechanisms are important (isotope effects sometimes make the results difficult to interpret, however). In particular, where paramagnetic impurities dominate strongly, one expects $1/T_{1(obs)}$ to be independent of α.

If a proton has more than one environment available to it, as in the case where it can occupy a site in the first hydration sphere of a

paramagnetic ion, it is possible that the substitution of deuterons for protons will disturb the original equilibrium which was established between the bulk liquid and the hydration sphere. Such isotope effects can be due to a change in the zero-point vibrational energy or to a difference in the tunneling rate across hydrogen bonds (41). In the present situation, we are therefore forced to consider the possibility that the parameter α may not be the same near the surface of a colloidal particle as it is in the bulk liquid. Toward that end, let H_S and H_B be the concentration of protons in the surface and bulk, respectively, (expressed as number per unit of bulk volume) and let D_S and D_B represent the deuteron concentration in each environment. One can then use chemical rate equations of the form

$$\dot{D}_S = -k'_{SB} D_S + k'_{BS} D_B \tag{169}$$

$$\dot{H}_S = -k'_{SB} H_S + k_{BS} H_B \tag{170}$$

where the dots indicate time derivatives, and where k's are rate constants, to obtain

$$\frac{D_S}{H_S} = \frac{k'_{BS} k_{SB}}{k'_{SB} k_{BS}} \cdot \frac{D_B}{H_B} = K \frac{D_B}{H_B} \quad . \tag{171}$$

Of course K is a true constant only at a fixed pH and temperature. The appropriate values of α are given by

$$\alpha_B = \frac{H_B}{H_B + D_B} \tag{172}$$

$$\alpha_S = \frac{H_B}{H_B + K D_B} \tag{173}$$

and one can rearrange the preceding equations to obtain

$$H_B(\alpha_B - 1) + D_B\alpha_B = 0 \tag{174}$$

$$H_B(\alpha_S - 1) + D_BK\alpha_S = 0 \quad . \tag{175}$$

If a non-trivial solution is to be obtained, one must have

$$\alpha_S = \frac{\alpha_B}{\alpha_B(1 - K) + K} \tag{176}$$

and this is the required relation between α_S and α_B.

In order to compute the proton T_1 which should be observed under D_2O dilution, we must also obtain an expression for the probability of finding a proton in the "surface" environment of the sol.[3] Under the assumption of rapid exchange, the equation derived in Chapter II can be combined with the one presented by Abragam to yield

$$\frac{1}{T_{1(obs)}} = \frac{P_S\alpha_S}{T_{1(S)}} + \frac{P_S}{T'_{1(S)}} + \frac{\alpha_B}{T_{1(B)}} + \frac{1}{T'_{1(B)}} \tag{179}$$

where

$T_{1(obs)}$ = measured proton T_1;

$T_{1(S)}$ = proton T_1 in surface due to dipole-dipole interaction;

$T'_{1(S)}$ = proton T_1 in surface due to paramagnetic impurities;

$T_{1(B)}$ = proton T_1 in bulk due to dipole-dipole interaction;

$T'_{1(B)}$ = proton T_1 in bulk due to dissolved paramagnetic oxygen;

P_S = probability that a given proton is in the "surface" environment.

---

[3] It is not possible to distinguish a "surface" paramagnetic impurity from one in the bulk; therefore, the term should not be interpreted literally.

In addition to the rapid exchange assumption, we have also taken $P_B \approx 1$ and $R \approx 0$ (see Equation 49). If V_S and V_B are the volumes of the surface and bulk phases, respectively, it can be shown that

$$P_S = \frac{V_S}{V_S + V_B[\alpha_B(1 - K) + K]} \quad . \tag{180}$$

If one starts out with an undeuterated sol, and then adds a volume of D_2O given by V_{ADD}, he will have

$$\frac{V_S}{V_B} = \frac{V_S}{V_{BO} + V_{ADD}} \tag{181}$$

and

$$\alpha_B \triangleq \frac{V_{BO}}{V_{BO} + V_{ADD}} \tag{182}$$

where V_{BO} is the original sample volume. Therefore

$$\frac{V_S}{V_B} = \frac{V_S}{V_{BO}} \alpha_B \tag{183}$$

and if $V_S << V_B$, one obtains the following expression for P_S from Equations 180 and 183:

$$P_S = \frac{V_S}{V_{BO}} \cdot \frac{\alpha_B}{\alpha_B(1 - K) + K} = P_{SO}\alpha_S \quad . \tag{184}$$

Inserting this expression into Equation 179, we obtain the final result that

$$\frac{1}{T_{1(obs)}} = \frac{P_{SO}\alpha_S^2}{T_{1(S)}} + \left(\frac{P_{SO}\alpha_S}{T'_{1(S)}} + \frac{\alpha_B}{T_{1(B)}}\right) + \frac{1}{T'_{1(B)}} \quad . \tag{185}$$

Therefore, if an experiment yields a linear relation between $T_{1(obs)}^{-1}$ and α_B, one is forced to assume that the first term is negligible and that $K \approx 1$. But, if the first term is negligible, the dipole-dipole interaction cannot be dominant in the environment labeled "s". This is precisely the situation which is encountered during the deuteration of Ludox LS.

In order to obtain these data, two samples of Ludox LS were carried through the deuteration procedure; one served as a control sample and was diluted with ordinary distilled water. Because the EFFP apparatus was not equipped with a temperature control, and further because the sample-containing coil was exposed to the local weather, it was necessary to preset the sample to some temperature near ambient. The prevailing weather conditions were such that 40°C seemed to be a reasonable choice (temperatures were in the region of 100°F). The sample temperature was monitored at all times and did not change more than $\pm$ 1°C during any set of measurements. Where smaller samples produced an acceptable S/N, an unsilvered Dewar flask was used as a sample container.

At low proton concentrations (i.e., small values of α), the free-precession signal is obscured by noise, and for that reason no attempts were made to obtain data from samples characterized by an α smaller than 0.22.

T_1 was also obtained as a function of field, and, at each field, up to six independent measurements were made with α held constant. If we were to report each measurement, we would have to list 168 values for T_1; if we were to list each data point (and five were used to determine T_1), we would have to list more than 1680 numbers, excluding such items as E_∞, etc. Obviously, such an attempt would be impractical, and we can

only report condensed tables of results. This will be the approach to be used throughout the remainder of this thesis, since it is physically impossible to do otherwise. It is hoped that the reader will understand that all subsequent data reported in this thesis were similarly condensed.

In order to perform the present experiment, we used D_2O whose purity exceeded 99% by weight. A sample of unmodified Ludox LS was diluted in several steps and the value of $T_{1(obs)}$ and $T_{2(obs)}$ was plotted as a function of α (V_{BO} was taken to be the original volume of the liquid phase, and was obtained from Equation 131). The resulting data were fitted to both a first degree and a second degree polynomial by means of a standard least-squares technique. Table VIII shows the results of the measurements, as well as the values of the coefficients obtained, and Figure 9 shows the data in graphical form, including the least-squares fit. Because the graph would be cluttered if all data were included, we have shown only the results at 0.89 G, 3.4 G, and 390 G. Note that the 0.89 G data are the only ones which exhibit noticeable curvature. It is our contention that the quadratic fit is the best one for this particular case since, as the table shows, a linear fit does not pass sufficiently close to the point (0,0).[4] An attempt to obtain a cubic fit results in the equation

$$\frac{1}{T_{1(obs)}} = 4.92\alpha^3 - 8.02\alpha^2 + 7.37\alpha - 0.697 \qquad (186)$$

and the negative intercept is unacceptable.

The quadratic fit is also quite reasonable in terms of the equation

[4]The point (0,0) was not included in the data to be fitted.

TABLE VIII

COEFFICIENTS OF LEAST SQUARES FIT TO D_2O DILUTION DATA WITH $T_1^{-1} = \sum_i a_i \alpha^{i}$ [1]

B_p	Linear Fit		Quadratic Fit			T_1^{-1} in sec^{-1}				
	A_0	A_1	A_0	A_1	A_2	α=1.0	0.88	0.45	0.66	0.22
376 G	Fitted Manually					1.50	1.29	0.675	0.900	0.355
112 G	-0.01	1.81	-0.17	2.48	-0.55	1.74	1.61	0.770	1.27	0.370
65 G	0.02	1.99	-0.19	2.92	-.715	2.00	1.72	0.910	1.49	0.425
35 G	0.03	2.26	-0.14	2.98	-0.59	2.24	2.02	1.03	1.61	0.500
21 G	-0.01	2.50	-0.25	3.49	-0.81	2.42	2.20	1.10	1.75	0.500
10 G	-0.07	2.88	-0.14	3.18	-0.25	2.78	2.50	1.23	1.85	0.555
3.4 G	-0.14	3.28	-0.18	3.45	-0.14	3.12	2.78	1.37	2.00	0.566
0.90 G [2]	-0.26	3.72	0.00	2.61	0.906	3.56	2.96	1.45	2.18	0.606

[1] Data are accurate to within 5%.

[2] This field is the vector sum of B_p and the earth's field.

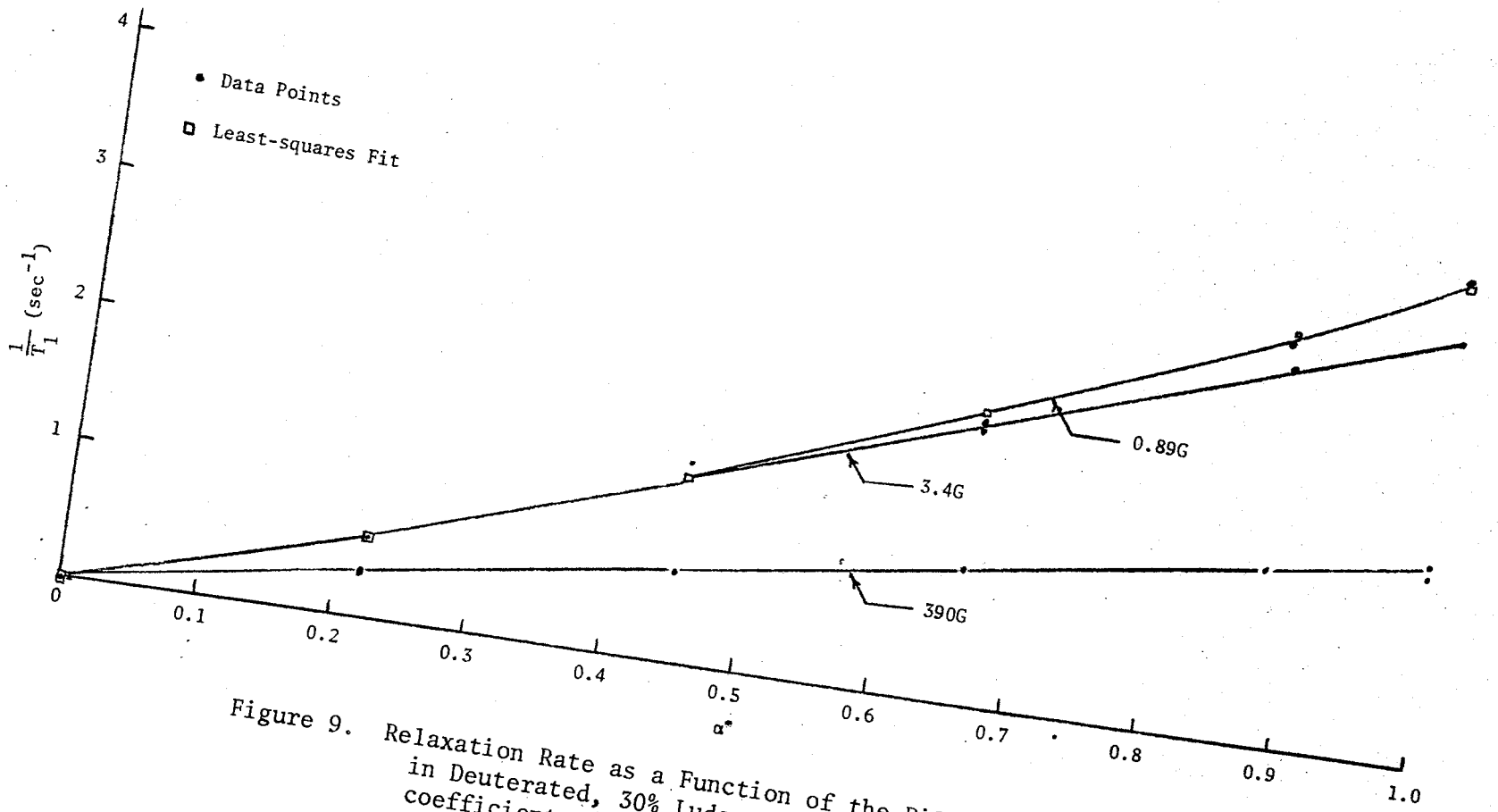

Figure 9. Relaxation Rate as a Function of the Dilution Parameter in Deuterated, 30% Ludox LS. See Table VIII for the coefficients of the least-squares fits.

previously developed, because it implies that, at very low fields, the environment labeled "s" is producing some dipole-dipole relaxation. Moreover, it is consistent with theory to expect such contributions to become important at low fields.

Curvature in the dilution plot does not in itself imply that dipolar contributions are important, since an examination of the preceding equations shows that a similar curvature can be expected when $K > 1$. However, since the curvature disappears at higher fields, and since K is independent of field,[5] one is forced to conclude that the preceding interpretation is correct.

By subtracting the relaxation rate for pure water at 40°C from the constant A, at 0.9 G, one can estimate that $P_{SO}/T'_{1(S)} = 2.61 - 0.29 = 2.32\ sec^{-1}$. Hence, $T'_{1(S)}/T_{1(S)}$ is 0.91/2.32 or 0.39 and one has

$$\frac{T_{1(S)}^{-1}}{T_{1(S)}^{-1} + (T'_{1(S)})^{-1}} = \frac{0.39}{1 + 0.39} = 0.28 \quad .$$

Thus, we estimate that the dipolar relaxation rate is roughly 28% of the total.

If the curvature of the 0.9 G plot is real, and is not the result of experimental error, some very interesting problems arise in trying to account for its disappearance at 10 G. However, this must be deferred to a later chapter where specific mechanisms for dipolar relaxation are discussed. For the present, it is sufficient to state that we have shown that paramagnetic impurities provide the dominant interaction at

---

[5] Strictly speaking, this is not true. However, the fields which are known to affect equilibrium constants are much larger than those produced here.

all but the very lowest of magnetic fields.

A Chelation Experiment

It has been observed that metal ions can combine with a large organic ion in such a way that the organic ion displaces all of the water that would normally be found in the first hydration sphere of the metallic cation (chelation). If the ion is paramagnetic, and if its influence on the water protons is being observed by NMR, it is quite possible that chelation will render the paramagnetic ions ineffective in producing proton relaxation. Therefore, one can use a suitable chelating agent such as EDTA as a test for the presence of such impurities.

Since the behavior of EDTA in the presence of a charged colloid was not predictable, it was necessary to examine its chelating ability in such a situation. For that reason, manganese ions were intentionally added to a sample of Ludox LS, diluted to 8% by weight of SiO_2, until the original high-field T_1 was reduced to roughly 10% of its initial value. As the data of Table IX show, the resulting "doped" sample had a proton T_1 which exhibited only a slight field-dependence. As the last column of the table shows, the addition of EDTA did not completely restore the original values of T_1, but it did restore the 2:1 field dependence.

In order to examine this effect further, two more samples were prepared, the first containing an identical concentration of EDTA in distilled water, and the second containing $MnCl_2$ and EDTA. The latter sample was doped with $MnCl_2$ until its T_1 was reduced to 0.2 seconds, whereupon EDTA was added in the amount of 0.044 g/ml. The results were (1) a field-independent T_1 of 3.47 seconds in the first sample, and (2)

a field-independent T_1 of 1.47 seconds in the second. Hence, we concluded that EDTA does not itself reduce the proton T_1 of water, and further, that EDTA does not completely shield the Mn ions. However, there was no evidence that the colloid interfered in any way with the normal behavior of EDTA, and that was our primary concern.

TABLE IX

ADDITION OF EDTA TO A SAMPLE OF LUDOX LS INITIALLY DOPED WITH $MnCl_2$[1]

Field	T_1 of Original Sample[2]	T_1 of Doped Sample	T_1 With EDTA Added[3]
540 G	1.90 sec	0.222 sec	1.36 sec
356 G	1.92 sec	0.218 sec	1.23 sec
155 G	1.90 sec	0.180 sec	0.870 sec
79.5 G	1.72 sec	0.173 sec	0.995 sec
41.4 G	1.56 sec	0.177 sec	0.963 sec
26.7 G	1.34 sec	0.167 sec	0.914 sec
12.8 G	1.19 sec	0.162 sec	0.876 sec
0.54 G	1.07 sec[4]	0.165 sec[4]	0.635 sec[4]

[1] $T = 40^{\circ}C$.

[2] pH = 9.

[3] 0.044 g EDTA.ml H_2O.

[4] T_2 in the earth's field.

A second problem, not recognized at the time these data were taken, must also be considered; namely, that the proton T_1 in Ludox tends to decrease with a reduction in pH. Because the addition of EDTA to an unbuffered sample results in a lowered pH, one could suspect that the last column of Table IX includes a pH effect. However, comparison with data taken at a later point quickly reveals that the pH must have remained above 6, where such changes are expected to be very small. Hence, the high-field colloid T_1 of 1.36 seconds appears to compare properly to the 1.47 second figure obtained with the test sample.

The addition of even more EDTA to the doped colloidal sample was observed to cause a decrease in the proton T_1 when the amount reached $\sim$ 0.1 g/ml. This was caused by the reduction of the sample pH and was eventually responsible for the discovery of a very interesting pH effect to be discussed later. As a result of this procedure, it was determined that the proton T_1 could not be increased any further and that the values reported in the last column of Table IX represent an upper limit.

The results of adding EDTA to a sample of 8% (by weight SiO_2) Ludox LS are shown in Table X. By comparing the figures given for sample I to those given for the original sample, it can be seen that the chelating agent had no measurable affect. In sample II there is some indication that, at higher fields, the value of T_1 may have been increased slightly, but it is not clear that the increase was due to chelation. The sample was unstable and was in the process of gelling. As will be shown later, gelling can produce an increase in the high-field T_1, and could be responsible for the results shown. We therefore conclude that, if paramagnetic impurities are present in the liquid phase, they are not sufficiently concentrated to be observable in a chelation experiment.

TABLE X

RESULTS OF CHELATION IN 8% BY WEIGHT SiO_2 LUDOX LS[1]

Field	Proton T_1 in Ludox LS With EDTA Sample I[2]	Proton T_1 in Ludox LS With EDTA Sample II[3]	Proton T_1 in Original Sample
510 G	2.07 sec	2.15 sec	2.03 sec
366 G	1.93 sec	2.28 sec	2.02 sec
162 G	1.92 sec	----	1.84 sec[4]
79.5 G	1.74 sec	----	1.70 sec
41.4 G	1.53 sec	1.46 sec at 32 G	1.53 sec
25.9 G	1.42 sec	----	1.42 sec
7.8 G	1.23 sec	1.26 sec at 15 G	1.24 sec

[1] $T = 40^{\circ}C$.

[2] 0.044 g/ml H_2O EDTA.

[3] 0.176 g/ml H_2O EDTA. Electrolyte caused sample to gel after several days. Results erratic.

[4] Computer indicated a probable error (high standard deviation).

A Washing Experiment[6]

Most of the iron group elements are highly soluble in an acidic medium at pH 2 or lower. Hence, it is possible to dry a colloidal silica and then to wash the solids left behind in order to extract those ions which are not intimately associated with the SiO_2. Because some

[6] See also Chapter IV.

compounds (such as ferric hydroxide) dissolve slowly, it is necessary to allow the sample to stand in concentrated acid for a sufficiently long time. In the present case, the solids obtained from Ludox LS[7] were allowed to stand in concentrated, reagent grade HCl for three days. They were then washed through filter paper with a series of HCl solutions of decreasing acidity. Finally, the liquid collected was diluted with distilled water until the volume of the original sample was obtained. The liquid was then examined by NMR.

It was found that the pH 1.30 sample had a T_1 at 440 G of 1.97 seconds. The 0.57 G T_2 was also 1.97 seconds,[8] and it was therefore concluded that T_1 was field-independent. Since a similar experiment with pH 1.30 HCl yielded a T_1 characteristic of pure water, it was also concluded that the result could not have been due to impurities introduced during the washing procedure (the sample was prepared by an identical series of steps, except that no solids were used).

A comparison of these values with the data included in Tables IX and X shows that they are typical of Ludox LS at high fields. Furthermore, unlike the original LS samples, this sample showed no field-dependence, and one can conclude that the field-dependence is somehow associated with the presence of the colloidal particles.

The remaining data which are to be discussed in this and in following chapters have a direct bearing upon the interaction mechanism(s) of importance. Therefore, it is necessary to briefly review the appropriate theory before proceeding.

---

[7]The original sample contained 8% by weight SiO_2.

[8]After correction for the field inhomogeneities discussed in Chapter II.

Nuclear Relaxation

From the previous material, it should be obvious that only two cases are of immediate interest, and they are: (1) the relaxation of water protons in a situation where the locally fluctuating magnetic fields are due only to the presence of other water protons; and (2) the relaxation of water protons in a situation where the local magnetic field is controlled by a nearby paramagnetic center. As has been previously stated, both the time scale of the locally fluctuating fields and the magnitude of these fields can influence T_1 or T_2.

To be a little more precise, the time scale of the local fluctuations is measured against the (average) time required for the nucleus of interest to precess about the externally applied magnetic field. If some of the Fourier components of the locally fluctuating field occur at or near the nuclear precession frequency, then energy may be exchanged between the spin system and the field, and T_1 is reduced. Additionally, if there is a steady component contained in the locally fluctuating fields (i.e., a zero-frequency Fourier component), the precession frequency itself will be affected, dephasing will occur, and the "phase memory time" T_2 will be reduced. If one changes the externally applied magnetic field B_0 he also changes the time scale which determines T_1. If it is in fact true that only the Fourier components of the fluctuating fields near γB_0 (the precession frequency) can affect T_1, one can "probe" the spectrum by altering B_0 and recording T_1 at each applied field. If a theory is also available which predicts the form of the locally fluctuating magnetic field, then one is in a position to use the experimental results to infer the magnitude of certain constants which are included in the theory.

It is reasonable to surmise that the fluctuating fields are produced, at least in part, by the relative motion of the magnetic dipoles making up the system. Therefore, an alteration of the temperature of the system can be expected to produce changes in both T_1 and T_2, and may afford yet another method for "probing" the character of the dominant interaction.

Since chemical exchange of atoms between molecules can also control the relative motion of the important magnetic dipoles, it is to be expected that, in aqueous media, the pH may also influence T_1 and T_2. Moreover, it is known that the magnitude of a dipole-moment is sometimes sensitive to the chemical environment in which it is found, since changes in the atomic valence state can for example cause a normally diamagnetic atom to become paramagnetic. Hence, alterations in the chemistry of a system may also be expected to change T_1 or T_2. In the following material, the influence of each of these variations will be discussed, but, at the present time we wish to present the specific theoretical framework.

The Correlation Time

Let us suppose that the position of some nuclear dipole can be specified as a function of time f(t). After τ seconds have elapsed, the new coordinates will be given by $f(t + \tau)$, and by using the function at these two different times one can define a correlation function $\phi(\tau)$ as[9]

---

[9]More properly, this is called the auto-correlation function of f(t).

$$\phi(\tau) = \lim_{T\to\infty} \frac{1}{T} \int_{-T/2}^{T/2} f(t)\ f(t+\tau)dt \quad . \tag{187}$$

In general, f(t) is not known, but statistical arguments can be employed to show that, for motion which either follows a diffusion equation or which represents a stationary random process

$$\phi(\tau) = K \exp\left(\frac{-|\tau|}{\tau_d}\right) \tag{188}$$

where K and τ_d are constants which are characteristic of the system. The latter constant (τ_d) is a measure of how long a particular coordinate position persists and has come to be called the translational correlation time. It is most often determined by experiment.

If more than one random process can be present in a given system, more than one correlation time may be defined; this is the situation which is encountered in most NMR experiments (e.g., rotational tumbling and translational diffusion may often be considered to be independent of one another), but the way in which these correlation times combine depends upon the nature of the processes being considered. If they are competing processes, then

$$\phi(\tau) = K \exp\left(-|\tau| \sum_i \tau_i^{-1}\right) \tag{189}$$

and the shortest correlation time dominates. If they are independent, then

$$\phi(\tau) = \sum_i K_i \exp\left(\frac{-|\tau|}{\tau_i}\right) \quad . \tag{190}$$

In their more usual form, such correlation functions are defined so that $\phi(0) = 1$. Hence

$$\sum_i K_i = 1 \quad . \tag{191}$$

The utility of these functions lies in the fact that, if f(t) describes the local field at a typical spin (rather than merely its position) as a function of the orientation and/or the position of all other spins, one can obtain the reduced spectral density of the locally fluctuating fields from the expression

$$S(\omega) = \int_{-\infty}^{\infty} \exp\ (i\omega\tau)\ \phi(\tau)d\tau \qquad (192)$$

where $S(\omega)$ is the Fourier transform, or spectrum of the function $\phi(\tau)$. If the "standard form" for $\phi(\tau)$ is assumed, then this integral is easily evaluated to give

$$S(\omega) = 2 \sum_i \frac{K_i\ \tau_i}{1 + \omega^2\ \tau_i^2} \quad . \qquad (193)$$

Note that, at this point, no specific interaction mechanism has been assumed. Its introduction determines the relationship between $S(\omega)$ and T_1 or T_2; additionally, it determines the K_i. The form of $S(\omega)$ is predetermined by the assumption of a stationary random process, and, as long as this is a valid assumption, it must be the same in any interaction.

Nuclear Relaxation in Water

One can assume that the locally fluctuating magnetic field at one water proton is due to the random motion of the nearest neighboring dipoles (e.g., the "other" proton attached to the same water molecule). This motion includes diffusion and rotation, and, if the standard dipolar field is used to calculate f(t), one obtains

$$\phi(\tau) = k_d \exp\ (\frac{-|\tau|}{\tau_d}) + k_r \exp\ (\frac{-|\tau|}{\tau_r}) \qquad (194)$$

with $k_d = 0.1$ and $k_r = 0.9$ (42). Here, the subscripts d and r refer to diffusion and rotation, respectively.

For isotropic motion, T_1 is related to $S(\omega)$ through the expression

$$T_1^{-1} = \frac{1}{3} m^2 \left[S(\omega) + 4\, S(2\omega)\right] \tag{195}$$

where m^2 is the mean squared dipolar field at a typical nuclear site. By combining the previous expressions, one finds that T_1 is composed of a diffusional and a rotational part such that

$$T_1^{-1} = T_{1d}^{-1} + T_{1r}^{-1} \tag{196}$$

with

$$T_{1d}^{-1} = \frac{2}{3} k_d\, m^2 \left[\frac{\tau_d}{(1 + \omega^2\tau_d^2)} + \frac{4\tau_d}{(1 + 4\omega^2\tau_d^2)}\right] \tag{197}$$

and

$$T_{1r}^{-1} = \frac{2}{3} k_r\, m^2 \left[\frac{\tau_r}{(1 + \omega^2\tau_r^2)} + \frac{4\tau_r}{(1 + 4\omega^2\tau_r^2)}\right] \tag{198}$$

These expressions are typical of those obtained with nearly any magnetic interaction, although many of them can be considerably simplified through a knowledge of the relative sizes of the constants involved. In the case of the previous expressions, for example, it is known that even at the highest magnetic fields available in the laboratory

$$\omega^2\tau_r^2, \quad \omega^2\tau_d^2 \ll 1 \tag{199}$$

so that one obtains

$$T_1^{-1} \doteq T_{1r}^{-1} \tag{200}$$

whereas for T_2

$$T_2^{-1} \doteq T_{2d}^{-1} = k_d\, m^2[\tau_d + (\tfrac{5}{3})\, \tau_d/(1 + \omega^2\tau_d^2) + (\tfrac{2}{3})\, \tau_d/(1 + 4\omega^2\tau_d^2)] \qquad (201)$$

again, $\omega^2\tau_d^2 << 1$, so that one can write

$$T_2^{-1} = T_1^{-1} \qquad (202)$$

The preceding expressions illustrate the fact that T_1 and T_2 become field-dependent whenever the product of the angular precession frequency by some correlation time approaches unity. In the case of pure water, the required precession frequency is so high that T_1 and T_2 are field-independent for all achievable fields.

It has not been the writer's intent to derive the important interaction equations since those derivations are already available in many standard sources. Rather, it was his intention that the concept of a correlation time be briefly reviewed in order that the point could be made that, because of certain assumptions about $\phi(\tau)$, the form of $S(\omega)$ is fixed and in turn controls the form (at least in the present case) of the theoretical expressions for T_1 and T_2. Furthermore, we wish to point out that, where a field-dependence exists, one can always use expressions such as those just given in order to determine τ and $k\, m^2$. Hence, the expression introduced in the second chapter is expected to fit a wide variety of field-dependence data, and the least-squares procedure discussed there is expected to yield meaningful data.

Temperature-dependence of T_1 and T_2

A change in the thermal environment most often manifests itself through a change in τ, although in some cases the factor $k\, m^2$ may change

also. The simplest theory arises from the empirical Arrhenius expression which gives τ as

$$\tau = \tau_0 \exp\left(\frac{H}{RT}\right) \tag{203}$$

where τ_0 is the so-called "pre-exponential factor", H is the activation enthalpy (often incorrectly called the activation energy), T is the absolute temperature, and R is the universal gas constant. τ_0 may be further expanded in the form

$$\tau_0 = \nu^{-1} \exp\left(\frac{-S}{R}\right) \tag{204}$$

where ν is the "frequency factor" and S is the activation entropy. In more refined theories H and S are associated with a change to a transition state (the activated complex) rather than with the difference between the initial and final states; it has become more or less standard to denote that activated state theory is being used by modifying the symbols to read $\Delta H^{\ddagger}$ and $\Delta S^{\ddagger}$. Thermodynamic arguments have been invoked to show that the factor τ_0 is actually temperature-dependent -- a result also obtained from statistical quantum mechanics with the result that $\nu = kT/h$ (43). However, the dependence is so slight that, over experimentally accessable temperature ranges, its presence may be ignored.

A second method of calculating τ (and hence T_1) has been to use the modified Debye formula

$$\tau = \frac{4\ \pi a^3 \eta}{3kT} \tag{205}$$

where a is the "molecular radius" and η is the viscosity. This formula was derived for a sphere of radius "a" tumbling in a liquid of viscosity η but, nevertheless, gives surprisingly good results. η is given by an

expression similar to Equation 203, so that the temperature appears twice, and the Debye formula does not agree with Equation 203, unless the temperature-dependence of τ_0 is included. However, over most accessible temperature ranges, it is not possible to see the curvature in a $\ln\tau$ vs. T^{-1} plot, and one cannot select a particular approach as being "correct". Finally, we note that an even more elaborate formula has been evolved by Cohen and Turnbill (44), which has

$$\tau = a^2(3ua^*)^{-1} \exp\{gv^*[\bar{v}_m\,\alpha(T - T_0)]^{-1}\} \quad , \qquad (206)$$

where $a^* = 6v^*/\pi$ is the diameter of a critical hole in the liquid, g is an overlap constant ≤ 1, $\bar{v}_m$ is the average molecular volume, T_0 is the glass temperature, T is the absolute temperature, α is the average value of the coefficient of thermal expansion, m is the molecular mass, and

$$u = \left(\frac{kT}{m}\right)^{\frac{1}{2}} \quad .$$

Typically, the very first expression given is inserted into the appropriate formula for T_1 or T_2 to obtain the temperature-dependence. The more elaborate theories are used only when this procedure completely fails and in the present study they were not required.

Relaxation Near Paramagnetic Centers

For dipolar coupling to unlike spins S, T_1 is given by (39)

$$T_{1\,dip}^{-1} = \frac{4}{30}\frac{S(S+1)\gamma_I^2 g^2\beta^2 P}{r^6}\left[\frac{\tau_{c2}}{1+(\omega_I-\omega_S)^2\tau_{c2}^2} + \frac{3\tau_{c1}}{1+\omega_I^2\tau_{c1}^2} + \frac{6\tau_{c2}}{1+(\omega_I+\omega_S)^2\tau_{c2}^2}\right] \qquad (207)$$

and T_2 is given by

$$T_{2\,dip}^{-1} = \frac{4}{60}\frac{S(S+1)\gamma_I^2 g^2 \beta^2 P}{r^6}\left[4\tau_{c1} + \frac{\tau_{c2}}{1+(\omega_I-\omega_S)^2\tau_{c2}^2} + \frac{3\tau_{c1}}{1+\omega_I^2\tau_{c1}^2} + \frac{6\tau_{c2}}{1+\omega_S^2\tau_{c2}^2} + \frac{6\tau_{c2}}{1+(\omega_I+\omega_S)^2\tau_{c2}^2}\right] \tag{208}$$

with $\tau_{c1,2}^{-1} = \tau_r^{-1} + T_{1,2e}^{-1} + \tau_h^{-1}$, and where τ_r is the rotational correlation time of the paramagnetic center, $T_{1,2e}$ the (two) relaxation times of an electron spin, and τ_h is the mean lifetime of the spin I (the one under observation) in the presence of the spin S. In addition, S is the spin quantum number of the paramagnetic center, γ_I is the magnetogyric ratio of the nucleus under observation, g is the Landé g factor, β the Bohr magneton, and P is the probability that the spin I is in the vicinity of the spin S.

In addition to the dipolar interaction, it is also possible for the spin I to relax due to the presence of the so-called isotropic spin exchange interaction. In this case, T_1 and T_2 are given by (39)

$$T_{1\,ex}^{-1} = \frac{2}{3}S(S+1)\left(\frac{A}{h}\right)^2 P\,\frac{\tau_{e2}}{1+(\omega_I-\omega_S)^2\tau_{e2}^2} \tag{209}$$

$$T_{2\,ex}^{-1} = \frac{1}{3}S(S+1)\left(\frac{A}{h}\right)^2 P\left[\tau_{e1} + \frac{\tau_{e2}}{1+(\omega_I-\omega_S)^2\tau_{e2}^2}\right] \tag{210}$$

with $\tau_{1,2e}^{-1} = T_{1,2e}^{-1} + \tau_h^{-1}$, and where A is the scalar coupling constant. Since both interactions may be operative, one uses

$$T_1^{-1} = T_{1\,dip}^{-1} + T_{1\,ex}^{-1} \tag{211}$$

and

$$T_2^{-1} = T_{2\,dip}^{-1} + T_{2\,ex}^{-1} \tag{212}$$

to compute the final relaxation rate. Additionally, since $\omega_S = 650\ \omega_I$, one can effect a considerable simplification of the preceding expressions by neglecting ω_I wherever it appears with ω_S. A further simplification is possible by noting that $\tau_c \gtrsim 10^{-11}$ sec, so that $\omega_I \tau_c << 1$ in most cases. If the frequency is sufficiently low, so that $\omega_S \tau_e << 1$, these expressions predict that $T_1 = T_2$.

Localized Dephasing

The field about which the spin I precesses may be very different than the externally applied field (B_0), when it is in the vicinity of a paramagnetic ion. In the case of an aqueous solution of paramagnetic ions, this may provide an additional mechanism for proton dephasing. Those water protons which exchange with protons in the hydration sphere of a paramagnetic ion can lose phase coherence with the majority water protons. If the exchange is sufficiently rapid, the net effect will be to reduce T_2, since the bulk protons will lose coherence with the average phase more rapidly than would normally be expected.

For "spin-only" ions (i.e., those whose orbital angular momentum is quenched) N. Bloembergen has shown that the fractional change in the angular resonance frequency is given by (45)

$$\frac{\Delta\omega}{\omega} = -S(S+1)\ \frac{\gamma_e A}{3kT\gamma_n} \tag{213}$$

where ω is the undisturbed resonance frequency in pure water, $\Delta\omega$ is the shift upon entering the paramagnetic hydration sphere, and γ_e and γ_n are the electronic and protonic magnetogyric ratios, respectively. The other symbols have their previous meaning.

If $\tau_h^{-1} >> \Delta\omega$ and if $\Delta\omega^2 >> (T_{2h}\tau_h)^{-1}$, where T_{2h} is the transverse relaxation time due to the presence of the paramagnetic ion, one finds from the material at the end of Chapter II that

$$T_{2h}^{-1} = P\tau_h\Delta\omega^2 \tag{214}$$

or

$$T_{2h}^{-1} = P_h[S(S+1)\frac{\gamma_e A B_0}{3kT}]^2 \quad . \tag{215}$$

Therefore, as the field B_0 increases, T_{2h} is expected to decrease -- an opposite effect to that normally observed and, as a result, an indication that this so-called "$\Delta\omega$-effect" is in operation. Under the previous assumptions, one also finds that the apparent resonance frequency of the bulk water protons is shifted by an amount $\Delta\omega_a$ given by

$$\Delta\omega_a = -P\Delta\omega \quad . \tag{216}$$

Since P is typically on the order of 10^{-4} - 10^{-6}, the shift may be quite small.

Moderately Long τ_h

As a final item of discussion, we also take note of the fact that when τ_h is of the same order of magnitude as T_1 or T_2, the previous expressions must be of the form

$$T_{1,2}^{-1} = \frac{P}{(T_{1,2}' + \tau_h)} \quad . \tag{217}$$

In this situation, one can have a T_1 which decreases with increasing temperature.

Relaxation Mechanisms in Ludox

Having briefly reviewed the interactions which the preliminary experiments indicated should be important in the Ludox series of colloidal silicas, we wish to present some further experiments which can be directly related to the expressions just presented. Because the most important series of experiments -- the pH dependence of T_1 in Ludox LS and HS -- requires a rather lengthy presentation, it seems appropriate to devote the better part of the next chapter to it.

CHAPTER VI

SYSTEMATIC EXPERIMENTAL INVESTIGATIONS

Some Preliminary Remarks

Since both Ludox LS and Ludox HS show a strong field-dependence in the range accessible to the EFFP apparatus, it is possible to use the techniques described in Chapter II to obtain a least-squares fit to the data. However, there are some additional points which must be considered before one embarks on such a course.

The first of these is, of course, the question of the validity of the function used to fit the data. Since, as we have indicated in Chapter V, the form of the field-dependence is largely established by the assumption of a stationary, random process, it is to be expected that in any simple situation (one dominant $J(\omega)$) the constants derived from our procedure will be meaningful. Having established that $T_1(\omega)$ can be described by a particular function, it then remains to identify that function as characteristic of a particular interaction.

The second question which arises has to do with the possibility that the EFFP apparatus does not really reveal the entire field-dependence of T_1. In order to dispose of that possibility, we had to resort to other equipment, capable of reaching fields far above our 600 G maximum. These results are reported in the next section, where it will be shown that the EFFP apparatus did obtain most of the important field-dependence information.

Field-dependence in Unmodified LS and HS

It has been previously established that the proton relaxation rate can be expressed as a rate per unit surface area and per unit volume (see Figure 8), thereby eliminating the particle concentration as an important parameter. The measurements reported here are therefore expressed in these terms, after correction for the relaxation due to bulk H_2O.

Figures 10 and 11 show the (typical) field-dependence of T_1 for both Ludox LS and HS over a range of fields extending from 1 G to 14 KG. It is evident from these data that there is no significant field-dependence above 1000 gauss (the lowest field readily available to a commercial instrument) and that, at temperatures above 30°C, the EFFP apparatus could be relied upon to give the important information. Furthermore, it is evident that only the EFFP device could have yielded the entire field-dependence -- a rather fortunate result.

The Field-dependence of T_2

Table XI also shows that we obtained some isolated measurements of T_2 as a function of field. Of particular interest is the fact that, after T_2 has increased with increasing field, it may actually reverse its behavior and begin to decrease as the field strength continues to rise. Since this type of field-dependence is not predicted by any of the "standard" interactions, it allows one to make only a very limited selection of possible mechanisms. We shall discuss those mechanisms in the next chapter.

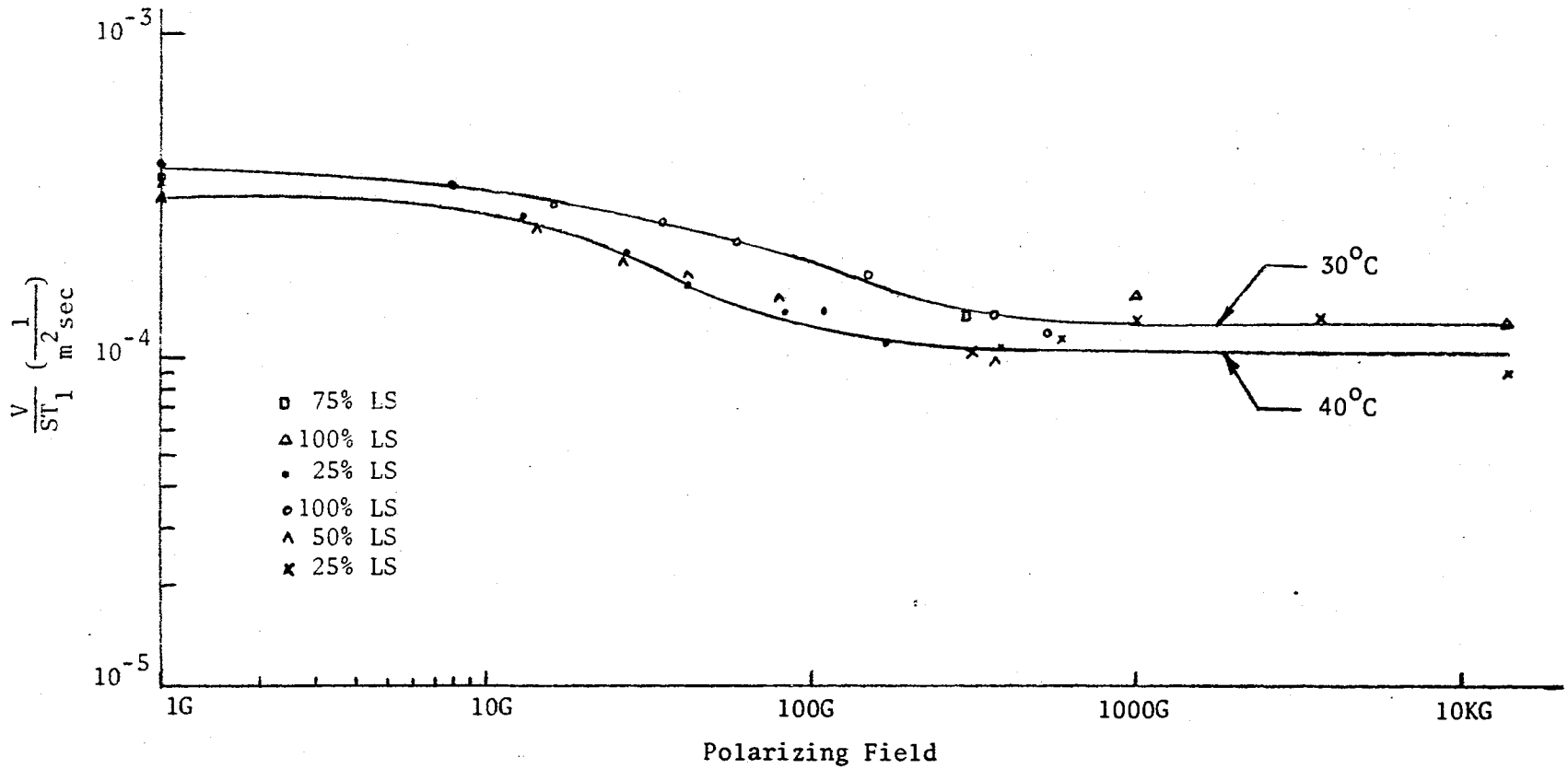

Figure 10. The Reduced Relaxation Rate in pH 9 Ludox LS as a Function of Field. The data were obtained from several instruments.

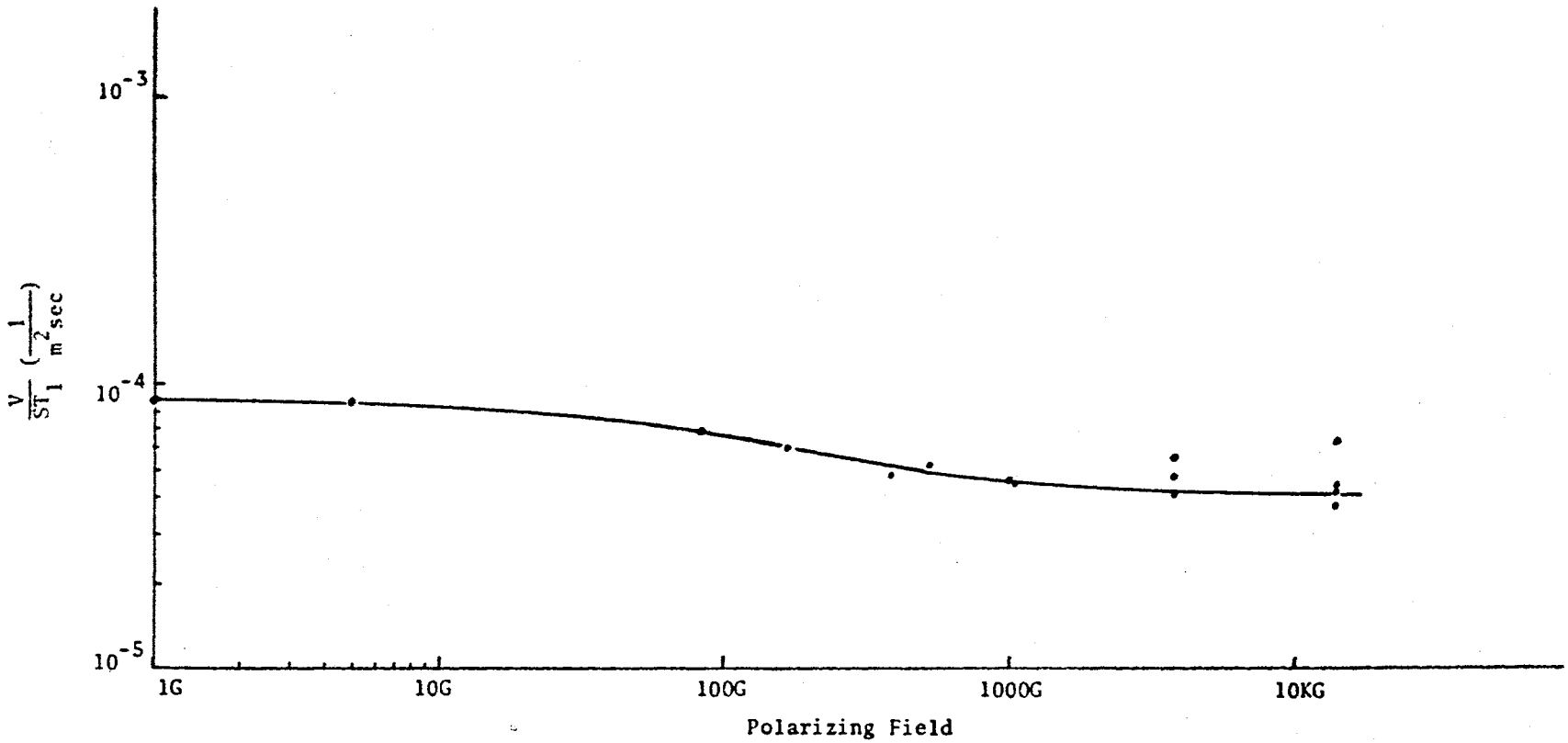

Figure 11. The Reduced Relaxation Rate in pH 9.5 Ludox 4HS as a Function of Field. The data were obtained from several instruments. The sample temperature was 30°C.

TABLE XI

DATA OBTAINED BY PULSED NMR

Sample	4.3 MHz (1010 G)					15.4 MHz (3730 G)			60 MHz (14,100 G)			
	D[3]	T_2	T_1	V/ST_2	V/ST_1	T_1	V/ST_1	T_2	T_1	V/ST_2	V/ST_1
HS-40	1.0	118MS	133MS	5.15×10^{-5}	4.57×10^{-5}	97MS		65MS	128MS	9.36×10^{-5}	4.76×10^{-5}
HS-40	0.25	515	550	4.62	4.32	440		290	557	8.15	4.24
HS-40	0.25	450	520	5.37	4.65			250	530	9.60	4.53
HS-40+D_2O	0.25	600	618					290	595		
HS-40 GEL[1]	0.75	134	180	6.35	4.73	203		72	217	11.6	3.85
LS	1.0	360	550	2.40	1.57	428		230	638	3.54	1.28
LS	0.25	1.23 sec	1.42 sec	1.52	1.32	1.42 sec		920	1.66 sec	14.1×10^{-6}	7.83×10^{-6}
LS	0.25	1.16	1.45	1.55	1.24			855	1.62	16.3	8.61
LS+D_2O	0.25	1.8	2.17					1.22 sec	2.4		
LS GEL[1]	0.75	53MS	750MS	20.1	1.42×10^{-5}	750MS		55MS	810MS	18.5×10^{-5}	1.26×10^{-5}
LS GEL[2]	0.41	95	1080		2.14	1000		87	1060		
SM GEL[2]	0.50	380	880	4.93	2.13	1030		250	1070	6.41	1.50

[1]pH = 3.99

[2]pH = 3.40

[3]Dilution factor discussed in the text (p. 123).

Data Reduction

It is worthy of mention that, although many of the samples represented in these figures had very different particle concentrations, the procedure of using the dimension "liters per m^2 sec" produced data which were entirely consistent.

Since large volumes of data were reduced to this form, a small computer (an IBM 1620) was programmed to make the calculations. The procedure was as follows:

1. The data obtained by L. P. Koegeboehn (46) for the temperature dependence of T_1 in distilled water[1] were fitted to a linear equation, yielding

$$T_{1(H_2O)} = (7.05 \times 10^{-2})T + 0.65$$

where T is the temperature in ^{o}C. It was found that, in the range $20^{o}C$ to $80^{o}C$, this equation produced a $T_{1(H_2O)}$ which was consistent with both the accuracy of the Koegeboehn data and also with our ability to measure T_1 at high fields ($\pm$ 5%).

2. Using the preceding equation, the corrected rate was obtained from the usual expression

$$T_1^{-1} = T_{1(obs)}^{-1} - T_{1(H_2O)}^{-1}$$

where T_1^{-1} is the corrected relaxation rate and $T_{1(obs)}^{-1}$ is the observed rate.

3. A "dilution factor" D was calculated from the expression

---

[1] Includes dissolved O_2.

$$D = \frac{V_0}{(V_0 + V_{add})}$$

where V_0 is the volume of an unmodified colloid and V_{add} is the volume of distilled water added to it to make up the sample of interest.

4. The Heston expression (Equation 131) was modified in such a manner that the adjusted rate R (in liters per m^2 second) could be obtained from

$$R = \frac{(100 - 0.438\ C_1 D)}{(10^{-3} C_2\ D\ T_1)}$$

with

$$C_1 = \begin{cases} 52.4 \text{ g/100 ml for 4HS} \\ 36.4 \text{ g/100 ml for LS} \\ 16.4 \text{ g/100 ml for SM} \end{cases}$$

and

$$C_2 = \begin{cases} 1.19 \times 10^4 \text{ m}^2\text{/per 100 ml sol for 4HS} \\ 7.26 \times 10^3 \text{ m}^2\text{/per 100 ml sol for LS} \\ 6.15 \times 10^3 \text{ m}^2\text{/per 100 ml sol for SM.} \end{cases}$$

Because the resulting plots (in terms of R) tend to obscure the original measurements of T_1, they were only used when it was found inconvenient to do otherwise.

The pH-dependence of T_1

Figures 12 and 13 summarize the results obtained with both Ludox LS and Ludox 4HS as samples were made progressively more acidic. The range of pH values was dictated by the fact that at pH 10 or higher the colloidal particles begin to dissolve; whereas to reach pH values below

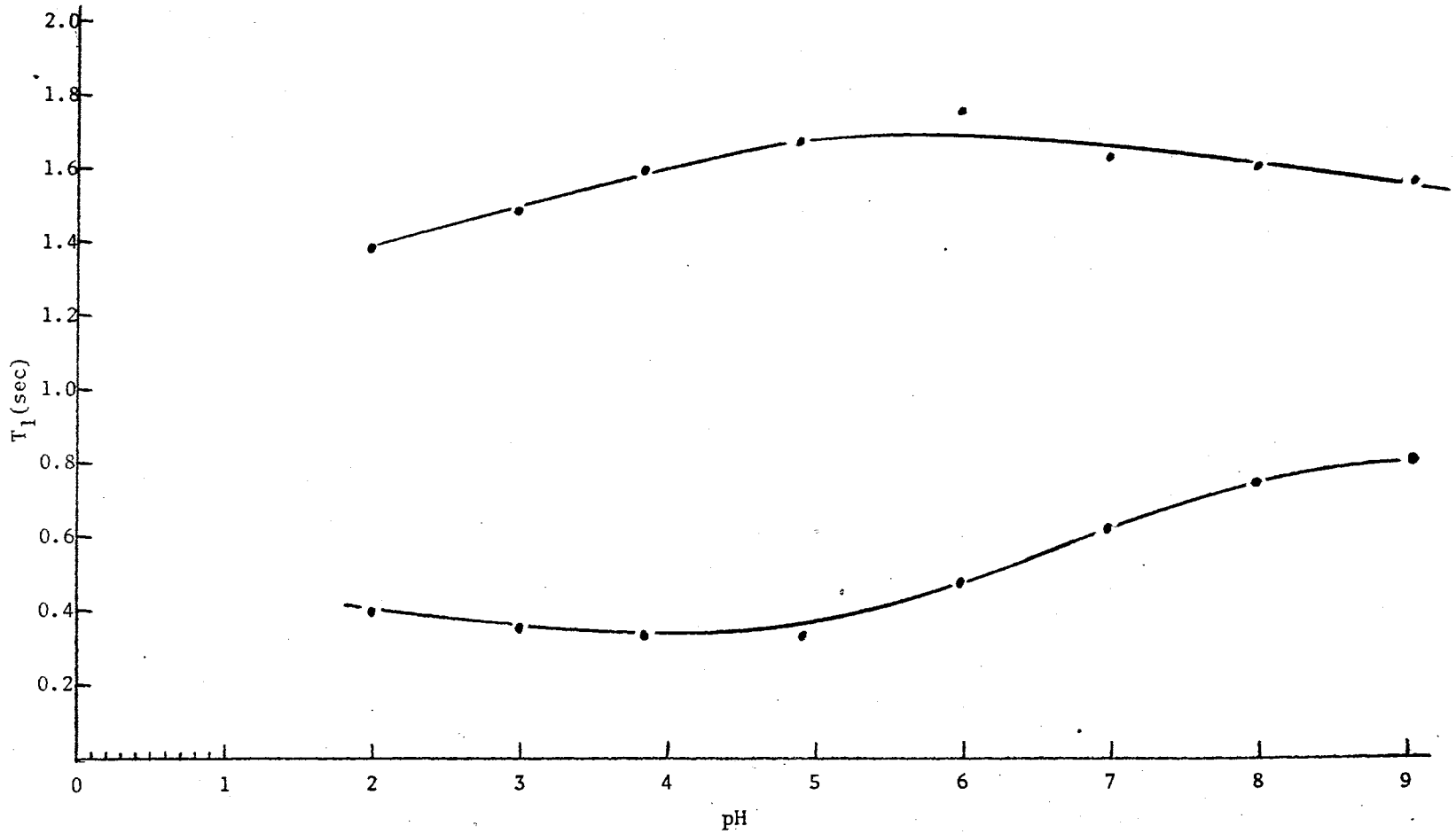

Figure 12. pH Dependence of T_1 in 8% by Weight SiO_2 Ludox LS at 30°C. Upper curve taken at 385 G; lower curve at 0.89 G.

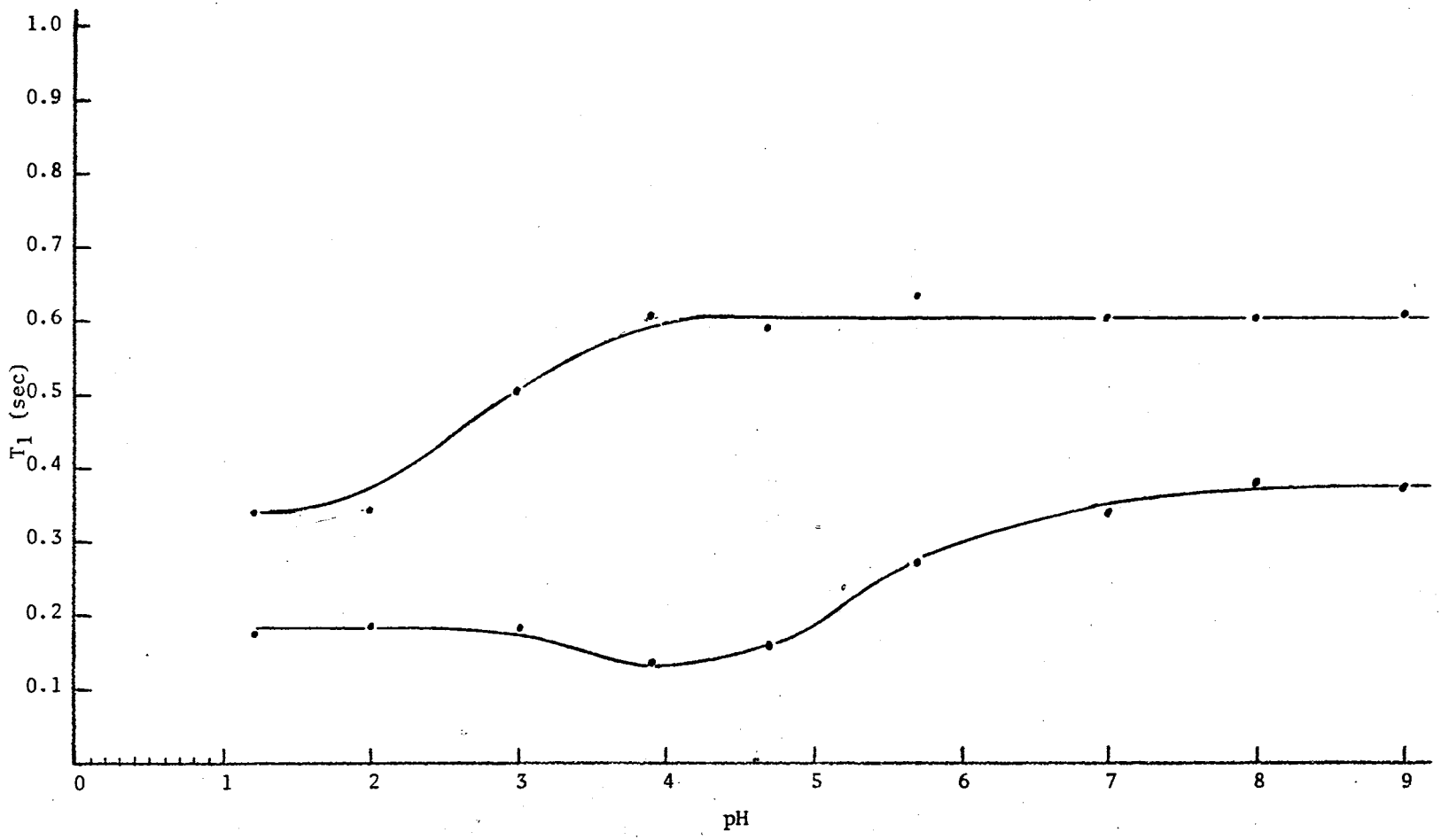

Figure 13. pH Dependence of T_1 in 10% by Weight SiO_2 Ludox HS at 30°C. Upper curve taken at 385 G; lower curve at 0.89 G.

l, it is necessary to add acid which is initially so concentrated that its addition to the sample produces localized gelling even under the action of vigorous stirring. It was found that the gelling phenomenon could be avoided by stirring the sample and simultaneously adding 1N acid solutions.

The pH values reported here were measured with a Beckman "zero-matic" pH-meter, using a standard glass electrode and a calomel electrode. Both were immersed directly into the colloid of interest after calibration against a suitable buffer solution. Once equilibrium was reached, it was possible to reproduce a given measurement to within $\pm$ 0.01 pH unit.

At a later point, we will discuss the problem of the reversability under NaOH addition, but for the present we wish to discuss both the influence of the acid used in the pH adjustment and the affect of the ionic strength.

The Influence of the Acid

During the initial examination of the pH effect in Ludox LS, reagent grade acetic acid (HAc) was used because of its immediate availability. After our initial observation that a large change in T_1 was in fact obtained, we repeated the experiment several times, but used Banco standardized 1N HCl instead. As may be seen in Figure 14, the change from a weak to a moderately strong acid had no measurable effect on the results. Thus, only the hydrogen ion activity (pH) seems to determine T_1 -- a result which is probably more general than this particular comparison has shown.

It was observed that samples acidified with HAc maintained their

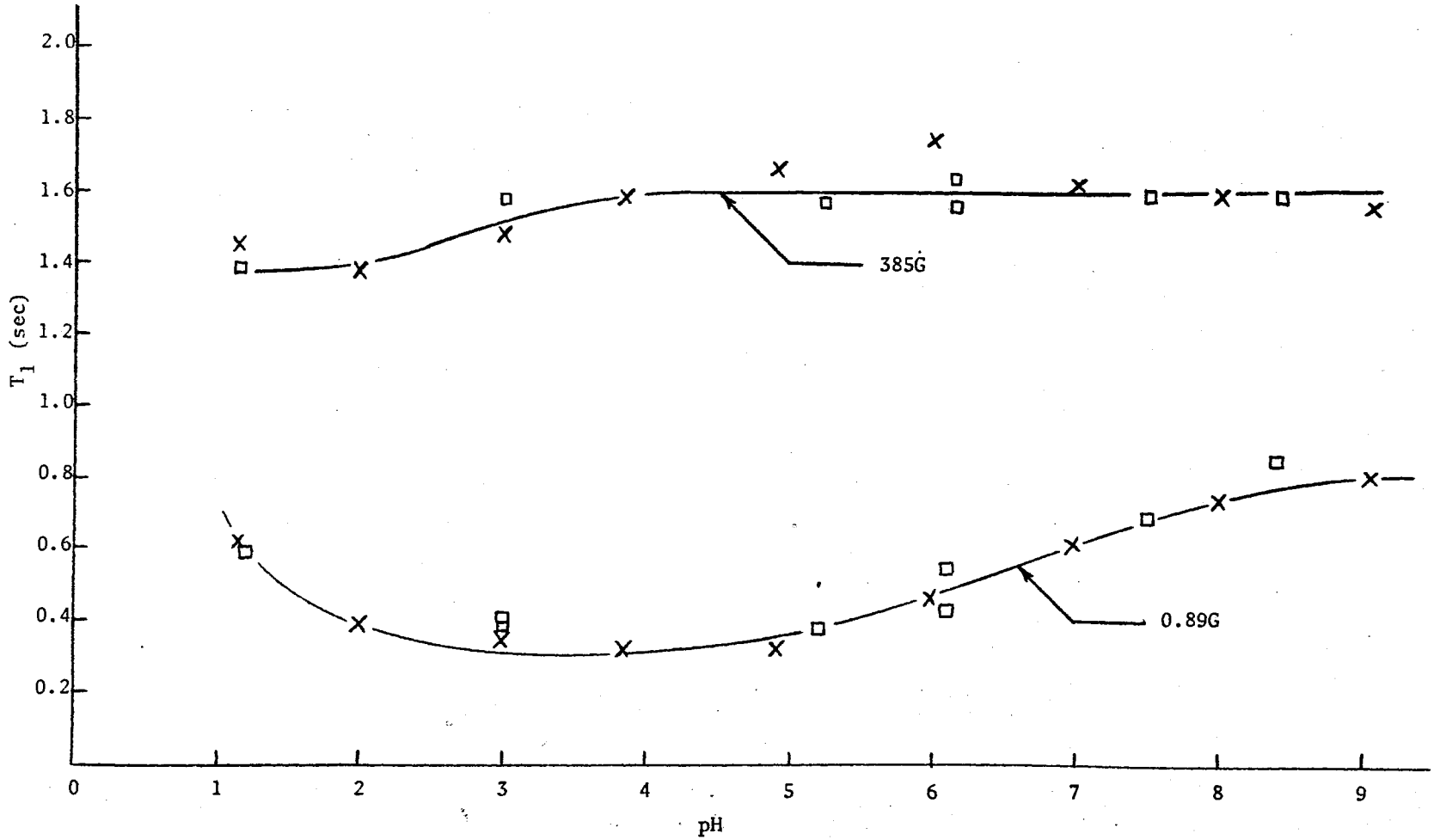

Figure 14. Comparison of Two Acid Types in a T_1 vs pH Experiment With 8% by Weight SiO_2 Ludox LS at 30°C. Squares: data points obtained with HAc; crosses: data points obtained with HCl.

pH with aging whereas the HCl acidified samples tended to show a pH increase, sometimes by as much as 0.5 pH unit. Such increases were always accompanied by an increased turbidity, indicating that the samples in question were undergoing slow gelling -- a process expected to produce the pH increase. Part of the reason that the samples were more stable under HAc addition may have had something to do with the known fact that organic molecules are capable of inhibiting the gelling phenomenon. DuPont, for example, markets an organic modified colloid which is stable even when frozen.

The Influence of the Ionic Strength

According to Debye-Huckel theory, part of an ion's ability to participate in a chemical reaction is dependent upon the amount of electrostatic work which must be done to remove it from its atmosphere of counter-ions. Thus, the activity of an ion depends upon the concentration of other ions, and may be modified if the concentration of non-participating ions is altered. In order to circumvent this possibility, chemists often study reactions which take place in a solution of highly-concentrated, non-participating ions. Changes in the concentration of the ion of interest are then assumed to have little affect on the net ionic strength. The "inert" ion usually favored is the perchlorate ion.

In our case, there is really no such thing as an inert ion. The addition of excess ions will reduce the thickness of the double-layer and hence destroy the stability of the colloid under test. For that reason, the problem had to be approached differently, and it was decided to drastically alter the ionic strength in those pH-regions where

the colloid stability should not be affected and to observe its influence upon T_1.

One such region lies between pH 1 and pH 6 where it is known that large amounts of NaCl can be added without promoting gelling. It also turned out that we could add NaF (a salt which does promote gelling) and that the gelling was sufficiently slow that T_1 could still be examined. In a later section, where we specifically discuss the influence of gelling, it will be seen that even at pH 9 (where gelling is extremely rapid) the added NaCl did not affect T_1.

Table XII gives the results of these experiments, and it can there be seen that, even when the Na-ion concentration is at least 100 times as large as that to be expected in the unmodified colloid, no measurable influence on T_1 is observed. Since a similar result was obtained with NaF, it does not appear that the ionic strength is a strongly important parameter.

The Field and pH-dependence Combined

Ludox LS, at 8% by weight SiO_2, was selected for a series of field-dependence measurements as the pH was varied throughout the range just discussed. A deuterated sample was also subjected to the same procedure, and, in each case, the least-squares method discussed in Chapter II was used to extract the constants K and τ. The primary virtue in using the least-squares method lay in the fact that all data were treated in an identical manner, and it was not our intention to extract "confidence intervals" or any of the other statistical parameters typically produced by such a study. The technique was viewed merely as a convenient method of curve-fitting which eliminated the type of bias

that could have influenced a manual technique (manual fitting was, in fact, attempted initially, but the results were generally unsatisfactory; this prompted the use of more elaborate methods).

TABLE XII

AFFECT OF ADDED ELECTROLYTES UPON T_1 AND T_2 AS MEASURED IN 8% BY WEIGHT SiO_2 LUDOX LS[1]

Temperature	Indicated pH	Observed T_1	Field	Added Electrolyte	Electrolyte Concentration in gm/ml H_2O
32°C	1.20	1.67 sec	443 G	None	
32°C	1.20	1.58 sec	324 G	None	
32°C	1.20	1.47 sec	14.5 G	None	
32°C	1.20	0.629[2] sec	0.54 G	None	
32°C	1.20	1.59 sec	330 G	NaCl	1.04×10^{-3}
32°C	1.20	0.629[2] sec	0.54 G	NaCl	1.04×10^{-3}
31°C	1.20	1.59 sec	330 G	NaCl	1.04×10^{-2}
31°C	1.20	0.629[2] sec	0.54 G	NaCl	1.04×10^{-2}
30°C	3.00	1.57 sec	443 G	None	
30°C	3.00	1.46 sec	322 G	None	
30°C	3.00	0.308[2] sec	0.54 G	None	
30°C	3.15	1.58 sec	443 G	NaF	1.46×10^{-3}
30°C	3.15	1.53 sec	328 G	NaF	1.46×10^{-3}
30°C	3.15	0.320[2] sec	0.54 G	NaF	1.46×10^{-3}

[1]Note that, even with NaF, the changes were very slight, but that in every case the Na-ion concentration was at least 100 times higher than in the normal colloid.

[2]This is the value of T_2, corrected by T_2^*.

Figures 15 through 36 show the experimental data along with the weighted least-squares fit (solid line) produced by the computer. For comparison, Figure 17 also shows an unweighted fit to the same data (dashed line). As expected, the unweighted fit is not drastically different, except that the high-field data are not as well represented. The reasons for the difference have been discussed in Chapter II.

Tables XIII and XIV list the relevant parameters as a function of pH, and Figures 37 through 39 show these same data in graphical form. Noting the large change in τ, the (unspecified) correlation time, it must be concluded that it is the single most important parameter which is influenced by the pH.

It may also be observed in Figure 39 that the constant "K" appears to increase in discrete steps as the pH is reduced, at least in the case of the undeuterated sample. Since these steps lie in the ratio 3:2:1, one immediately considers the possibility that stepwise dissociation is modifying an occupation probability. However, discussion of this phenomenon must also be deferred until all of the data have been presented.

The Reversability of the pH-dependence

Up to this point, we have only spoken of samples whose pH was changed in a definite direction; namely, from the initial value as supplied (ca pH 9) toward lower values which approached pH 1. The question naturally arises as to the reversability of the procedure, and it was of definite interest to take a pH 1 sample back up to pH 9 through the addition of NaOH. At the same time, it had to be recognized that a sample which had gone through a pH 9-pH 1-pH 9 cycle was in fact altered, since the concentration of NaCl would be increased. In view of

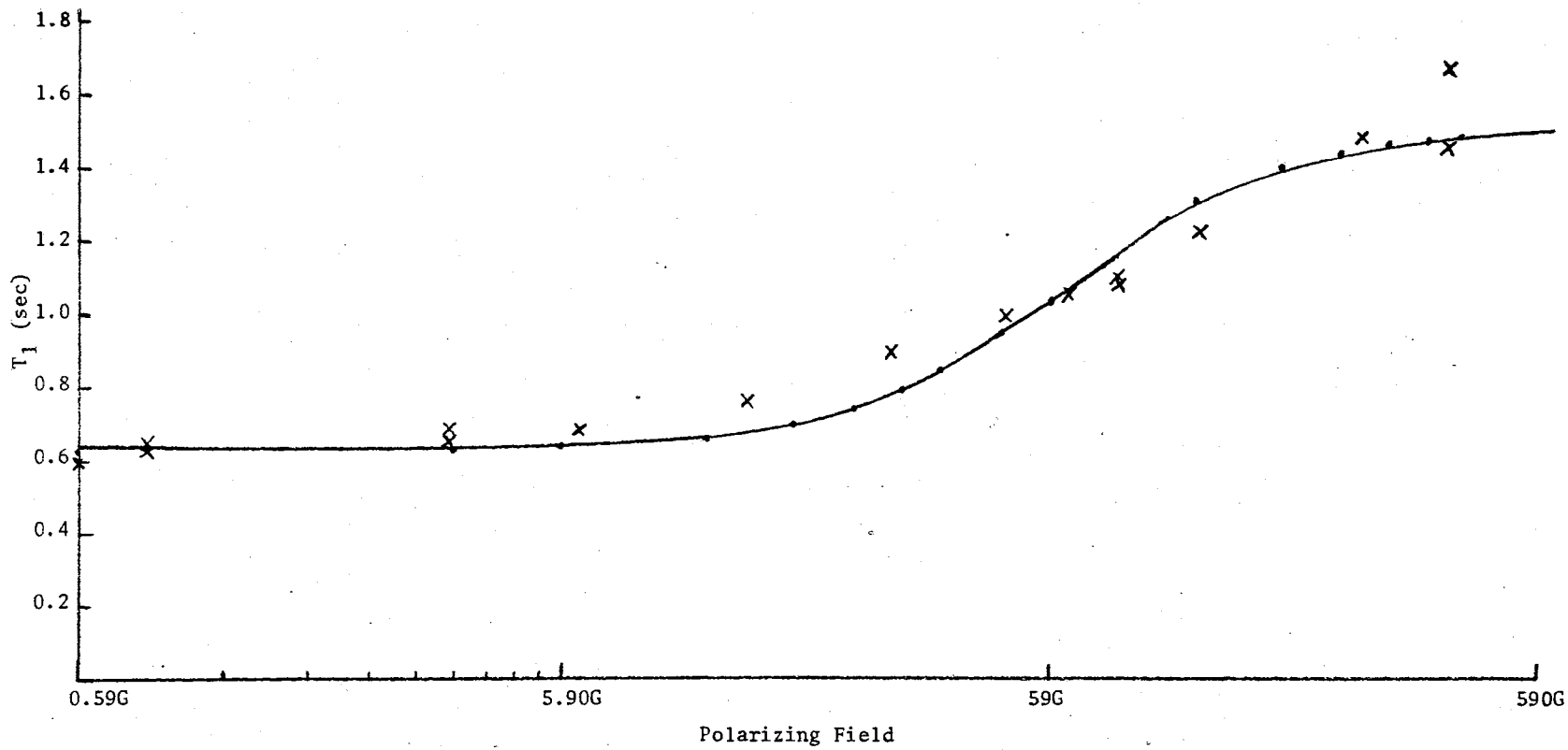

Figure 15. Least-squares Fit to 8% by Weight SiO_2 Ludox LS Field-dependence Data at pH 1.15 and at 40°C. The crosses represent the data points. See Table XIII for the least-squares parameters.

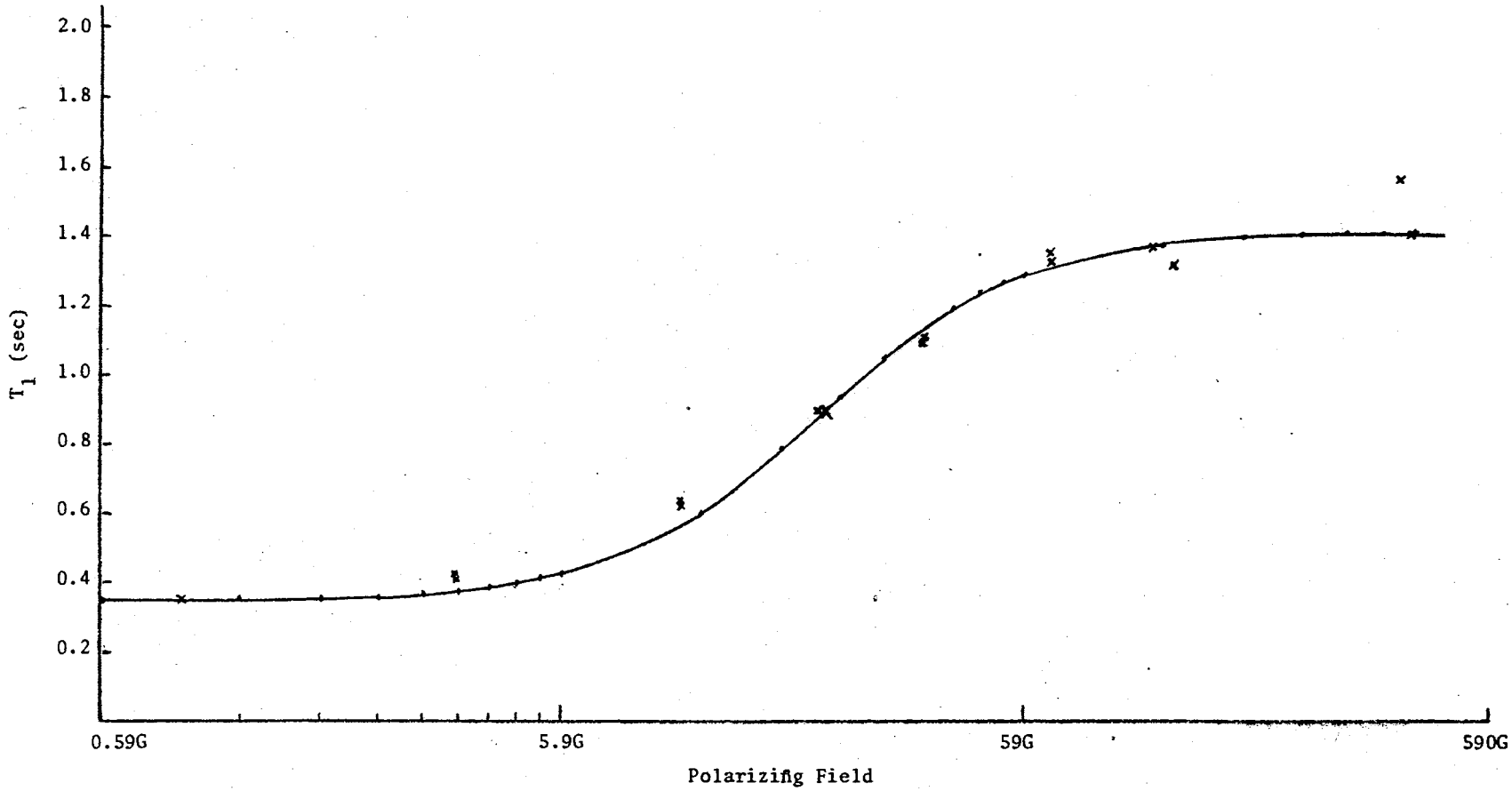

Figure 16. Least-squares Fit to 8% by Weight SiO_2 Ludox LS Field-dependence Data at pH 2.00 and at 40°C. The crosses represent the data points. See Table XIII for the least-squares parameters.

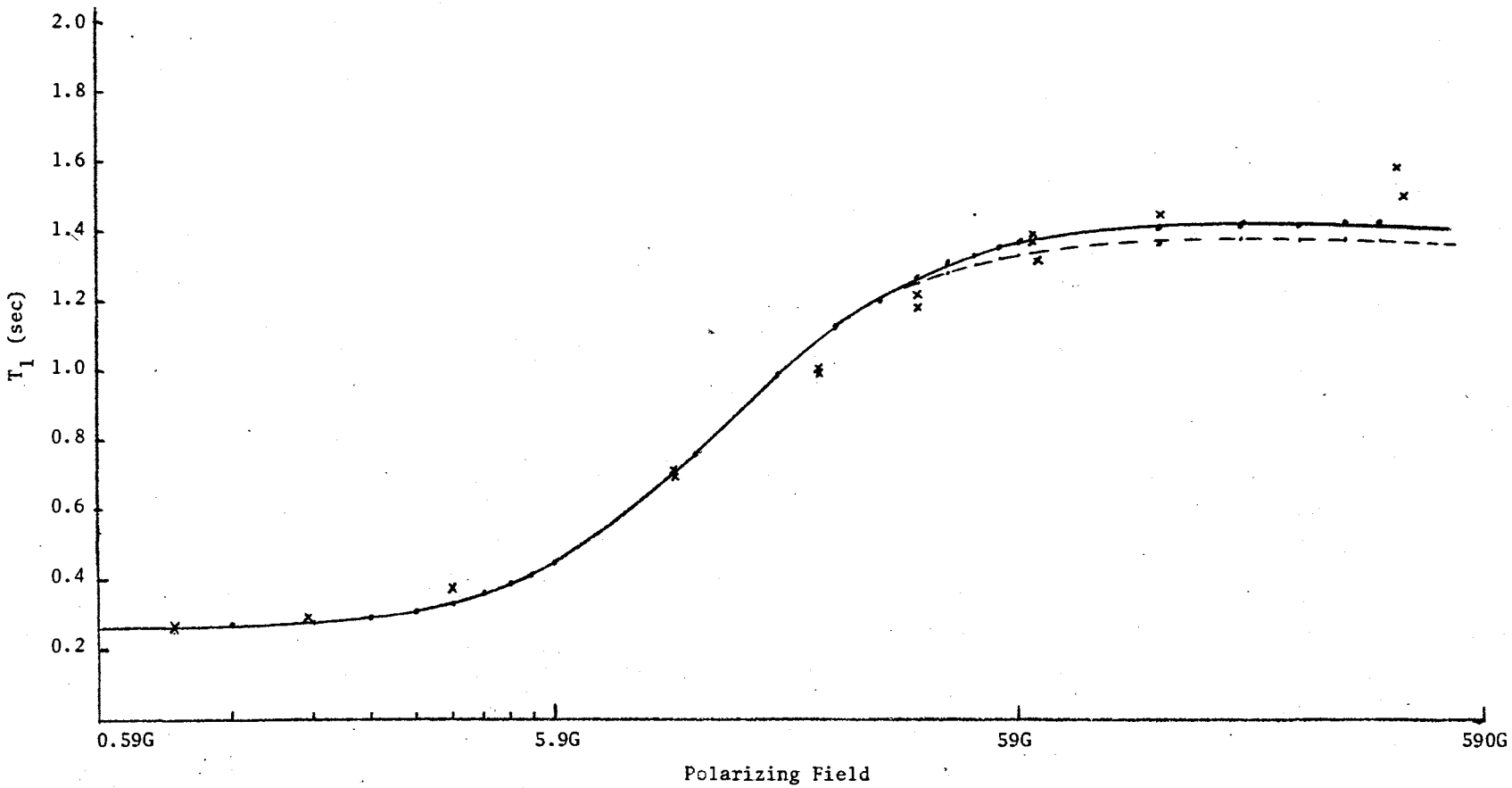

Figure 17. Least-squares Fit to 8% by Weight SiO_2 Ludox LS Field-dependence Data at pH 3.10 and at 40°C. The crosses represent the data points. The dashed segment represents the results of the unweighted fit discussed in the text. See Table XIII for the least-squares parameters.

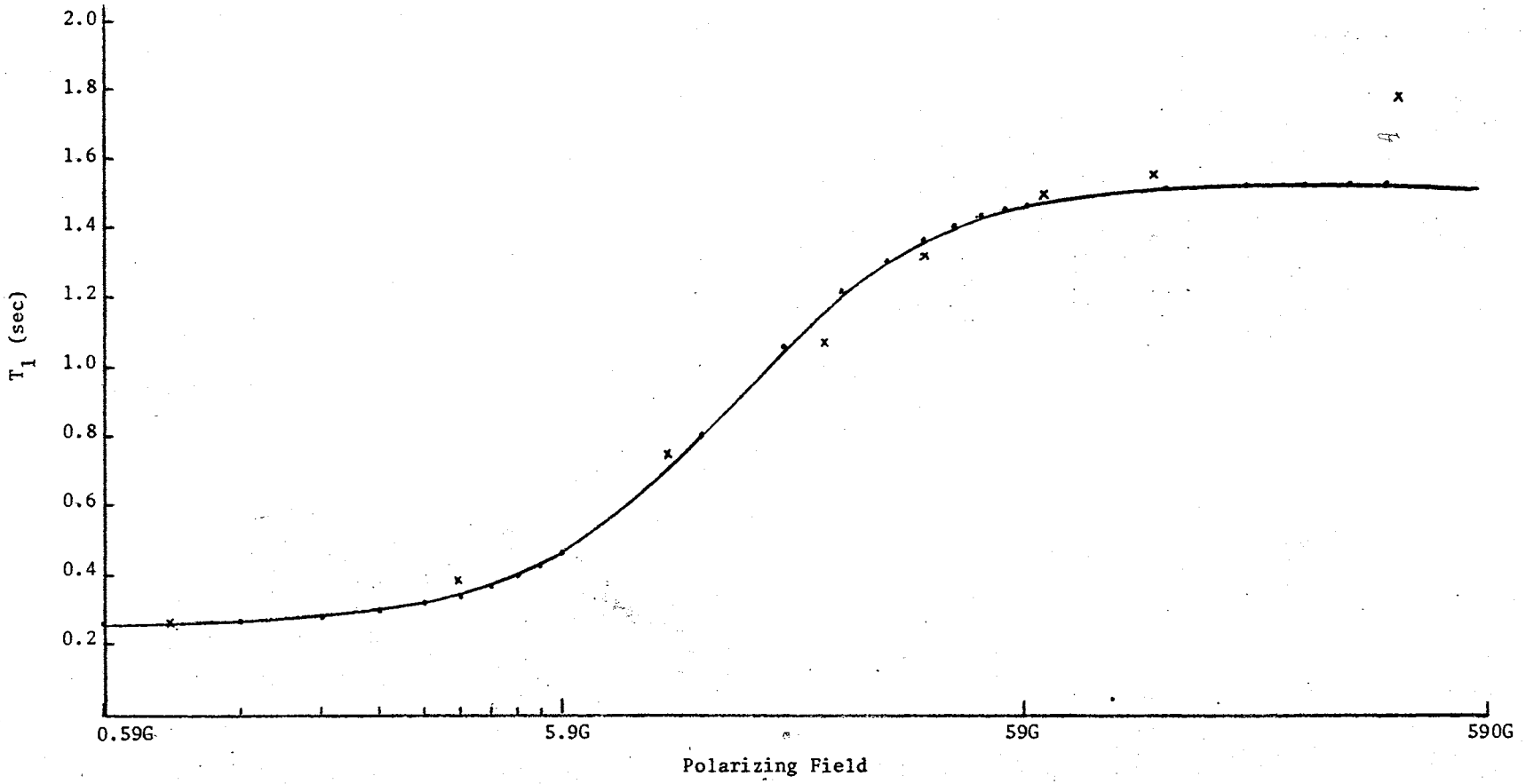

Figure 18. Least-squares Fit to 8% by Weight SiO_2 Ludox LS Field-dependence Data at pH 4.00 and at 40°C. The crosses represent the data points. See Table XIII for the least-squares parameters.

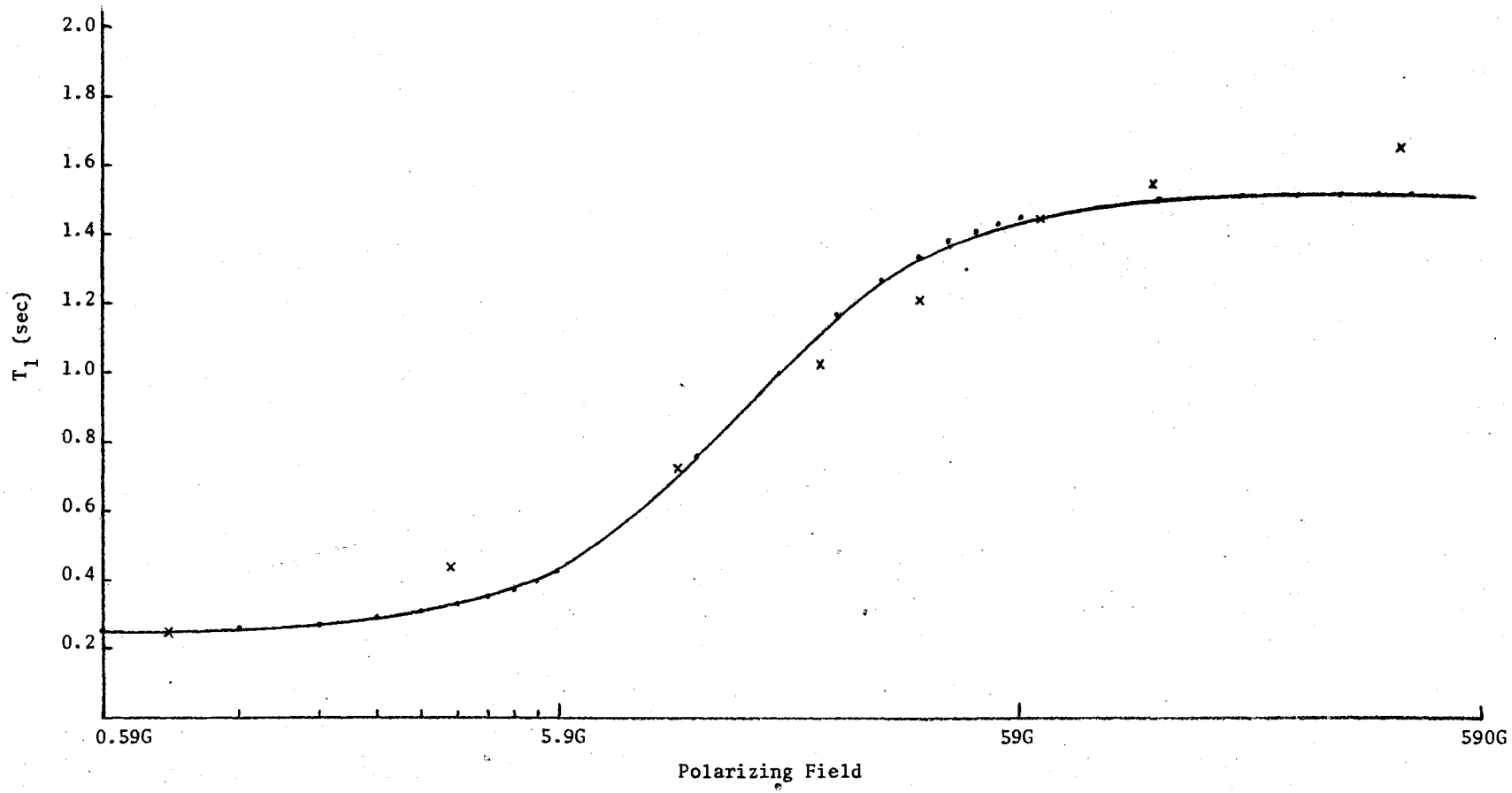

Figure 19. Least-squares Fit to 8% by Weight SiO_2 Ludox LS Field-dependence Data at pH 4.00 and at 40°C. The crosses represent the data points. See Table XIII for the least-squares parameters.

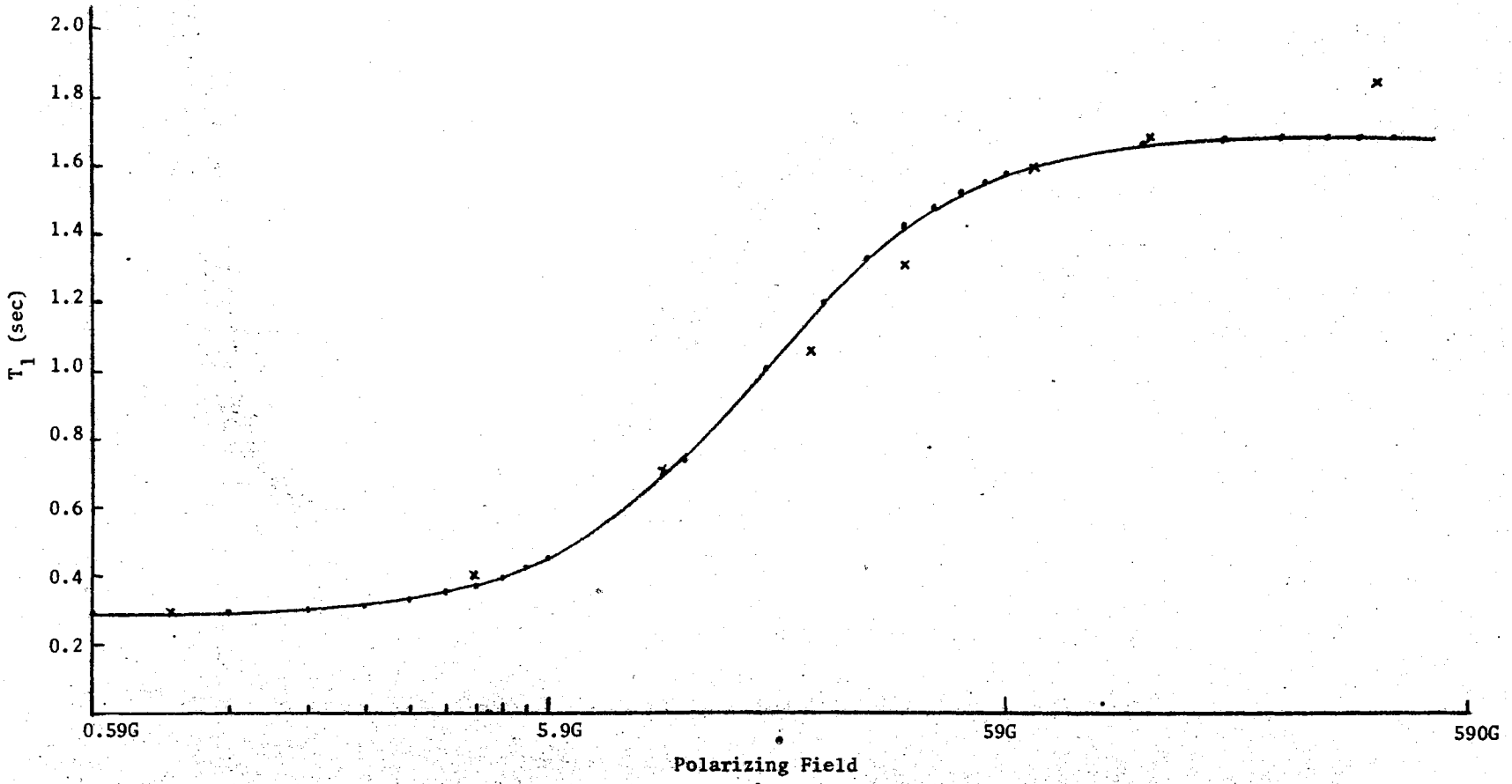

Figure 20. Least-squares Fit to 8% by Weight SiO_2 Ludox LS Field-dependence Data at pH 5.00 and at 40°C. The crosses represent the data points. See Table XIII for the least-squares parameters.

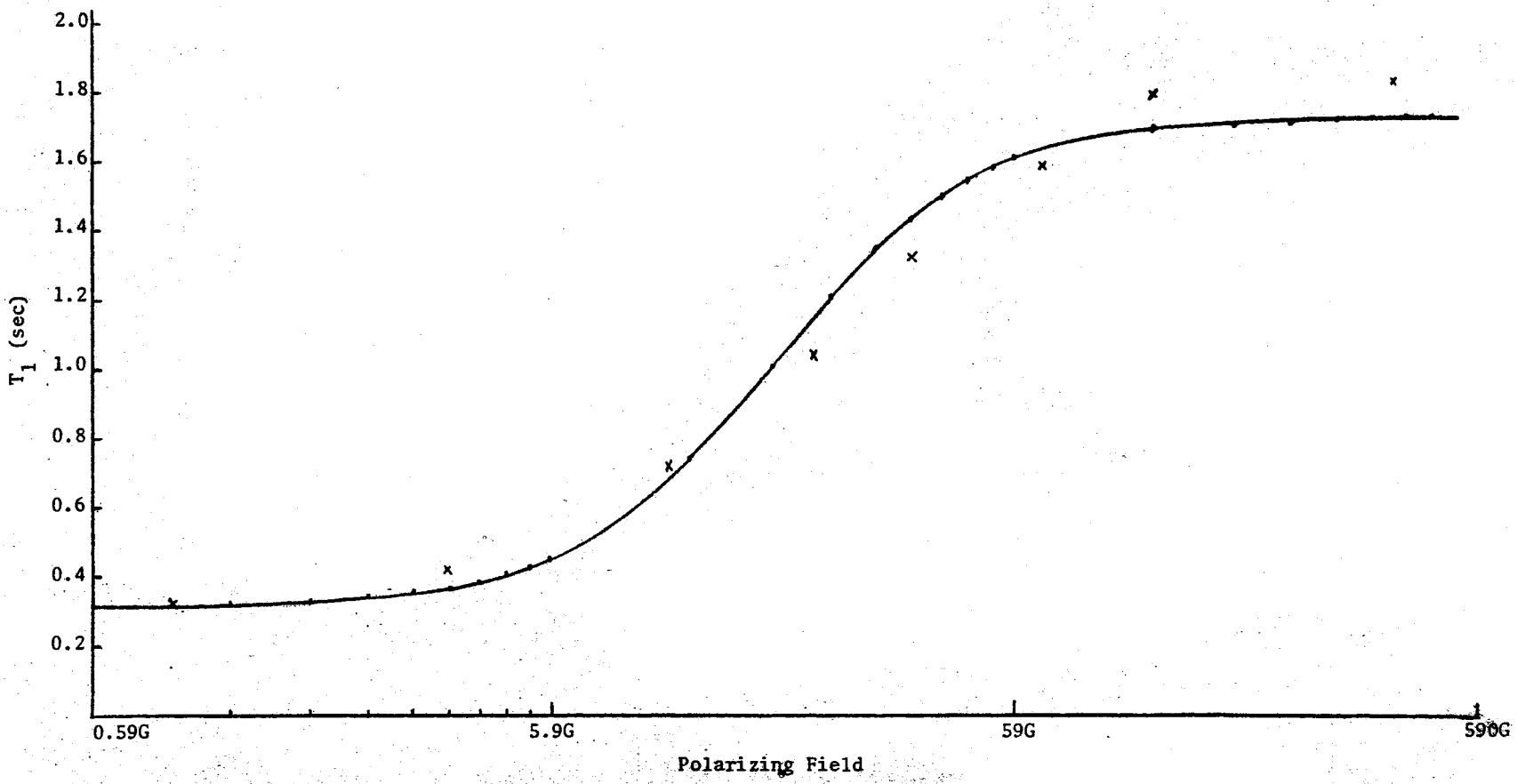

Figure 21. Least-squares Fit to 8% by Weight SiO_2 Ludox LS Field-dependence Data at pH 5.00 and at 40°C. The crosses represent the data points. See Table XIII for the least-squares parameters.

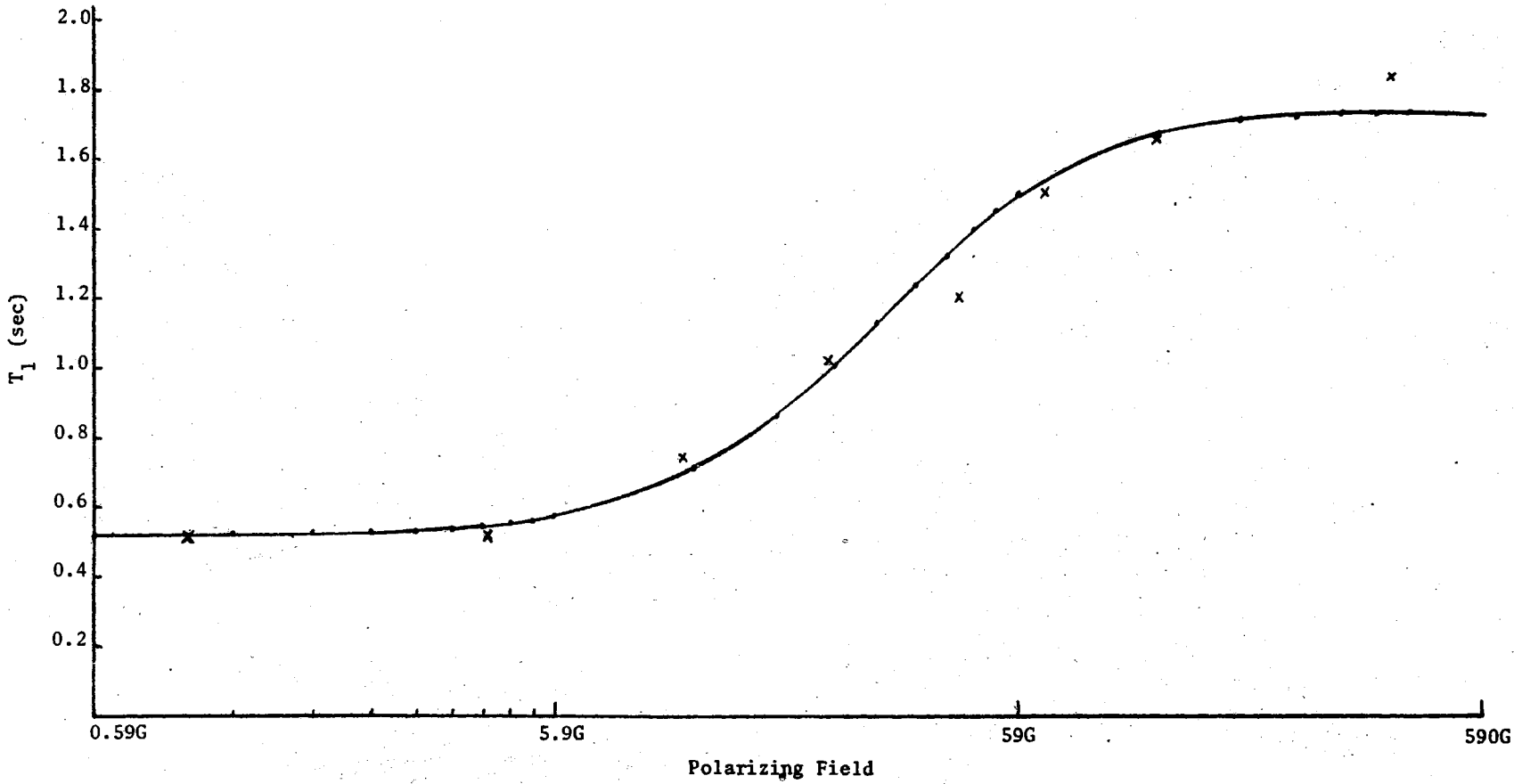

Figure 22. Least-squares Fit to 8% by Weight SiO_2 Ludox LS Field-dependence Data at pH 6.00 and at 40°C. The crosses represent the data points. See Table XIII for the least-squares parameters.

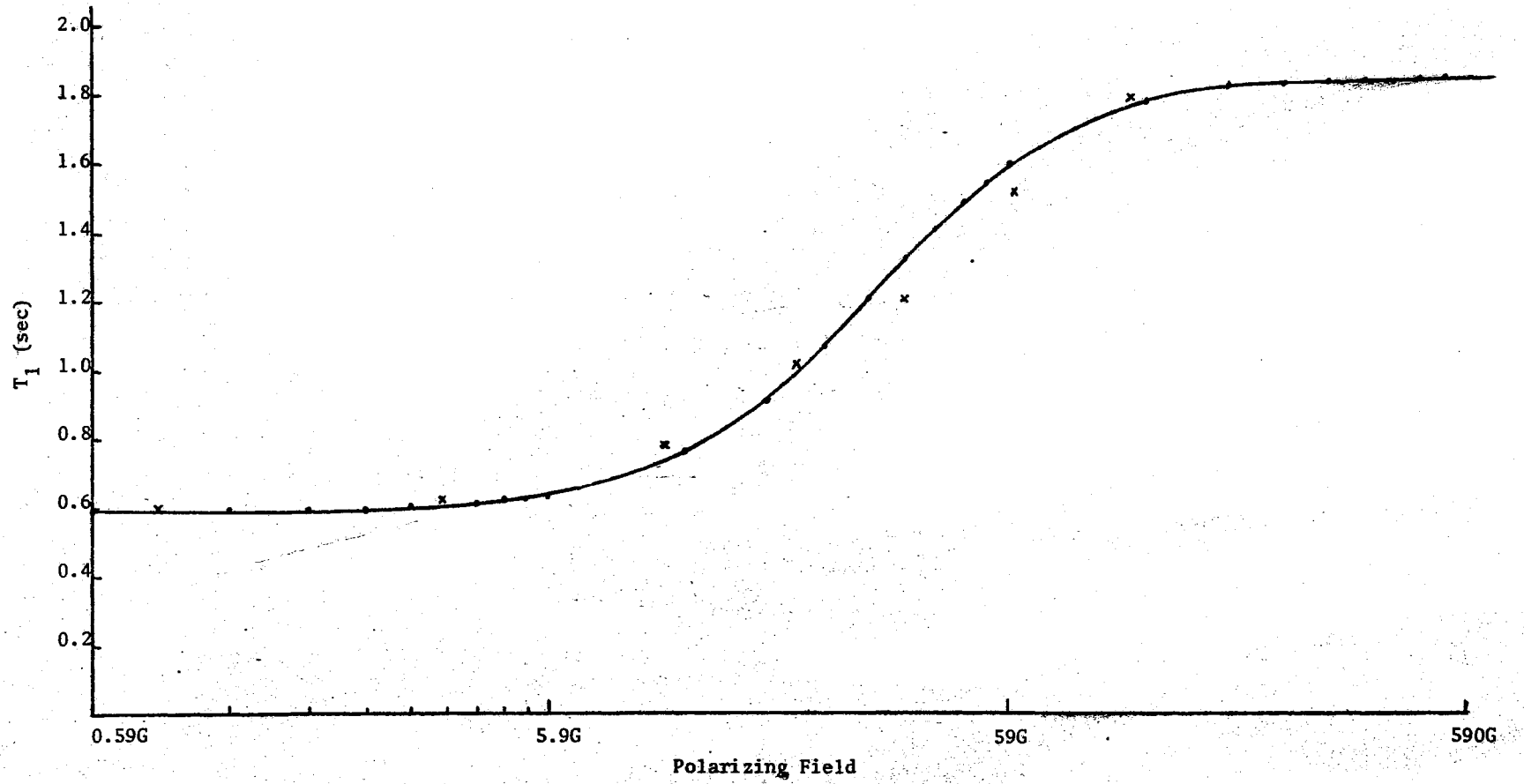

Figure 23. Least-squares Fit to 8% by Weight SiO_2 Ludox LS Field-dependence Data at pH 6.00 and at 40°C. The crosses represent the data points. See Table XIII for the least-squares parameters.

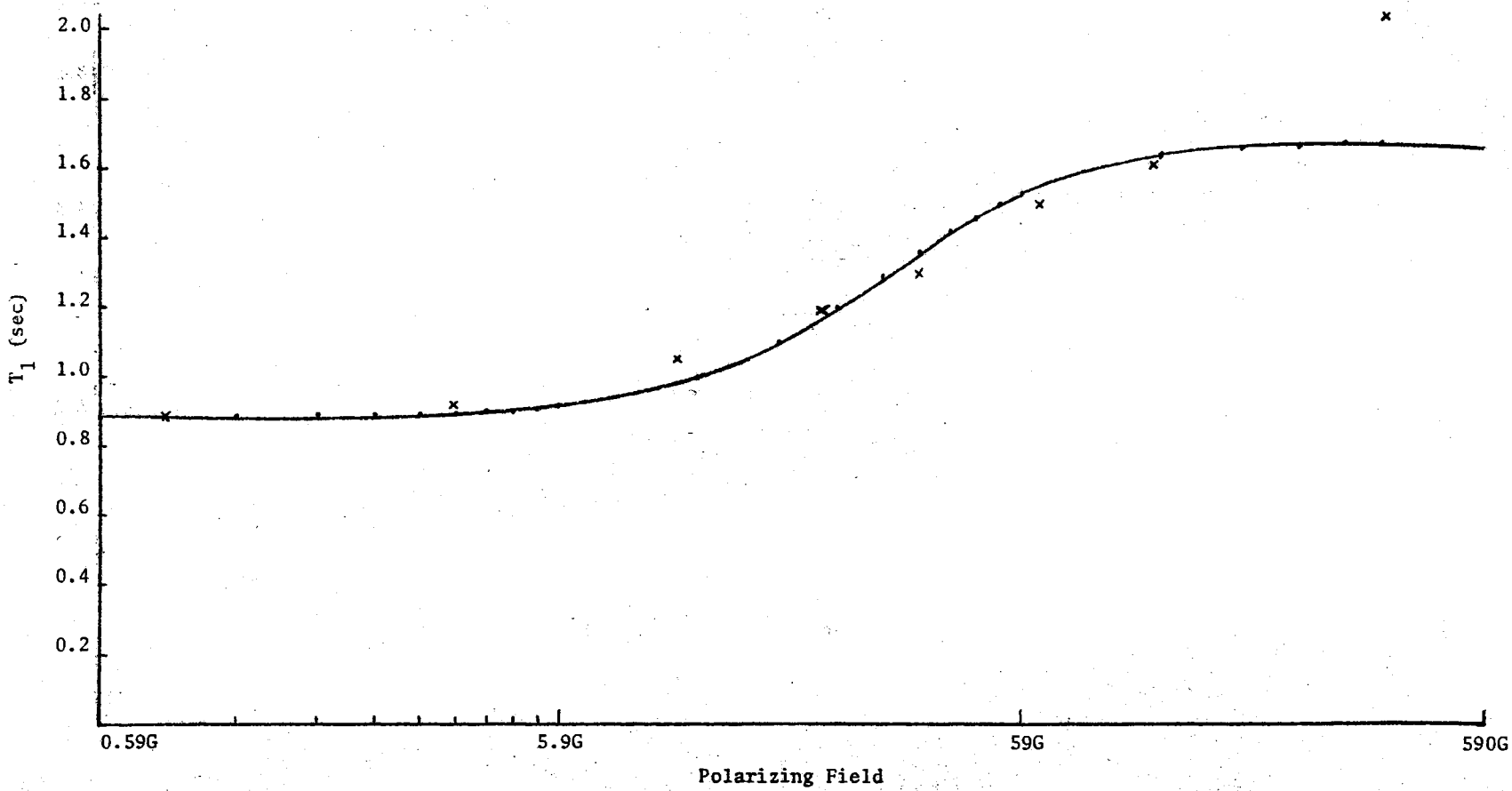

Figure 24. Least-squares Fit to 8% by Weight SiO_2 Ludox LS Field-dependence Data at pH 7.00 and at 40°C. The crosses represent the data points. See Table XIII for the least-squares parameters.

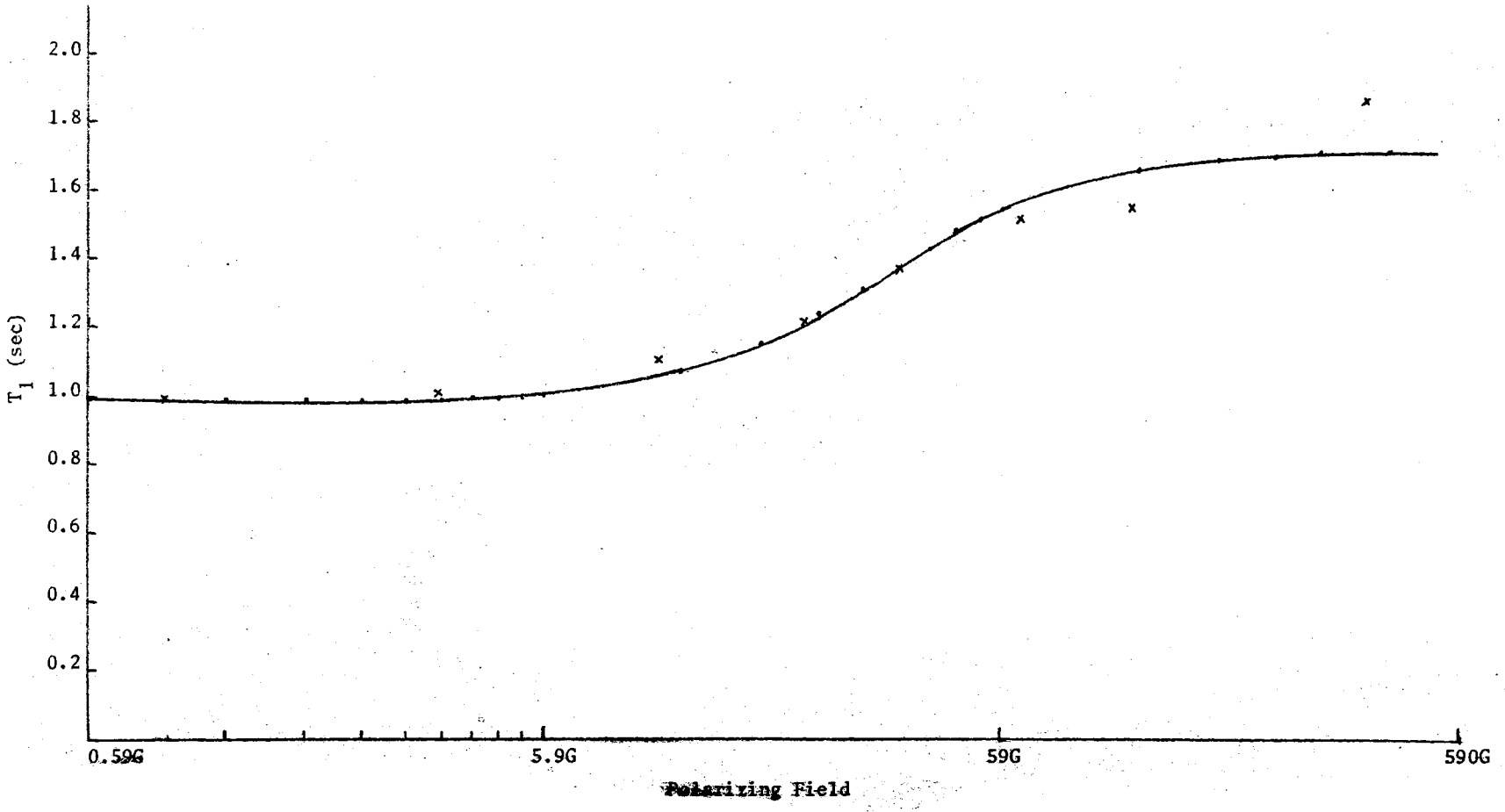

Figure 25. Least-squares Fit to 8% by Weight SiO_2 Ludox LS Field-Dependence Data at pH 7.00 and at 40°C. The crosses represent the data points. See Table XIII for the least-squares parameters.

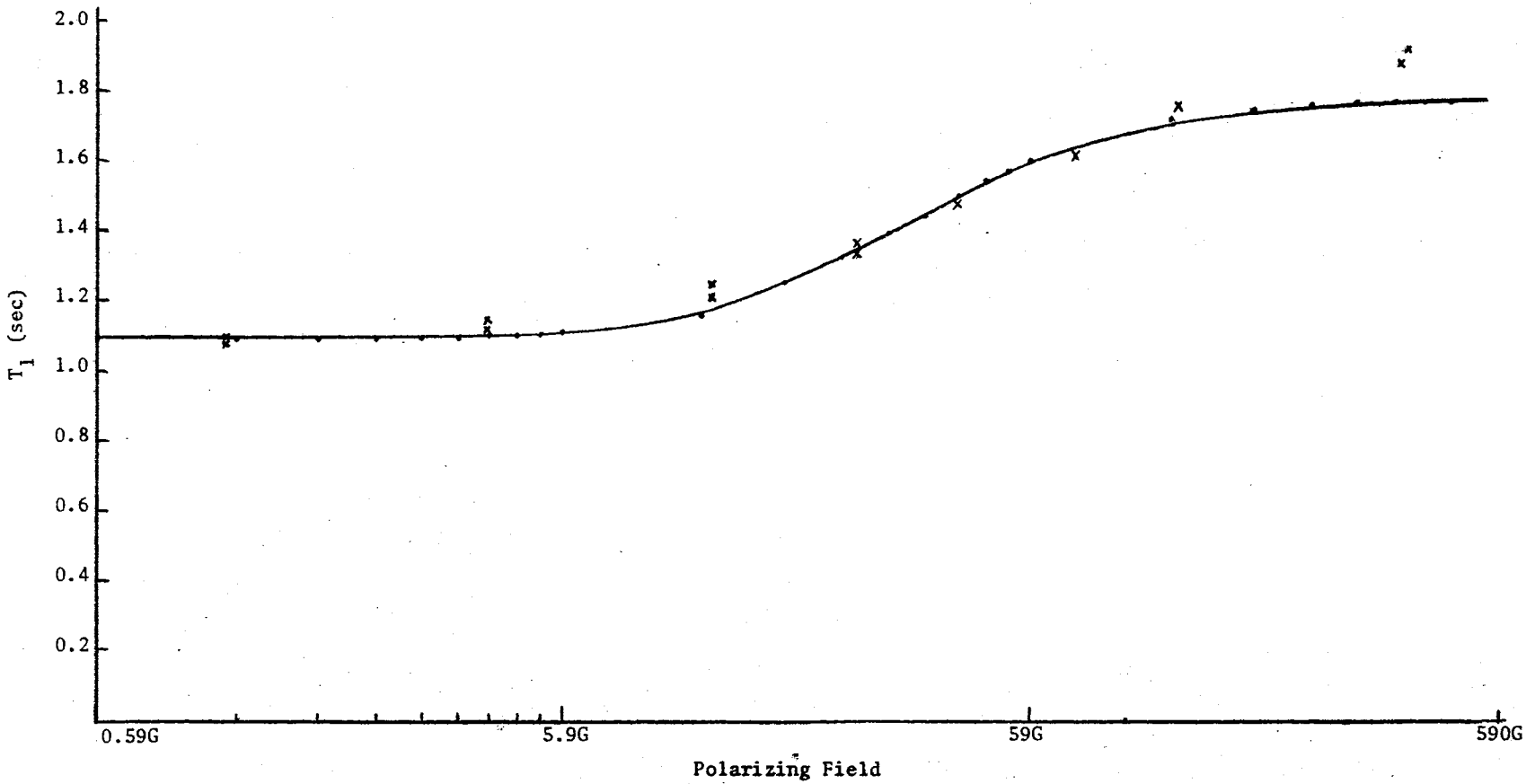

Figure 26. Least-squares Fit to 8% by Weight SiO_2 Ludox LS Field-dependence Data at pH 9.00 and at 40°C. The crosses represent the data points. See Table XIII for the least-squares parameters.

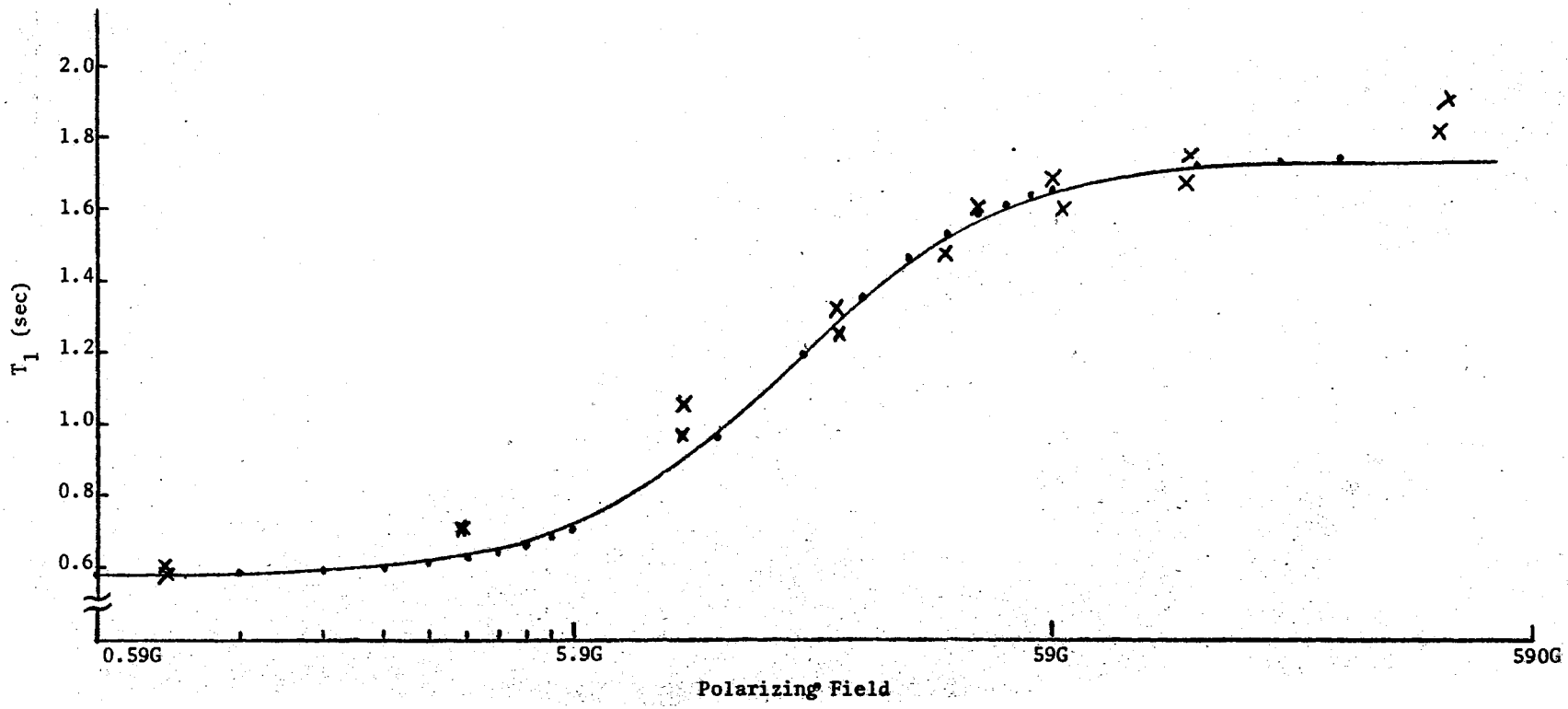

Figure 27. Least-squares Fit to Deuterated 8% by Weight SiO_2 Ludox LS Field-dependence Data at pH 2.04 and at 40°C. The crosses represent the data points. See Table XIV for the least-squares parameters.

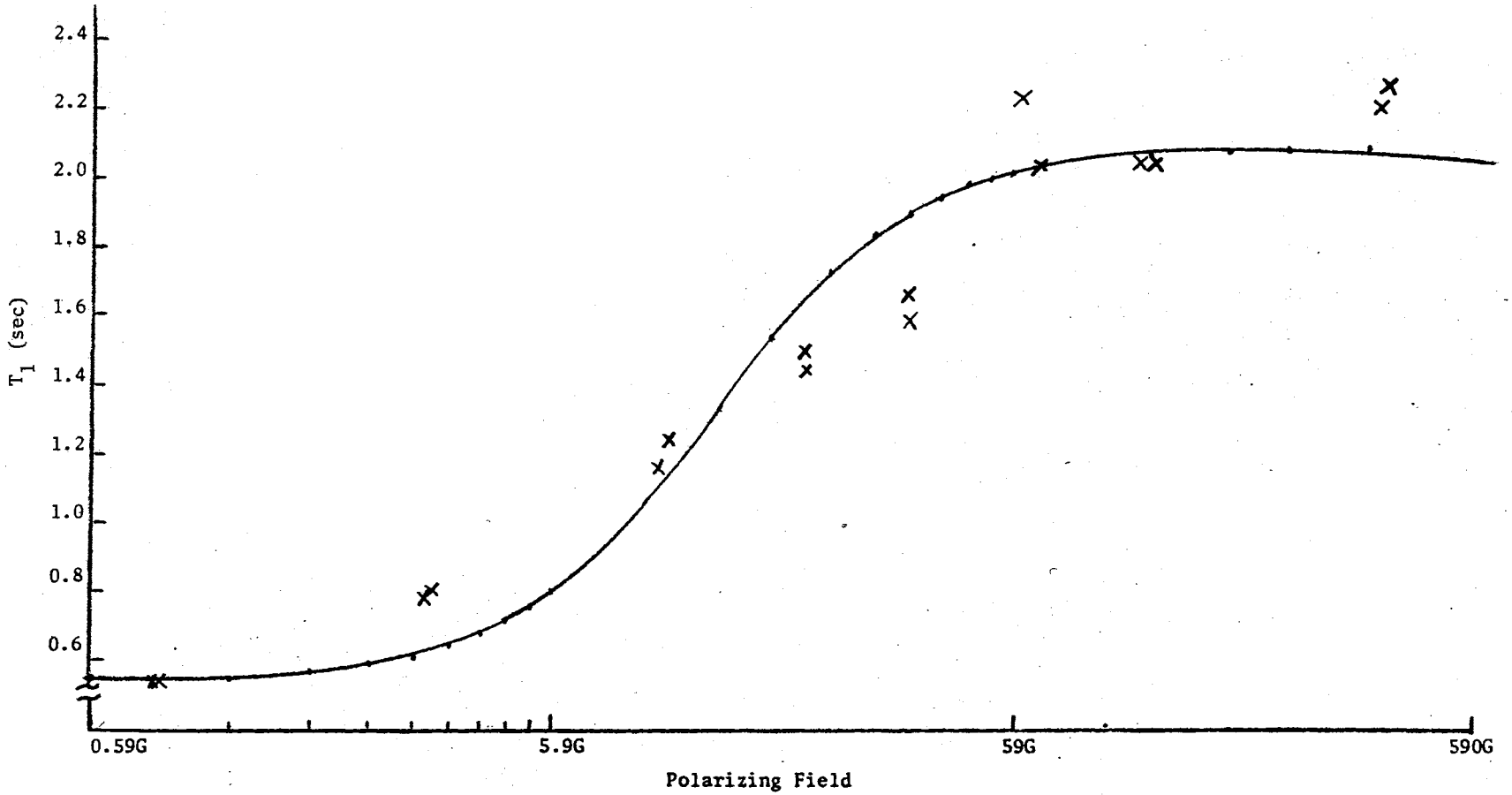

Figure 28. Least-squares Fit to Deuterated 8% by Weight SiO_2 Ludox LS Field-dependence Data at pH 3.00 and at 40°C. The crosses represent the data points. See Table XIV for the least-squares parameters.

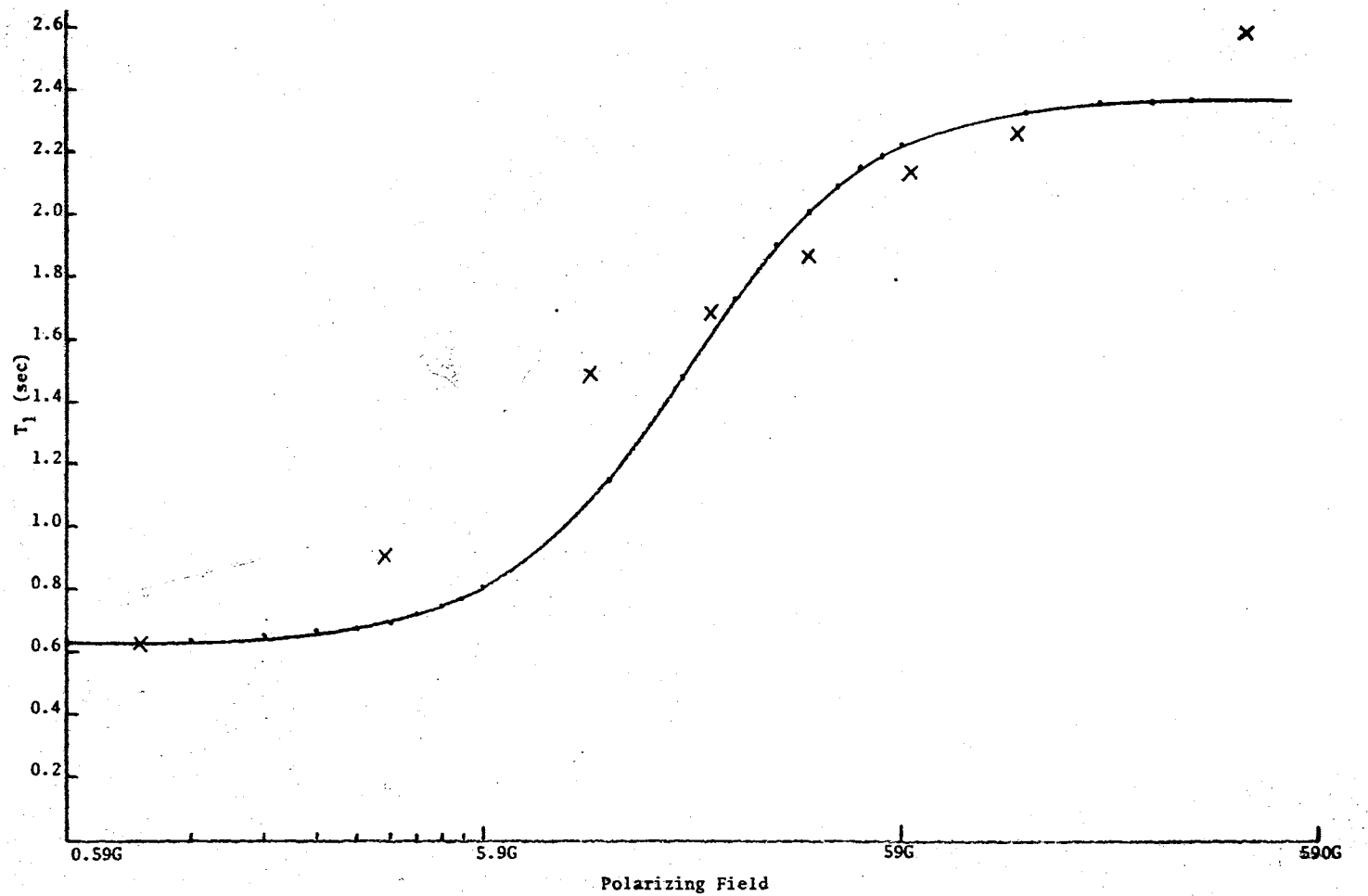

Figure 29. Least-squares Fit to Deuterated 8% by Weight SiO_2 Ludox LS Field-dependence Data at pH 4.00 and at 40°C. The crosses represent the data points. See Table XIV for the least-squares parameters.

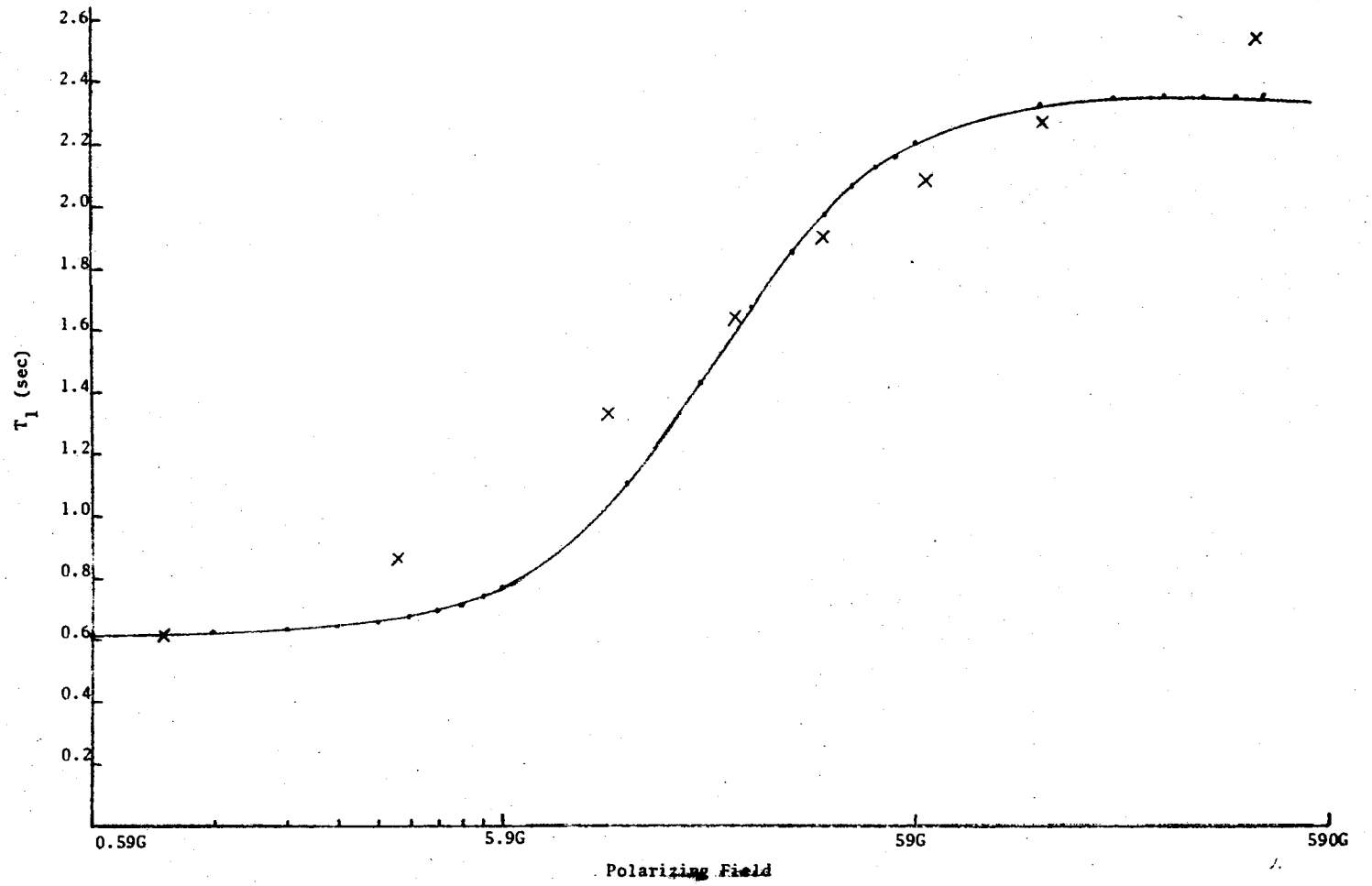

Figure 30. Least-squares Fit to Deuterated 8% by Weight SiO_2 Ludox LS Field-dependence Data at pH 4.00 and at 40°C. The crosses represent the data points. See Table XIV for the least-squares parameters.

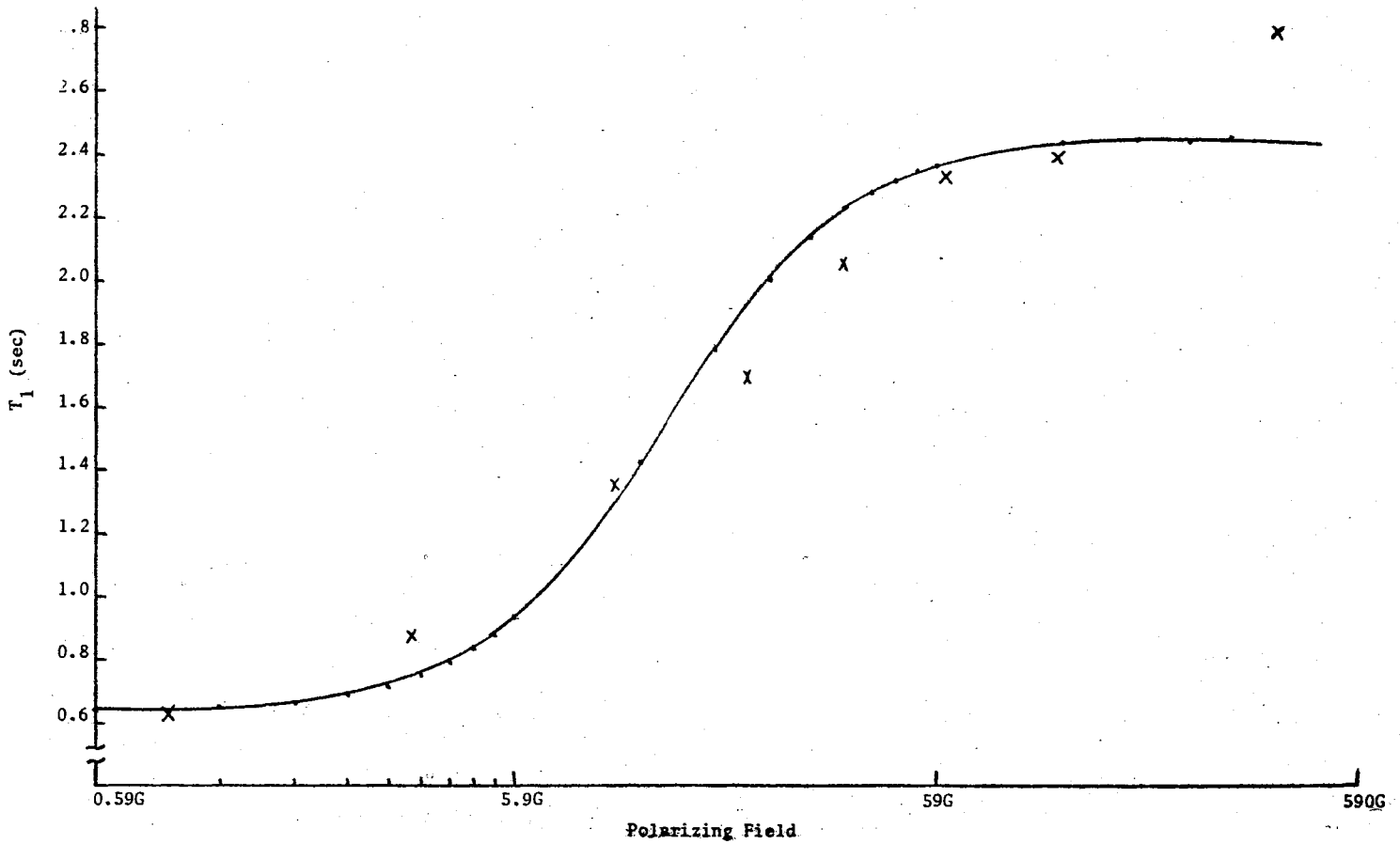

Figure 31. Least-squares Fit to Deuterated 8% by Weight SiO_2 Ludox LS Field-dependence Data at pH 4.90 and at 40°C. The crosses represent the data points. See Table XIV for the least-squares parameters.

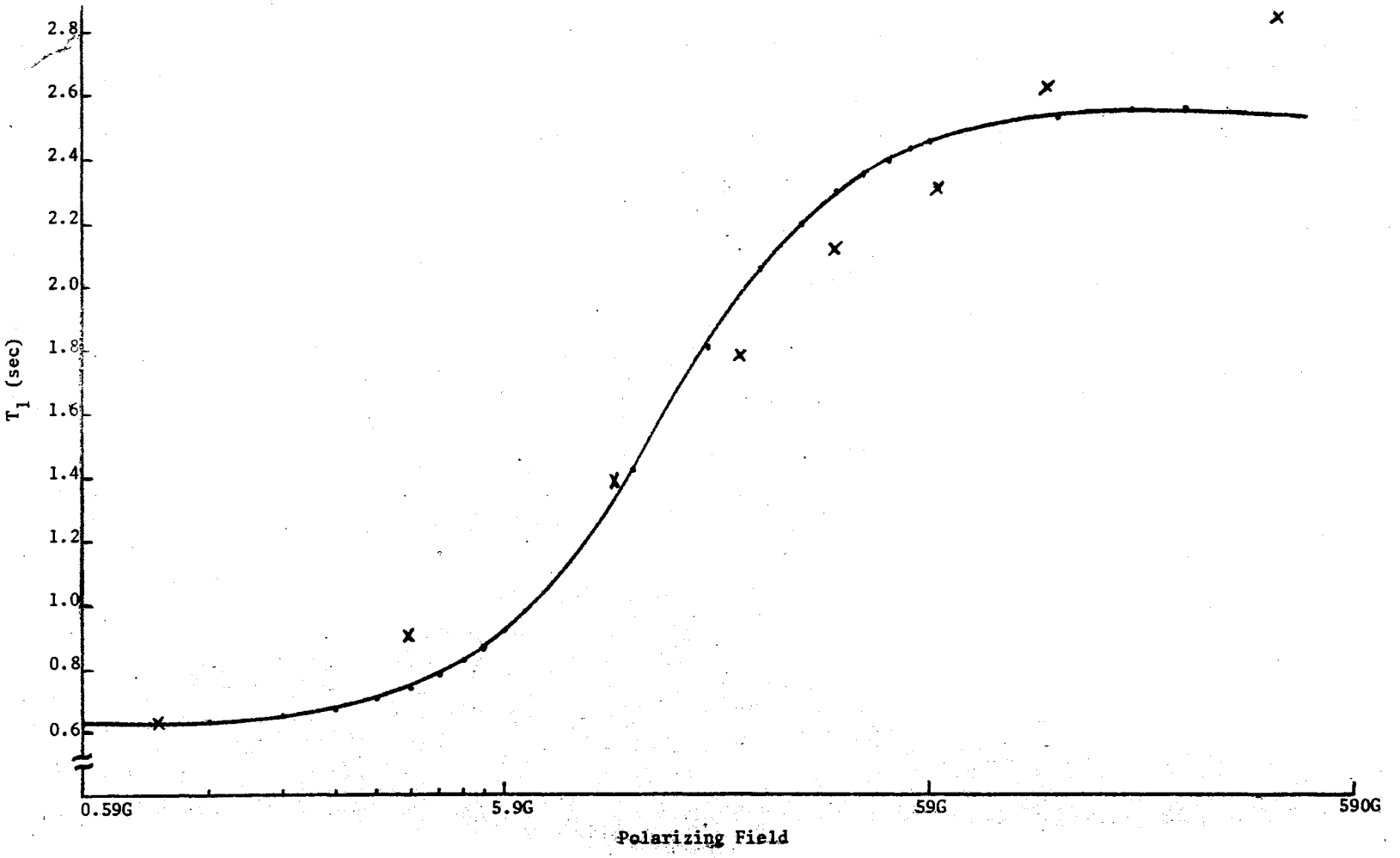

Figure 32. Least-squares Fit to Deuterated 8% by Weight SiO_2 Ludox LS Field-dependence Data at pH 4.90 and at 40°C. The crosses represent the data points. See Table XIV for the least-squares parameters.

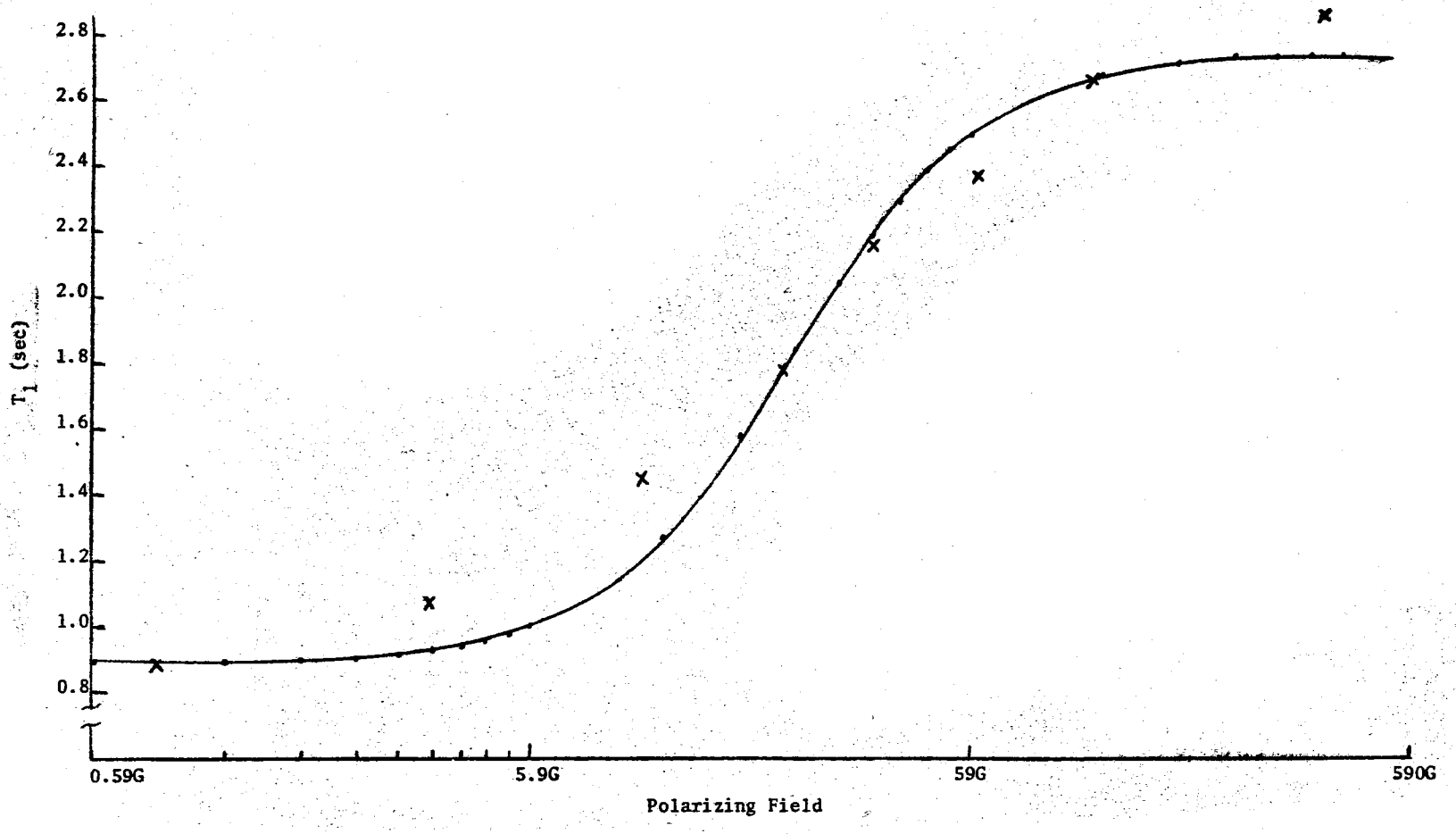

Figure 33. Least-squares Fit to Deuterated 8% by Weight SiO_2 Ludox LS Field-dependence Data at pH 6.00 and at 40°C. The crosses represent the data points. See Table XIV for the least-squares parameters.

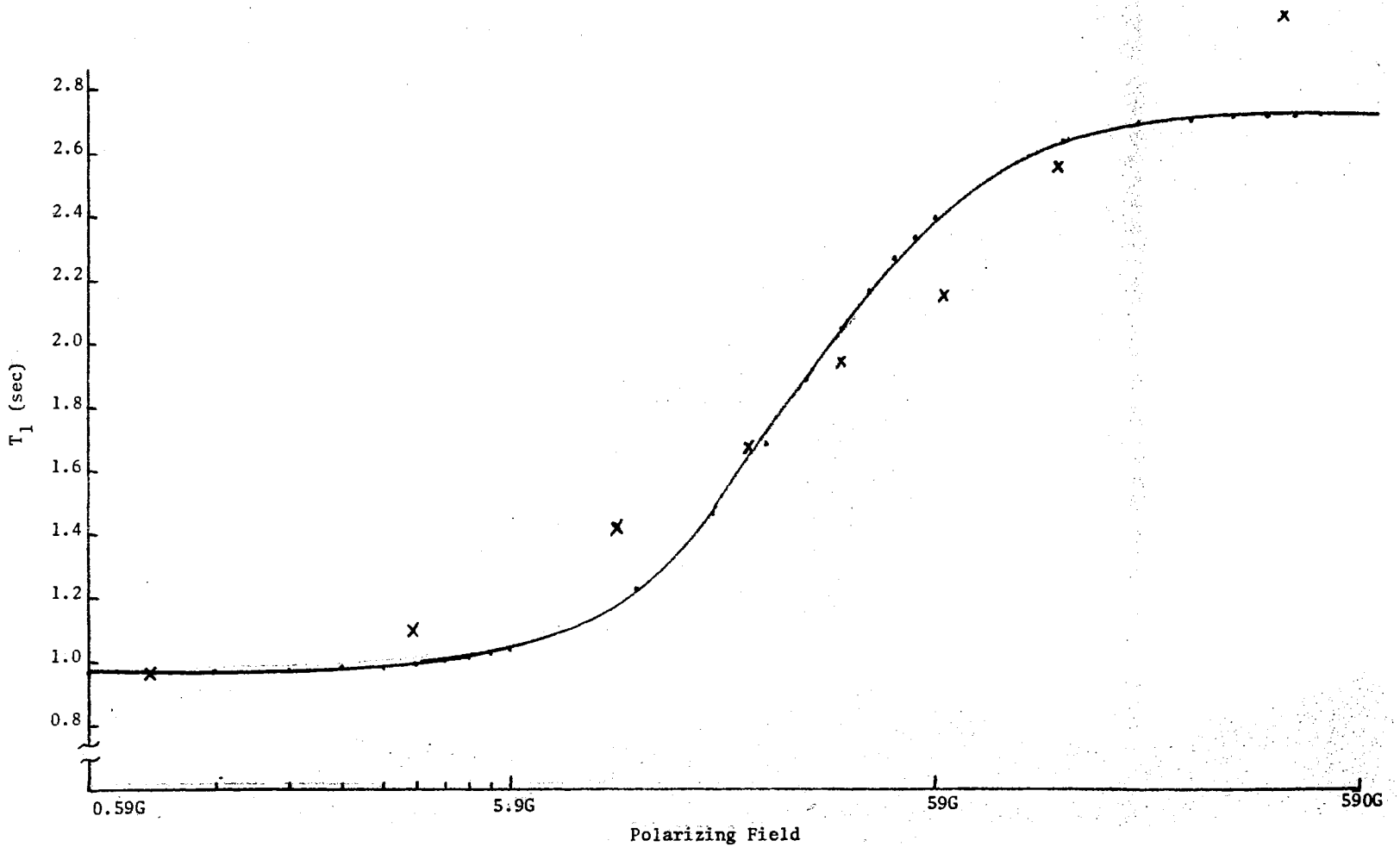

Figure 34. Least-squares Fit to Deuterated 8% by Weight SiO_2 Ludox LS Field-dependence Data at pH 6.00 and at 40°C. The crosses represent the data points. See Table XIV for the least-squares parameters.

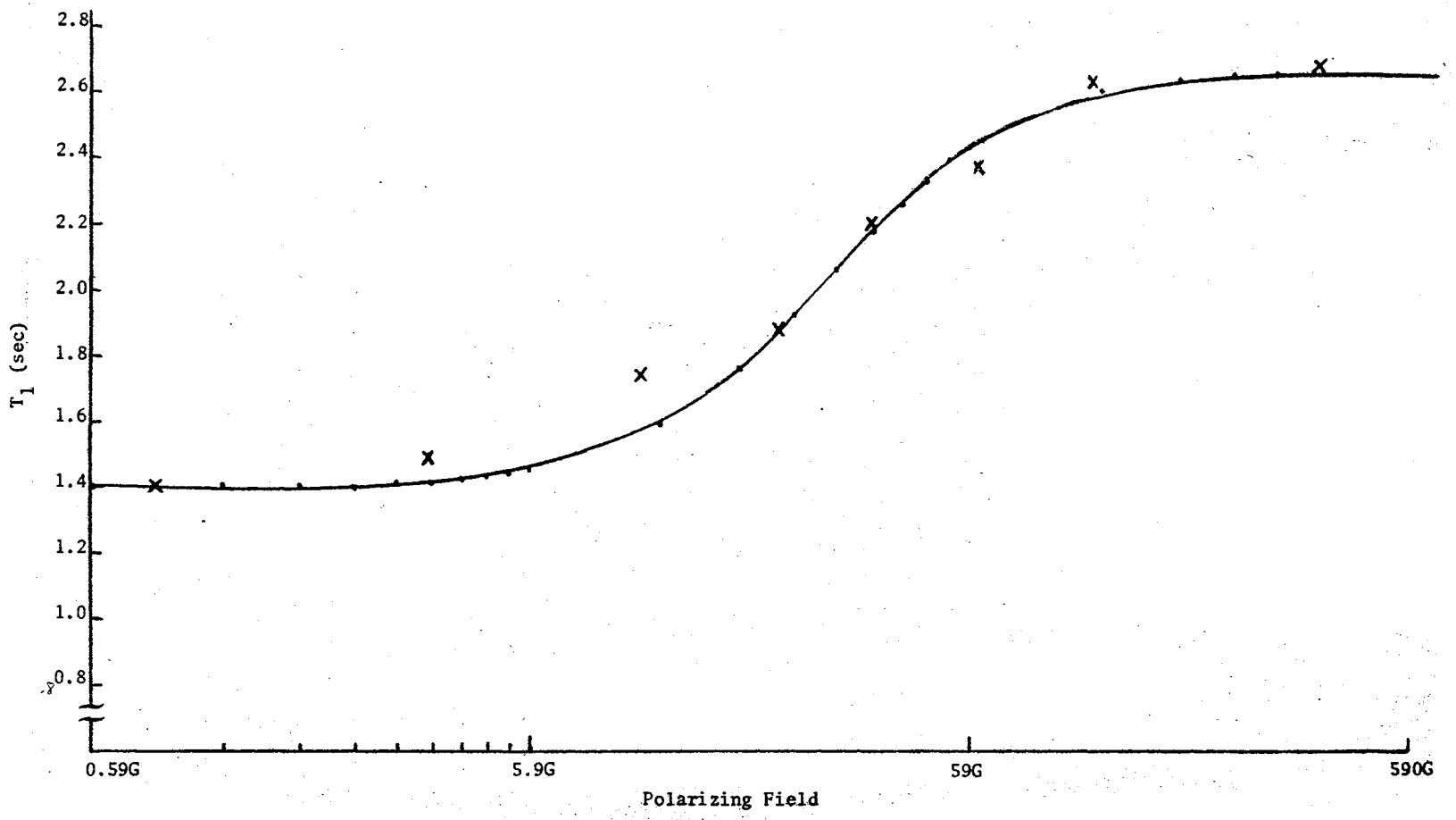

Figure 35. Least-squares Fit to Deuterated 8% by Weight SiO_2 Ludox LS Field-dependence Data at pH 7.00 and at 40°C. The crosses represent the data points. See Table XIV for the least-squares parameters.

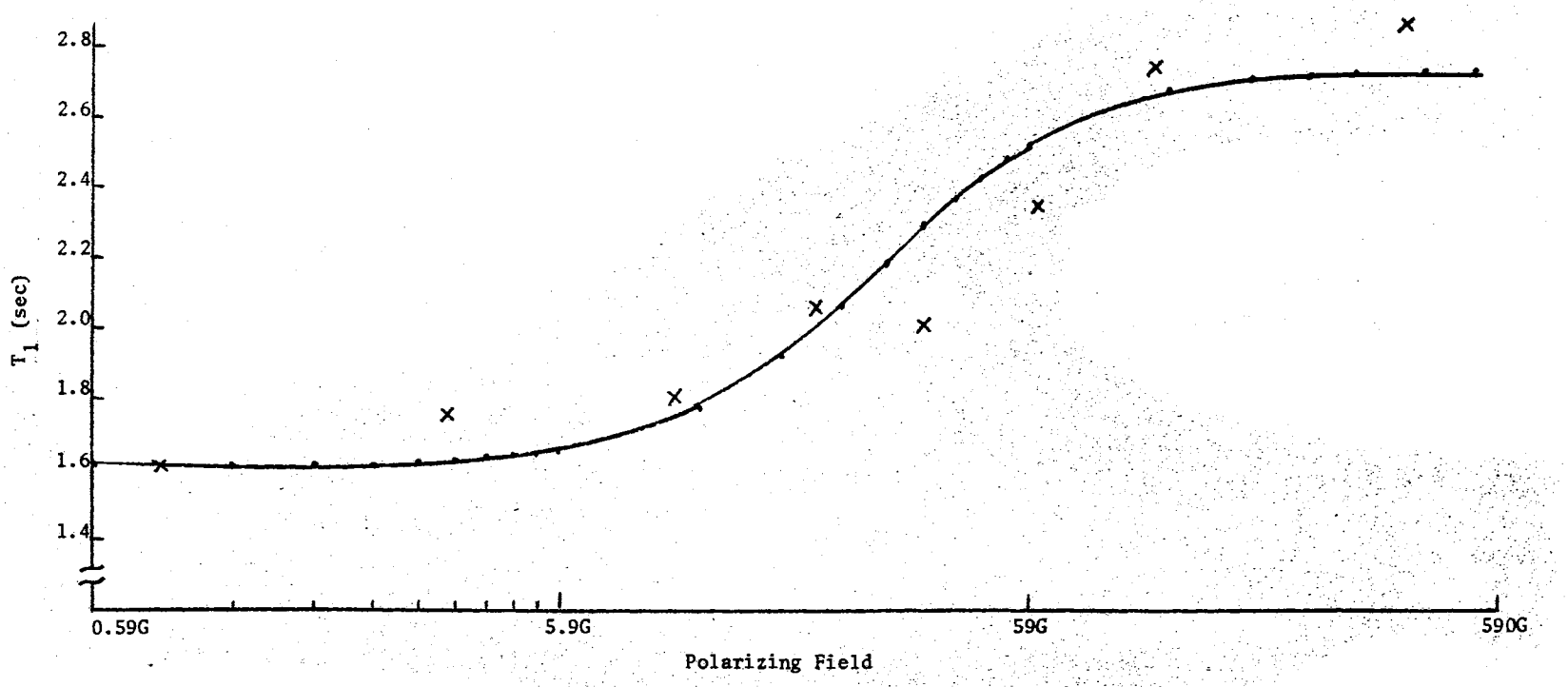

Figure 36. Least-squares Fit to Deuterated 8% by Weight SiO_2 Ludox LS Field-dependence Data at pH 9.00 and at 40°C. The crosses represent the data points. See Table XIV for the least-squares parameters.

TABLE XIII

LEAST-SQUARES PARAMETERS DERIVED FROM THE FIELD-DEPENDENCE OF 8% BY WEIGHT SiO_2, LUDOX LS

Indicated pH	Data Set Number	$Kx10^{-8}$ (sec^{-2})	$\tau x10^{9}$ (sec)	T_{1hf}	Temperature
1.15		5.00	1.50	1.48 sec	40°C
2.00		4.10	5.34	1.43 sec	40°C
3.10[1]		3.28	9.65	1.43 sec	40°C
4.00	1	3.28	9.83	1.60 sec	40°C
4.00	2	3.39	9.82	1.53 sec	40°C
5.00	1	3.55	8.04	1.68 sec	40°C
5.00	2	3.41	7.47	1.73 sec	40°C
6.00	1	2.80	3.56	1.75 sec	40°C
6.00	2	3.10	2.93	2.17 sec	40°C
7.00	1	1.86	2.35	1.73 sec	40°C
7.00	2	2.97	2.38	1.84 sec	41°C
9.00		1.65	2.15	1.78 sec	40°C

[1]At 16% by weight SiO_2, a least-squares fit yielded $K=2.56x10^{8}$, $\tau=10x10^{-9}$, and $T_{1hf}=1.03$ sec, showing that the derived constants behave in the expected manner as the concentration is varied.

TABLE XIV

LEAST-SQUARES PARAMETERS DERIVED FROM THE FIELD-DEPENDENCE OF 8% BY WEIGHT SiO_2, DEUTERATED LUDOX LS (α = 0.22)[1]

Indicated pH	Data Set Number	$Kx10^{-8}$ (sec^{-2})	$\tau x10^{9}$ (sec)	T_{1hf}	Temperature
2.04	1	1.91	5.96	1.76	40°C
2.04	2	2.13	5.32	1.80	40°C
3.00	1	1.41	9.68	2.05	40°C
3.00	2	1.58	8.65	2.10	40°C
4.00	1	2.02	5.94	2.37	40°C
4.00	2	1.88	6.16	2.38	40°C
4.90	1	1.40	8.37	2.46	40°C
4.90	2	1.46	8.30	2.57	40°C
6.00	1	1.94	3.41	2.74	40°C
6.00	2	1.73	4.42	2.75	40°C
7.00	1	1.20	2.83	2.67	40°C
7.00	2	0.944	4.16	2.66	40°C
9.00	1	0.940	2.60	2.49	40°C
9.00	2	0.986	2.03	2.74	40°C

[1]The pH 1 data are missing, due to the impossibility of maintaining α at this pH. The increased scatter in the data reflects the fact that the assumed relation (see text) does not represent the deuterated samples as well as it should.

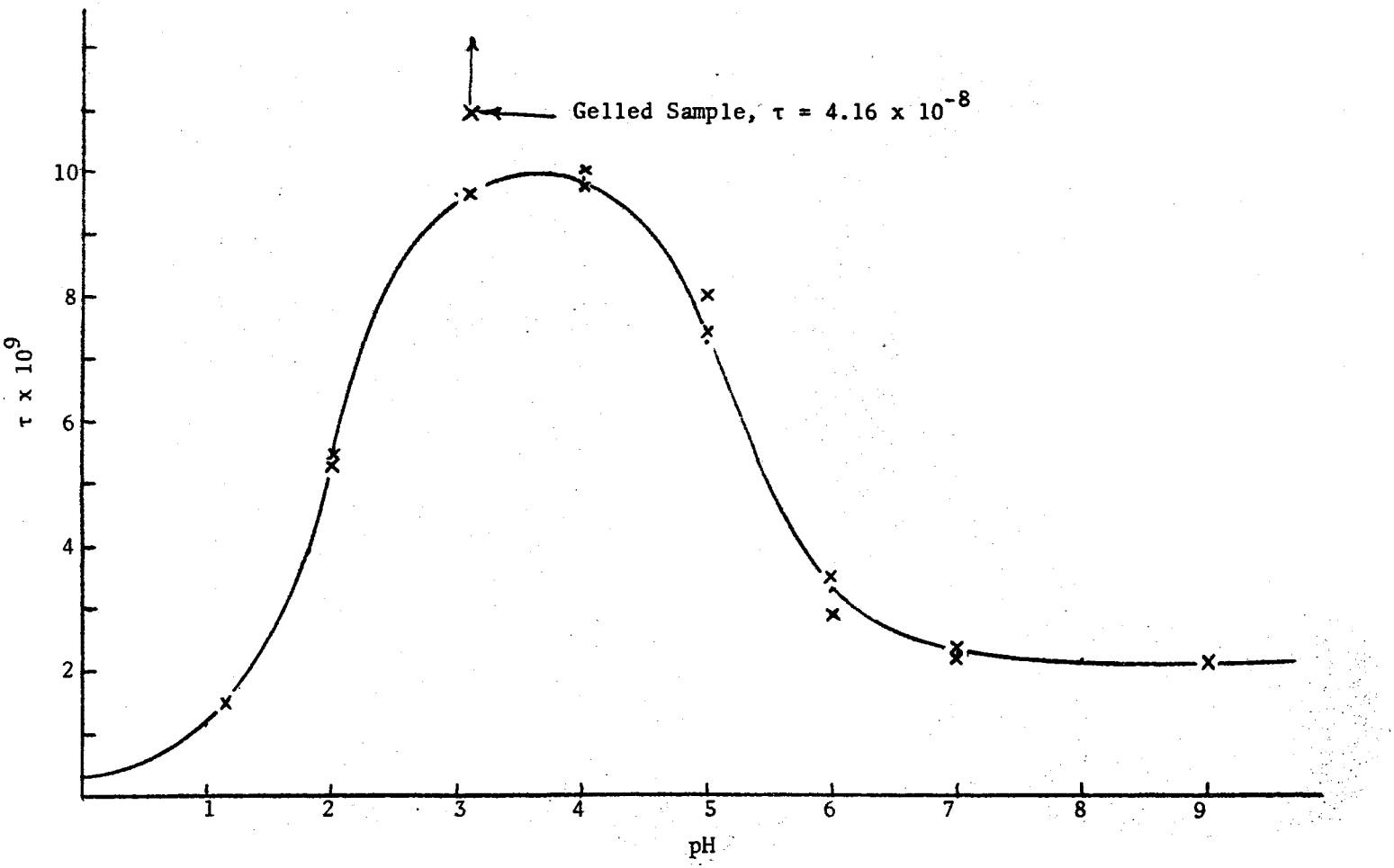

Figure 37. τ vs pH for 8% by Weight SiO_2 Ludox LS as Derived From the Preceding Field-dependence Plots. The isolated data point represents the τ typical of a gelled colloid.

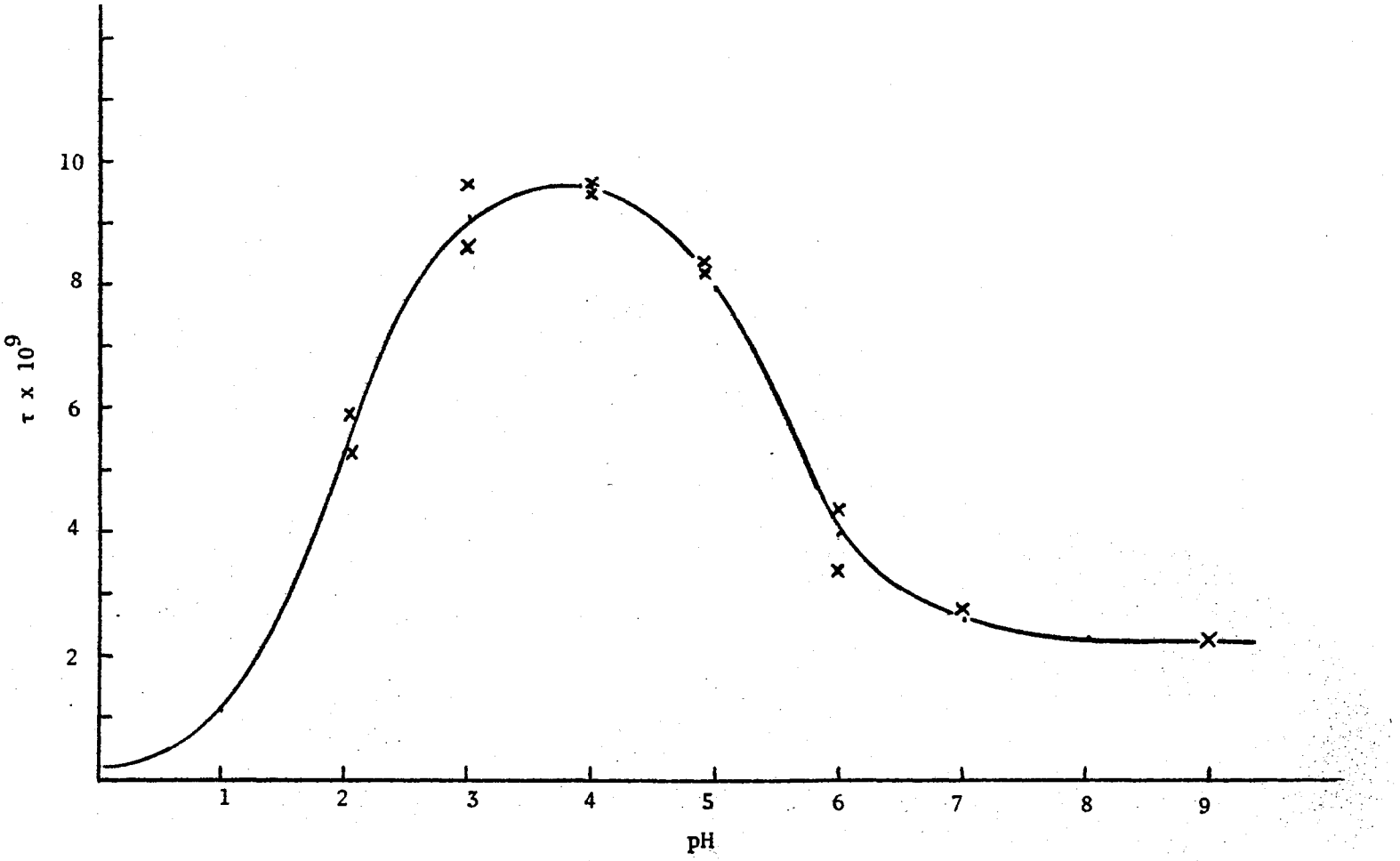

Figure 38. τ vs pH for 8% by Weight SiO_2 Deuterated Ludox LS as Derived From the Preceding Field-dependence Plots

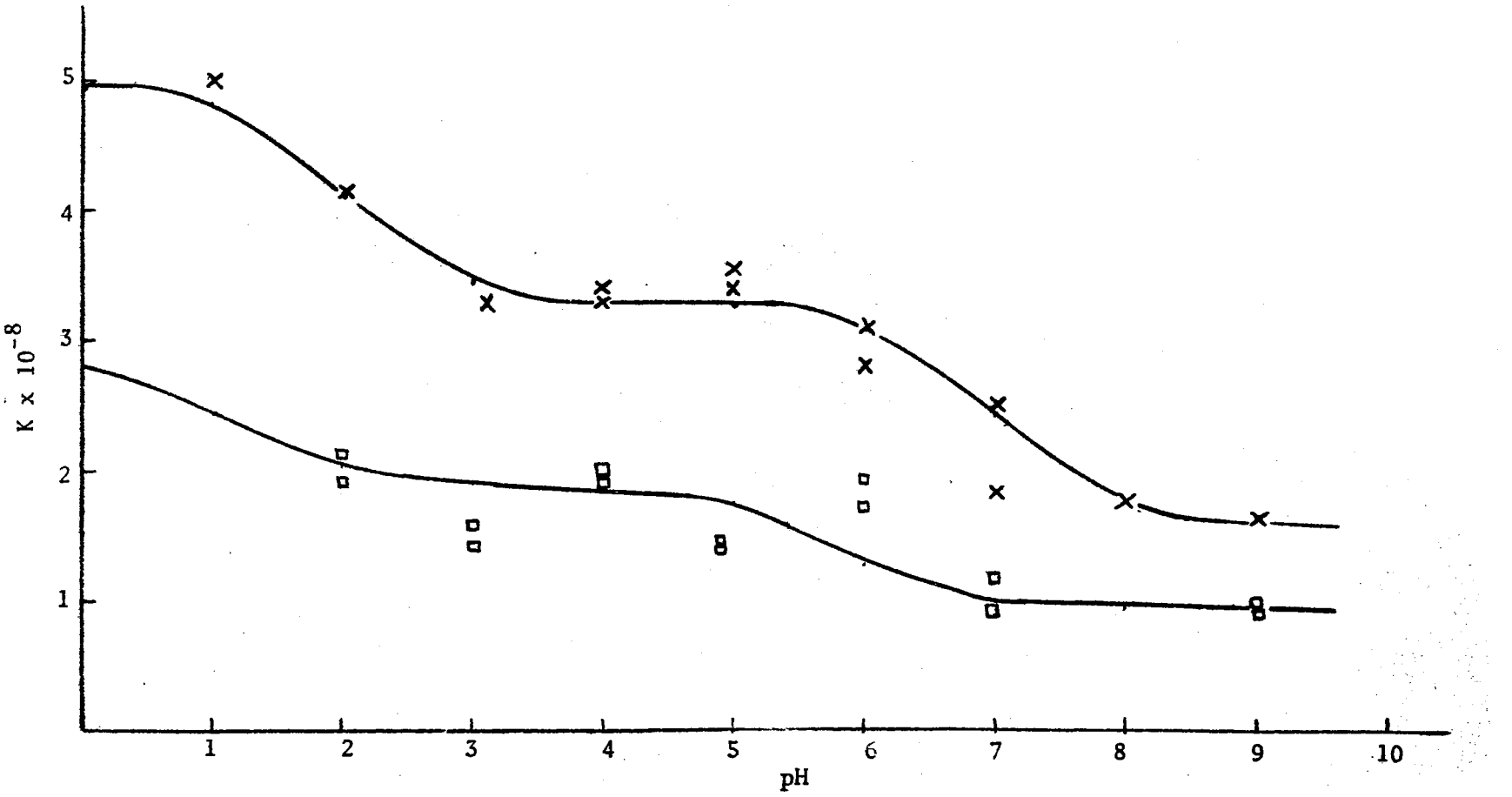

Figure 39. K vs pH for 8% by Weight SiO_2 Ludox LS as Derived From the Preceding Field-dependence Plots. Squares: deuterated samples; crosses: undeuterated samples.

the gelation experiments at pH 9 (to be described later), it is now felt that the increased NaCl concentration cannot account for the results we are about to describe.

Table XV shows that the low-field results were found to be reversible whereas the high-field results were not -- a situation which indicates that the value of T_1 at high fields was not directly related to the mechanism giving rise to the observed field-dependence. Furthermore, since the high-field relaxation rate irreversibly increases with decreasing pH, it seems highly likely that it is the result of a paramagnetic ion which dissolves into the bulk solution as the pH is reduced. When we begin to present our explanations for the total experimental results it will be seen that this interpretation is consistent with the activation energies obtained by measurement of the temperature-dependence of T_1.

Unfortunately, this particular experiment was performed prior to the detailed investigation of τ vs pH, and the complete field-dependence curves were not obtained as a result of our ignorance of their importance. Although it is strongly felt that τ had returned to its initial value, we cannot unequivocally state that that was the observed result.

The pH-dependence of Aqueous $FeCl_3$ Solutions

In previous sections we have alluded to the fact that T_1 seemed to be controlled by iron impurities, and it was of interest to determine whether or not such iron impurities could be expected to produce the observed pH-dependence. Toward that end, we produced several aqueous

$FeCl_3$ samples and subjected them to a measurement of T_1 vs pH.[2]

TABLE XV

DATA EXHIBITING THE HYSTERESIS IN THE HIGH-FIELD RESULTS WITH pH

	T_1	Field	Temperature
Sample Returned to pH 9 (from pH 1.15)	1.66 sec	392 G	40°C
Average Over Four Measurements	1.03 sec	0.991 G[1]	40°C
pH 9 Sample	1.92 sec	381 G	40°C
Average Over Four Measurements	1.09 sec	1.24 G[1]	40°C

[1]Polarizing and earth's field, combined.

Table XVI shows the results of such a series of measurements and demonstrates the fact that the observed pH-dependence was quite different from that observed in the Ludox series of colloids. Hence, we conclude that the presence of the colloid is very necessary if iron is assumed to control the proton T_1.

[2]In all cases, the iron concentration was kept below the so-called "mononuclear wall" (10^{-4}M). In this way one can avoid the production of iron polymers.

TABLE XVI

T_1 IN 6×10^{-5} MOLAR $FeCl_3$ SOLUTIONS AS A FUNCTION OF pH[1]

pH	T_1	Field	Temperature
1.00	0.600 sec	404 G	30°C
2.15	0.800 sec	404 G	30°C
2.70	1.00 sec	389 G	30°C
4.00	2.74 sec[2]	392 G	30°C
10.5 → 2.00	1.57 sec	398 G	30°C

[1]Note (1) that T_1 and T_2 were always identical (T_2 measured at 0.54 G), and (2) that the data were not reversible, as indicated by the last line, where an initially pH 10.5 sample was reduced to pH 2.00.

[2]This is identical to T_1 in distilled H_2O at 30°C.

T_1 in Gelled Colloids

During the first experiments with the Ludox series of colloids, we had felt that the rotational correlation time of the colloidal particles was probably important. For that reason, a pH 9 sample of Ludox LS (8% by weight SiO_2) was gelled through the action of some added reagent grade NaCl and since T_1 remained essentially unchanged, it was assumed that further experiments of this type were of little interest.

After the pH-dependence of T_1 was investigated, a number of samples in the pH 4-pH 6 range were on hand which eventually gelled. A reexamination of the gelled samples revealed that the low-field T_1 had decreased significantly and for that reason we attempted to reproduce the effect under more carefully controlled conditions.

The first experiments were therefore designed to reveal whether or not the way in which a sample was gelled had any influence on T_1. We allowed samples to gel by (1) heating to 80°C and holding for 24 hours, (2) by adding NaF or NaCl and (3) by aging. Once stable samples were obtained, T_1 was the same for any of the three methods and we concluded that the precise history of the sample was unimportant. Although there was some initial difficulty in obtaining stable samples the following procedure was found to eliminate the problem:

1. The pH was reduced to the desired value and T_1 was measured as a function of field at 40°C;
2. The sample temperature was elevated to 80°C and held there for 24 hours;
3. After the temperature was once again lowered to 40°C T_1 was measured as a function of field (the sample was gelled at this point);
4. Steps 2 and 3 were repeated until no further changes in T_1 could be detected.

The aged samples, on the other hand, were measured once each week until no further changes could be detected. This was a time-consuming process and could only be taken to completion in the case of the least stable samples. Typical aging times were on the order of three months.

Once stable gels had been formed, it was found that K and τ had undergone significant changes (see Figure 37). Although K did not change appreciably, the increase in τ was quite large.

Although we have indicated that we do not believe τ to be a rotational correlation time, it should be pointed out that when some samples are gelled at pH 4 it is possible to demonstrate that the relaxation

rate per unit surface area is independent of the colloid being examined (see Table XI, and compare Ludox LS, SM and HS which were all intentionally adjusted to have identical specific surface areas), whereas such was not the case prior to gelation. Were it not for our other experimental results, this would certainly seem to indicate that the particle correlation time is important near pH 4. However, it is necessary to continue with the presentation of the data before any further interpretation is attempted.

The Equality of T_1 and T_2 at Low Fields

In many of the experiments that are reported here, we have used either the measurement of T_2 in the earth's field or the measurement of T_1 at 1 gauss to define the low-field limit of T_1. This procedure is justified because, as Table XVII shows, it has been verified by experiment that $T_1 = T_2$ at these fields. The measurement of T_1 at 1 gauss was preferred on the basis of experimental expediency, since it was time consuming to change the EFFP apparatus' pulsing units over to the configuration necessary for an accurate T_2 measurement. Furthermore, the field-gradients at the sample coil were subject to daily (and even hourly) fluctuations, making it necessary to remeasure T_2^* each time a T_2 measurement for a colloidal sample was required. For these reasons, the measurement of T_2 was not a routine procedure and was undertaken only when a new type of sample was under initial examination.

The Temperature-dependence of T_1

Ideally, one would measure the temperature-dependence of T_1 as a function of pH and field in both liquid and gelled samples. However,

over much of the pH range of interest, the samples are not stable, and the act of heating them produces permanent (and measurable) changes. This has restricted the measurements to those samples which were stable against heating and has eliminated large segments of the pH range from further consideration. The situation was probably not too serious, because later evaluation revealed that the activation enthalpy is only weakly influenced by pH changes, field changes, and gelling.

TABLE XVII

A COMPARISON OF T_1 AND T_2 IN DEUTERATED LUDOX LS SAMPLES AS A FUNCTION OF THE DILUTION PARAMETER α[1]

α	T_1 at 1 G	T_2 at 0.47 G
1.0	0.280 sec	0.280 sec
0.45	0.620-0.680 sec	0.660 sec
0.22	1.60 sec	1.60 sec

[1] T_2 corrected by a T_2^* of 7.50 sec, and α referred to solvent water, exclusive of suspended solids.

All measurements were taken with the sample in an unsilvered vacuum DeWar flask.[3] The temperature was initially set in a Haake liquid bath to within $\pm$ 0.1°C and then the sample was transferred to the sample

[3] Because of eddy currents, a completely silvered flask will reduce the coil inductance and Q. It was therefore, necessary to use either a "partially silvered" flask, in which insulating strips are left behind, or to leave the silvering out altogether.

coils. The temperature was then monitored by visual inspection of a mercury thermometer which was permanently installed in the DeWar. Some attempts were made to use a remote reading thermistor thermometer, but when it was discovered that the thermistor probe reduced T_2^* the attempt was dropped. Finally, it should also be mentioned that an in situ temperature controller was available in which a thermally controlled liquid could be circulated about the sample of interest via an external jacket. It was found that the method had several disadvantages which forced us to abandon it, and these disadvantages were as follows:

1. Since the total volume that could be contained inside the sample coil was fixed, the presence of the jacket for the circulating liquid reduced the available sample volume to 200 ml. In cases where T_2^* was quite small, this reduced the S/N to a point where the measurements became very unreliable;
2. At the time these measurements were being made, the circulating liquid was water, doped with a paramagnetic ion to reduce T_2. Nevertheless, a brief signal from the circulating water could still be observed, and it masked the signal from the sample of interest for a sufficiently long time that, when the sample T_2 was short, it was necessary to wait for too long a time to measure the free-precession signal from the sample;
3. If a gelled sample was to be observed, it was virtually impossible to clean the container. Since it was a specially-constructed, double-walled container, it became a rather expensive proposition to discard it when the experiments were finished.

It should be mentioned that objection 2 was later eliminated by B. F.

Melton, who found a non-corrosive, non-toxic, proton-free liquid which could be used as the circulant.[4]

Figures 40 through 43 show the results of the temperature-dependence measurements, after correction for bulk water. The activation enthalpies, obtained from the simple Arrhenius expression discussed previously, are also shown. Note that very low activation enthalpies were obtained in all cases, and that in one case a negative result was obtained. The interpretation of these experiments will be considered in the next chapter.

[4]At the time of writing this thesis, the precise identity of the liquid was unavailable to the author, but memory seemed to indicate that it was a member of the Freon family. See Melton's Ph.D. thesis (54) for further details.

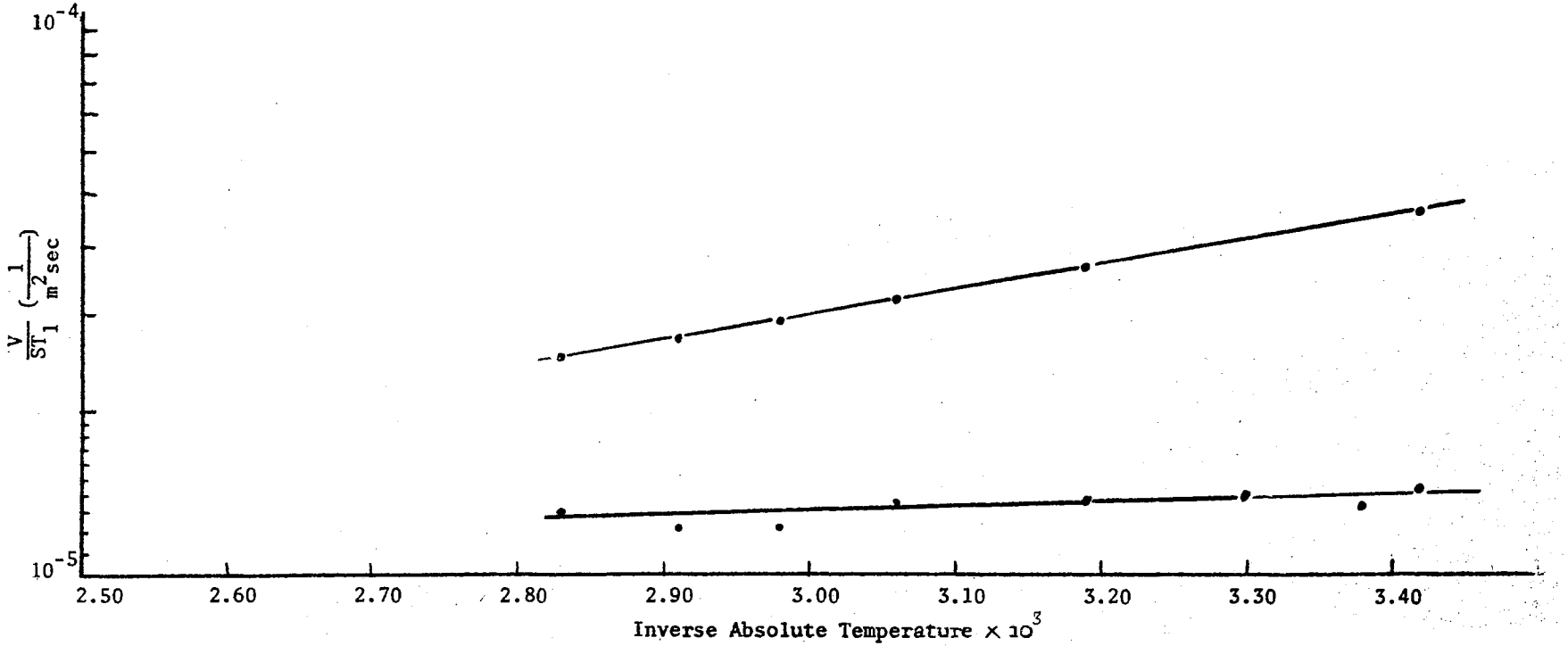

Figure 40. Reduced Relaxation Rate Versus Inverse Absolute Temperature for pH 9 Ludox LS. Upper curve taken at 1 G, E_a = 2.09 K cal/mole. Lower curve taken at 320 G, E_a = 4.30 K cal/mole.

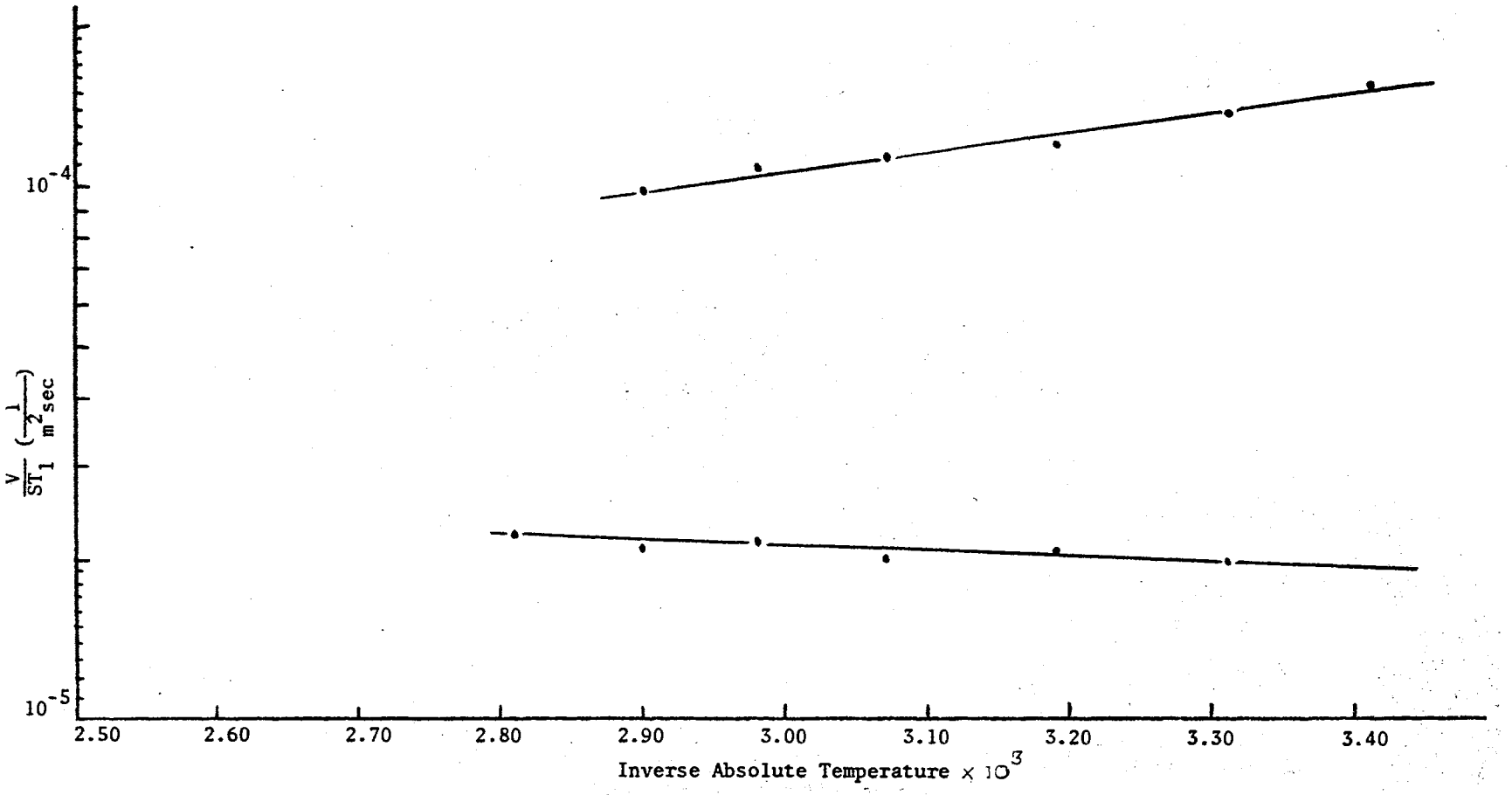

Figure 41. Reduced Relaxation Rate Versus Inverse Absolute Temperature for pH 2 Ludox LS. Upper curve taken at 1 G, E_a = 1.44 K cal/mole. Lower curve taken at 320 G, E_a = -0.771 K cal/mole.

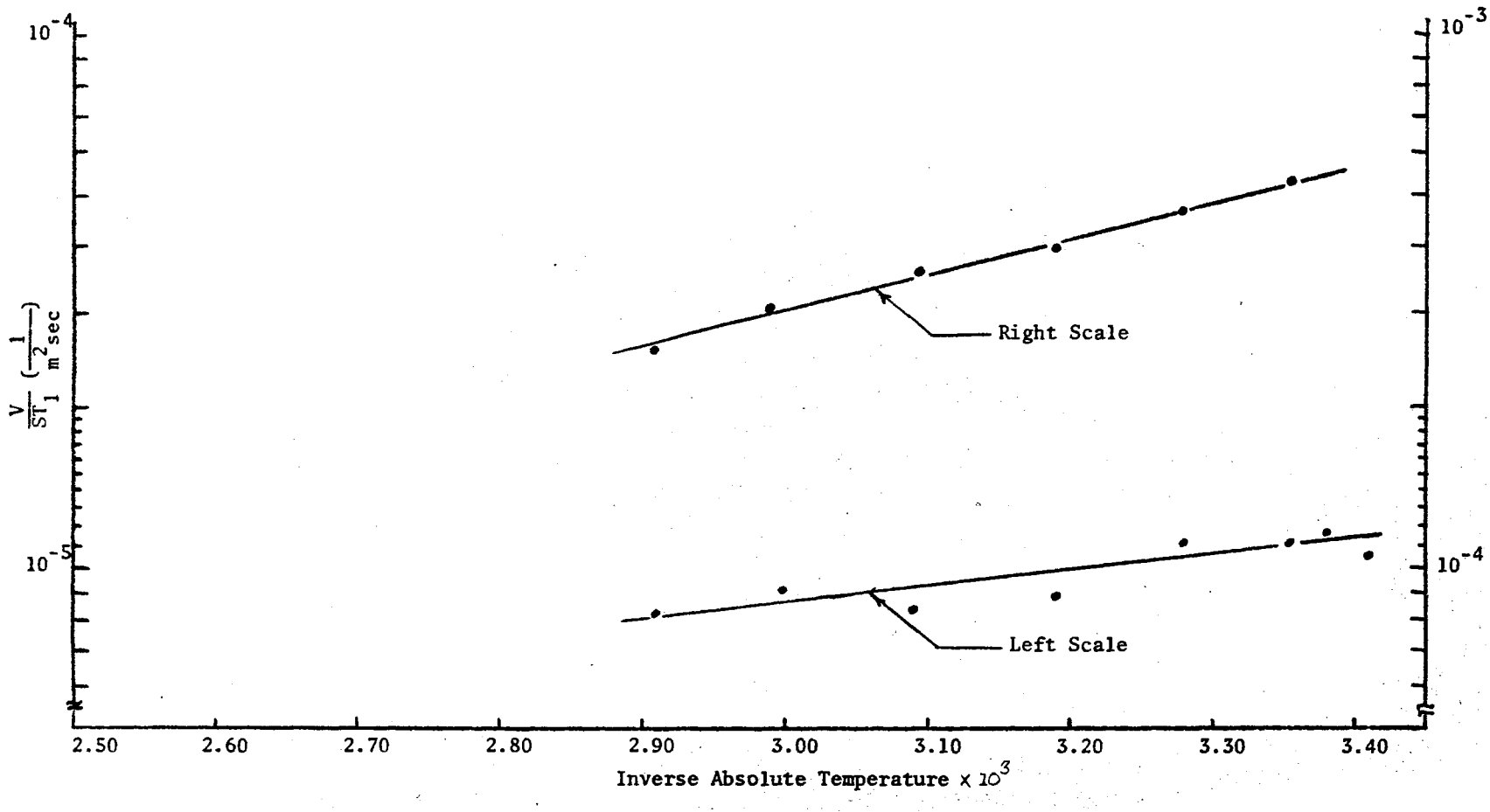

Figure 42. Reduced Relaxation Rate Versus Inverse Absolute Temperature for pH 4 Ludox LS Gel. Upper curve (right scale) taken at 0.54 G, E_a = 3.10 K cal/mole. Lower curve (left scale) taken at 390 G, E_a = 1.15 K cal/mole.

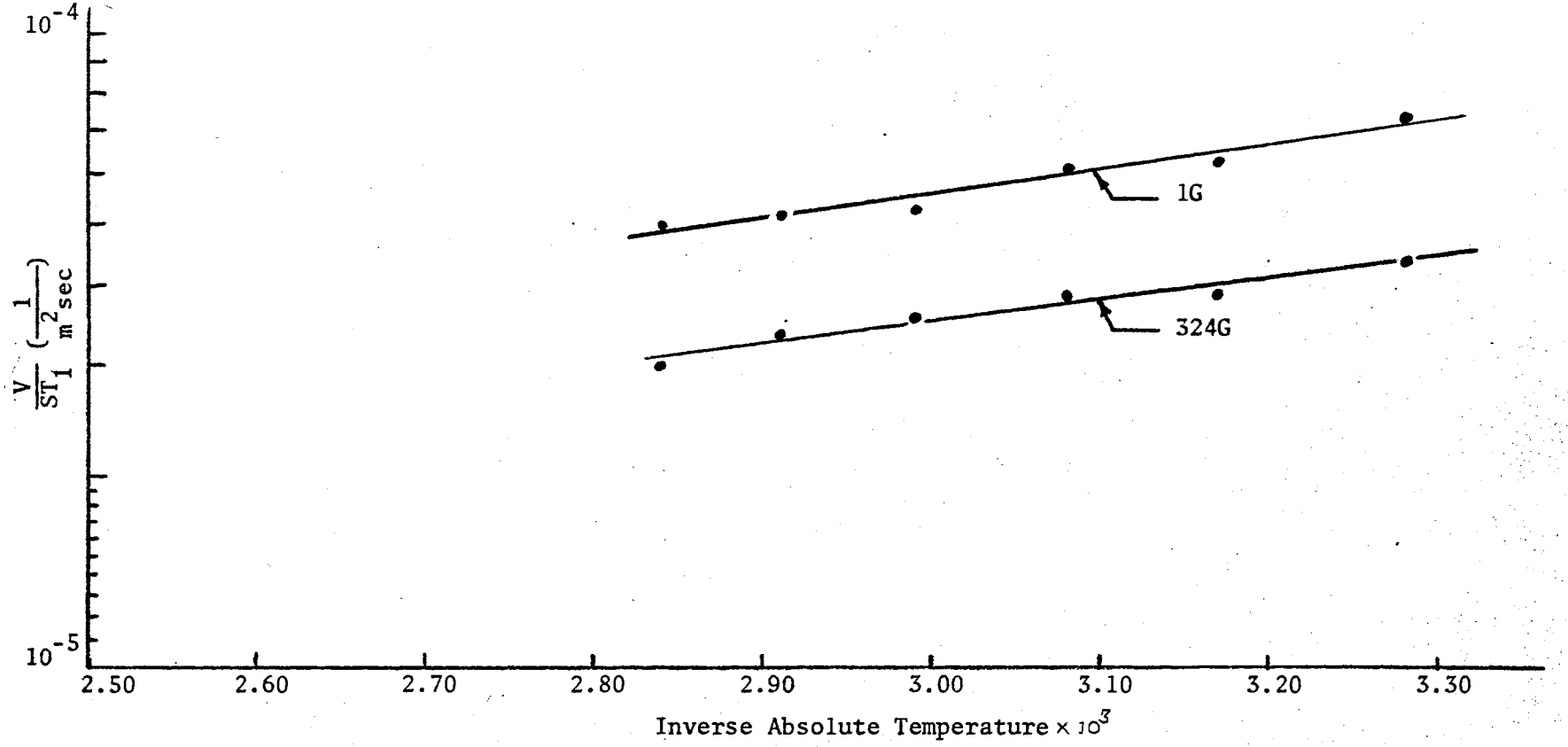

Figure 43. Reduced Relaxation Rate Versus Inverse Absolute Temperature for pH 9.5 Ludox HS. Upper curve taken at 1 G, E_a = 1.78 K cal/mole. Lower curve taken at 324 G, E_a = 1.56 K cal/mole.

CHAPTER VII

INTERPRETATION

A Qualitative Discussion of the Data

It should be obvious that the most interesting result of the previously described experiments is the variation of T_1 (and τ) with indicated pH[1] -- a variation probably related to a change in the physical and/or chemical properties of the colloid with hydrogen-ion activity, and one which may offer considerable insight into the dominant relaxation mechanism(s).

We categorize the pH-dependent mechanisms which may change T_1 in the following manner:

1. Electric field effects (through a change in the surface charge)
   a. Changes in the double layer thickness;
   b. Changes in the particle correlation time (through a change in the effective radius of the particle);
   c. Changes in the motional behavior of sorbed water molecules (e.g., anisotropic rotation due to the electric field).
2. Lifetime effects -- a change in the mean proton lifetime near the particle surface.
3. Chemical effects -- a change in the chemical state of the

[1]The term "indicated pH" is used here to designate the pH measured directly by a standard pH meter.

surface (number of adsorbed protons, change in the spin state of paramagnetic impurities, change in the type of reactive species present, etc.).

These effects are considered separately in the following paragraphs.

Electric Field Effects

One may consider the prime effect of an electric field to be one which inhibits the normal rotational motion of the dipolar water molecules, and under (1a) of the preceding list, we wish to consider the total number of water molecules so inhibited.[2]

If one takes the thickness of the double-layer to be the distance between the surface of the colloidal particle and that point at which the product of the electrostatic field by the electric dipole-moment of a water molecule is on the order of $kT(|\overline{E}| \cdot |\overline{P}| \sim kT)$ he finds that the thickness decreases with decreasing surface charge. If T_1 were to depend solely upon the total number of water molecules included in this region, its value would have to assume a maximum at the isoelectric pH, since it is at this point that the electric field is theoretically absent. (Li (47) has shown that for Ludox SM and LS the electric field is actually weak enough that, even at pH 9, $|\overline{E}| \cdot |\overline{P}| < kT$ at all distances from the particle surface). Hence, it is necessary to abandon the notion that this mechanism can qualitatively account for the observed results.

---

[2]An inhibited water molecule will either have an increased rotational correlation time, or else its motion will be describable in terms of more than one correlation time (anisotropic rotation). In either case, the observed T_1 will be inversely proportional to the total number of water molecules which can be considered to be "inhibited".

Under (1b), we consider a monolayer coverage of the colloidal surface, and assume that the water molecules are bound so rigidly that the rotational correlation time of the colloidal particle assumes control over T_1 through the intramolecular dipole-dipole interaction. Neglecting gelling effects, one expects the correlation time to decrease as the isoelectric pH is approached, and once again the low-field T_1 is expected to reach a maximum at zero surface charge. If a paramagnetic impurity were to dominate, and if that impurity controlled T_1 through its rotational correlation time, Equation 207 of Chapter V would apply with $\tau_c = \tau_r$ and a maximum low-field T_1 would still be expected near pH 4. Furthermore, if a rotational correlation time dominates through a paramagnetic complex (A = 0 in Equation 209), it is not possible for the ratio of T_1 at high-fields to T_1 at low-fields to exceed 10/3. The inclusion of any other field-independent relaxation mechanism must reduce this ratio, so that it represents an upper limit whenever the rotational correlation time of a paramagnetic complex is assumed to control the field-dependence of T_1. But the preceding data show that this ratio exceeds 10/3, in several cases, and we conclude that the value of T_1 cannot be simply dependent upon either the rotational correlation time of a colloidal particle or upon the tumbling rate of a paramagnetic complex.

One could attempt to salvage the situation by claiming that, near the isoelectric pH, the colloidal particles have partially agglomerated and that the rotational correlation time of an agglomerated group of particles is actually much longer than would be expected. However, when one recalls the experimental fact that the gelation of a pH 9 colloid changes T_1 only slightly, whereas the gelation of a pH 4 sample has

a profound effect upon the low-field T_1, he is again forced to reject the notion that the low-field value of T_1 is related in some simple way to the rotational correlation time of a group of colloidal particles.

Under (1c), we wish to briefly consider the effect of the electrostatic field on the motional behavior of those water molecules which are contained within the double-layer. Since the dipolar water molecules will tend to align themselves with such a field, τ_r will increase, and, at low magnetic fields, the value of T_1 will be shorter than that expected for the bulk water protons. Even if the motion is anisotropic, so that it is possible to assign more than one rotational correlation time to a "surface" water molecule, one is eventually led to the result that the low-field T_1 should reach its maximum value at the isoelectric pH, since at this point the electric field is absent. However, the experimental data show that the T_1 in question actually reaches a minimum near the isoelectric point, and this final contradiction leads one to the conclusion that it is not possible to assign the obvious electric field effects any dominant role in determining T_1.

Lifetime Effects

Equations 206 through 209 explicitly include a parameter τ_h which is the mean lifetime of a water proton in the hydration sphere of a paramagnetic ion. Equation 216 shows that, even where paramagnetic ions are not assumed to be present, the availability of multiple magnetic environments may be sufficient to produce a lifetime-dependent T_1 or T_2. It is therefore natural to inquire into the possibility that the parmeter τ_h may depend upon pH in such a way as to produce the observed results. Equation 216 can be eliminated from this qualitative discussion

on the grounds that (1) it does not explicitly account for the observed fact that the field-dependence of T_1 is a function of a pH-dependent correlation time, and (2) it predicts that, where τ_h dominates (and contrary to our experiments), one should expect to observe a T_1 which decreases with increasing temperature -- assuming, of course, that τ_h follows a simple Arrhenius law. We turn, then, to a consideration of Equations 206 through 209, since they do predict a field-dependence which changes with τ_h, and since they are also in keeping with the earlier finding that paramagnetic impurities control T_1.

Inspection of these equations reveals that, in the simplest situation (paramagnetic contributions only), we are suggesting that $\tau_c \tilde{\gtrsim} \tau_h$ (dipolar term) and/or $\tau_s \tilde{\gtrsim} \tau_h$ (scalar term). The most troublesome aspect of such an assumption will be due to the fact that one must take $\tau_h \ll T_{1e}, T_{2e}$ where T_{1e} and T_{2e} are the relaxation times for an electron spin. In studies of aqueous solutions of paramagnetic ions, one typically finds that $T_{1e} \sim 10^{-9} - 10^{-10}$ seconds so that it is of the same order of magnitude as the value we wish to assign τ_h. Fortunately, such electronic relaxation times are important to those who are doing Mössbauer spectroscopy of Fe^{3+} substituted into various crystalline solids, and it has been found that they are typically 10^{-7} seconds or longer (Poole gives 10^{-7} seconds as a lower limit to T_{1e} (47)). Hence, if the results are attributed to the Fe^{3+} present in the SiO_2 lattice, it is quite reasonable to take $\tau_h \ll T_{1e}$.

It should be reiterated at this point that, if the dipolar part of Equations 207 through 210 controls the field-dependence of T_1, one expects to have present a "10/3 affect", i.e., the ratio of the first high-field plateau in T_1 to the low-field limit of T_1 cannot exceed

10/3.[3] Since the experimental ratio has been observed to exceed 10/3, it is natural to assume that the field-dependence must reside in the scalar term, and in this assumption we would agree with D. Michel (39) who found a similar result in a colloidal silica of German manufacture (the present author reached this conclusion prior to the publication of Michel's work).

In summary, one can conclude that it is qualitatively reasonable to assume that lifetime effects will manifest themselves through a strong, paramagnetic, scalar interaction controlled by τ_h and arising from the presence of Fe^{3+} in the crystal lattice of SiO_2. It is an attractive assumption because it is in harmony with the experimental results, and especially, because it assigns a unique role to the "lattice iron" in good agreement with the washing experiment that was described earlier. One can even rationalize the high-field value of T_1 on the basis of non-lattice Fe^{3+} ions, and can invoke desorption phenomena at low pH to explain the fact that the restoration of the original pH does not result in the original high-field T_1 (hysteresis), whereas the low-field value is restored. Similarly, the "anomolous" temperature-dependence of the pH 1 high-field T_1 becomes understandable because it is precisely what one would expect from aqueous Fe^{3+} (see later paragraphs). For all of these reasons, our qualitative arguments show that this viewpoint is one which may have merit.

---

[3] The first increase in T_1 will be expected to occur when $\omega_s \sim 1/\tau_{c2}$. Since $\tau_{c2} \leq \tau_{c1}$, it is easily shown that the subject ratio cannot exceed 10/3. It may be argued (after Bloembergen) that as many as six electron relaxation times may be important, but the conclusion is valid even in that event.

Chemical Effects

It has been shown experimentally that the charging process in colloidal silica involves an excess of OH groups associated with the particle surface. Although the workers who performed this measurement took the viewpoint that excess OH-ions were actually adsorbed at the particle surface, it is equally plausible to assume that hydrogen ions were desorbed when excess base was added to the system. This would imply that in the discharging process the excess OH-ions on the surface combine with bulk protons to form bound water, and that the total water on the surface would then reach a maximum at the isoelectric point. If T_1 were to be inversely proportional to the surface occupation probability (see Equation 49) one would obtain the desired minimum at pH 4.

Measurements by Iler and others indicate that, below pH 9, the surface charge is never greater than about 8% of its maximum possible value (12,23). Since our own titration experiment tends to confirm this result for the case of Ludox LS, the percentage variation in the total number of bound water molecules is too slight to account for the strong pH-dependence at 1 gauss. Furthermore, such an assumption does not account for the variations in the correlation time, and it must therefore be considered to be unsatisfactory.

Returning again to the discussion of paramagnetic impurities, it is possible that the spin state of such an impurity will change with pH. For example, J. F. Gibson, et al. have observed that, in haemoglobin complexes, the Fe^{3+} ion may have a spin of either 5/2 or 1/2, depending upon the axial ligand (49). Since the spin appears explicitly in expressions for T_1 and T_2, it is conceivable that changes in complexing with a change in pH could be responsible for the observed results.

Furthermore, the spin appears in theoretical expressions for the electron relaxation times T_{1e} and T_{2e}, so that if one identified one of them with the dominant correlation time τ, it would be reasonable to expect it to change with pH. However, French and Howard (50) have noted that the spin state of Fe^{3+} is unchanged in the process of sorption onto silica gel and, moreover, the constant "K" derived from the least-squares analysis would reflect such changes through the (hidden) factor S(S+1). If the occupation probability were to remain constant, then the values S = 5/2, 3/2, 1/2 would produce a set of K values in the ratio 35:15:3, or roughly 12:5:1. This is quite different from the observed ratio of 3:2:1, and it would be a remarkable coincidence if the occupation probability varied simultaneously in such a way as to give the observed variation in K. For these reasons, we have abandoned this type of interpretation of the data.

One chemical effect which has not yet been considered in this section is a change in the surface occupation probability through stepwise dissociation. Such a mechanism can reasonably be expected to give a 3:2:1 ratio in K with increasing pH. Furthermore, this mechanism restricts any chemical reactions which may be proposed in a quantitative theory to those which will produce the expected "steps" in K.

Summary of Qualitative Discussion

The present author's reasoning has led him to look for a quantitative explanation under the following restrictions:

1. The intramolecular dipole-dipole interaction, normally assumed to be dominant in pure H_2O, cannot entirely explain the experimental results. Instead, one must assume that paramagnetic

impurities are present and, specifically, that the dominant impurity is Fe^{3+} substituted into the crystal lattice of SiO_2;

2. The scalar interaction dominates through the correlation time conventionally called τ_h;
3. The spin state of the iron probably does not change with pH;
4. The high-field T_1, which changes irreversibly with pH, is probably due to iron which desorbs from the colloidal particles, especially at low pH; and
5. The changes in K with pH are probably due to stepwise dissociation.

Aqueous Fe^{3+}

It is appropriate to digress momentarily to consider the type of behavior to be expected from an aqueous Fe^{3+} complex. It turns out that, at this writing, only a few of the important facts are known, and for these we have had to rely mainly upon the Ph.D. thesis of Judkins (51), who has made the following pertinent points:

1. First and second hydration sphere effects are both important;
2. The electronic T_2 is on the order of 10^{-11} seconds;
3. The lifetime of a water molecule (based on O^{17} resonance) in the first hydration sphere of $Fe(OH)^{2+}$ is roughly 10^{-7} seconds;
4. The lifetime of a water molecule in the first hydration sphere of Fe^{3+} is ca. 10^{-3} seconds;
5. The dominant O^{17} relaxation mechanism can be expressed as a combination of scalar coupling and the $\Delta\omega$ effect, with the dominant correlation time being controlled by the electron

relaxation time in the second hydration sphere. In the first hydration sphere T_2 is exchange limited (0^{17});

6. The proton lifetime on $Fe(H_2O)_6^{3+}$ is $4x10^{-7}$ sec at 25°C;
7. The proton lifetime on $Fe(H_2O)_5(OH)^{2+}$ lies between 10^{-8} and 10^{-10} seconds at 25°C; and
8. The activation enthalpy for water exchange never falls below 9 K cal/mole in either hydration sphere.

Clearly, these results are far different than those that have so far been induced for the dominant mechanism in colloidal silica. It is obvious that the exchange of whole water molecules is far too slow to account for the least-squares τ, and that the important correlation times are far too short to account for the observed field-dependence no matter what kind of paramagnetic interaction dominates. Hence, ordinary aqueous iron cannot begin to account for our low-field results, although it can account for the high-field limit of T_1. At pH 1, for example, we found a high-field T_1 which, after being corrected for the bulk water relaxation, decreased with increasing temperature whereas the low-field T_1 showed just the opposite behavior. This is an "anomolous" result in the sense that it cannot be rationalized on the basis of a single type of paramagnetic center. If aqueous Fe^{3+} is responsible for the high-field results, however, one can note that it should be predominantly $Fe(H_2O)_6^{3+}$ at pH 1, and that the proton lifetime τ_h is approaching the proton T_1 (which is conventionally called T_{1p} and which should be on the order of $7x10^{-6}$ seconds).[4] Since T_{1p} is dominated by the electron relaxation time, it will have only a slight temperature dependence

[4]This value is obtained with $A/h = 5 \times 10^6$ sec^{-1} and $S = 5/2$.

whereas τ_h should follow an Arrhenius law. Hence, if the expression

$$\frac{1}{T_{1(obs)}} = \frac{P}{T_{1p} + \tau_h} + \frac{1}{T_{1(H_2O)}} \tag{218}$$

is valid, the observed T_1 should decrease with increasing temperature (after the correction for $T_{1(H_2O)}$ because τ_h will decrease rapidly enough to dominate the first term. Thus, Judkin's results are in apparent agreement with the fourth point made in the summary of the qualitative arguments. They are in agreement at higher pH values too, because the presence of $Fe(H_2O)_5(OH)^{2+}$ should so drastically reduce τ_h that the normal type of temperature-dependence should be observed, and because the dominance of an electron relaxation time should produce low activation enthalpies of the type derived from our high-field data (42).

Phenomenological Theory

The pH-dependence

In order to obtain an interpretation of the fact that τ_h changes with pH, one can look to phenomenological chemical kinetics. Specifically, one can search for a set of acid and base-catalyzed reactions which "explain" the fact that τ_h is very short when either excess acid or base is present. It must be recognized, however, that the uniqueness of any set of reactions will necessarily be an open question, if for no other reason than that the nature of the colloidal particle surface is very poorly understood. Therefore, the author states at the outset that he only intends to show that such an explanation is reasonable and can "explain" the observed behavior; it is not his intent to lay claim to the fact that he has found the reactions which are actually

operative. In fact, such a selection does not appear to be possible unless a whole new study is undertaken. The kinetic details of even the aqueous Fe^{3+} system are not yet available, but if the recent study of aqueous Al^{3+} can serve as a guide (52), they will probably turn out to be rather complicated, and their elucidation will not be a short-term affair. Hence, the study of the surface Fe^{3+} kinetic mechanism was considered to be too far beyond the province of the present effort, which was necessarily limited to the study of PMR in colloidal silica.

Returning to the prime topic of this section, we note that base and acid-catalyzed exchange can be represented by reactions of the type

$$A \underset{k_{-1}}{\overset{k}{\rightleftharpoons}} C^* \tag{219}$$

and

$$C^* + D \xrightarrow{k_2} E + F \tag{220}$$

where C* is some species which is particularly reactive, where D is an acidic or basic group, and where either E or F is chemically (but not magnetically) identical to A. It is, of course, assumed that A carries all of its "tagged" protons with it when it is converted into C* (e.g., by the addition of a solvent proton to its second hydration sphere).

If one solves this system for the mean lifetime for proton exchange between A and F, defined by

$$\tau_{AF} = [A_0]^{-1} \int_0^\infty \frac{d[F]}{dt} \cdot t \cdot dt \tag{221}$$

where a group of tagged protons is assumed to reside on the species A at $t = 0$, and where $[A_0]$ is the equilibrium concentration of chemical species A (which is now assumed to be identical to E), he finds that if

$k_2[D] >> k_{-1}$

$$\tau_{AF} = (k_2[D])^{-1} + k_1^{-1} \quad . \tag{222}$$

This expression can be converted into the mean proton lifetime on a particular iron species by means of including certain multiplicative constants (statistical factors), and it is therefore useful in testing the idea of catalyzed exchange by applying it to the extremes of the pH region studied.

In the case of the base-catalyzed exchange of tagged protons between an Fe^{3+} complex (A) and the solvent water, one would identify D as the OH-ion complex. Ignoring statistical factors, the expression for τ_h at high pH would then take the form

$$\tau_h = \frac{[H_3O]}{k_2K_w + k_1^{-1}} \tag{223}$$

where K_w is the ion product for water. Such an expression has the correct functional form to fit the high pH data, but it is easy to show that it is not acceptable.

From the τ vs pH data, it is obvious that k_1 must be on the order of 10^9 per second. Since the curvature in the τ vs pH plot should first be noticed when the pH is reduced to the point where

$$\frac{[H_3O]}{k_2K_w} \sim k_1^{-1} \tag{224}$$

and inspection of Figure 37 reveals that this happens when $[H_3O] \sim 10^{-6}$, one can estimate that k_2 should be on the order of 10^{17} per mole-second. This value is clearly too large to be reasonable, and we conclude that the idea of a base-catalyzed exchange, as contained in

Equations 219 and 220 is not applicable to the high pH region.

In the low pH region (and again neglecting statistical factors), one would consider that species D should be the H_3O^+ ion, and he would obtain a mean lifetime of the form

$$\tau_h = k_2^{-1} [H_3O]^{-1} + k_1^{-1} \tag{225}$$

This also has the desired functional form since, as $[H_3O]^+$ gets very large, τ_h approaches the limiting value k_1^{-1}. Taking k_1 as 10^9 per second (which is probably too small), and assuming that $k_2[H_3O] \approx k_1$ at pH 2, one finds that k_2 is on the order of 10^{11} per mole-second and, unlike the previous situation, acid-catalyzed exchange is not an obvious candidate for rejection.

Further High pH Mechanisms

Considering the high pH region further, one could speculate that the same reaction scheme which leads to stepwise dissociation (to produce the changes in the value of K) could also be invoked as a means to obtain proton exchange. However, such an assumption invariably leads to a situation in which the high pH "step" in K can be related to the equilibrium constant for the reaction which is assumed to dominate. In fact, when considering the reactions normally operative for aqueous Fe^{3+}, one finds that the pH at which the step occurs is equal to the pK of the dominant exchange reaction. At high pH, the equilibrium stant, K, for the reaction in question will have to be on the order of 10^{-6}. Since $K = k_f/k_r[OH]$, and since the experimental data demand that $k_f \approx 10^9$ sec^{-1}, one obtains the unreasonable result that $k_r[OH] \approx 10^{15}$ sec^{-1}. It appears that no amount of improvisation will allow this

difficulty to be defeated, and we have therefore abandoned this sort of scheme also.

Having abandoned base-catalysis and stepwise dissociation as possible explanations for the high pH variation in τ, we are left with (1) concerted exchange, which is supposedly not diffusion limited, and (2) the assumption that the exchange rate is set by the major iron species present and that this exchange mechanism is neither base-catalyzed nor directly related to the mechanism which produces one iron species out of another.

We can adopt a combination of the preceding ideas, and it may be noted that one very simple reaction which is satisfactory is the two-center mechanism shown in Equation 226.

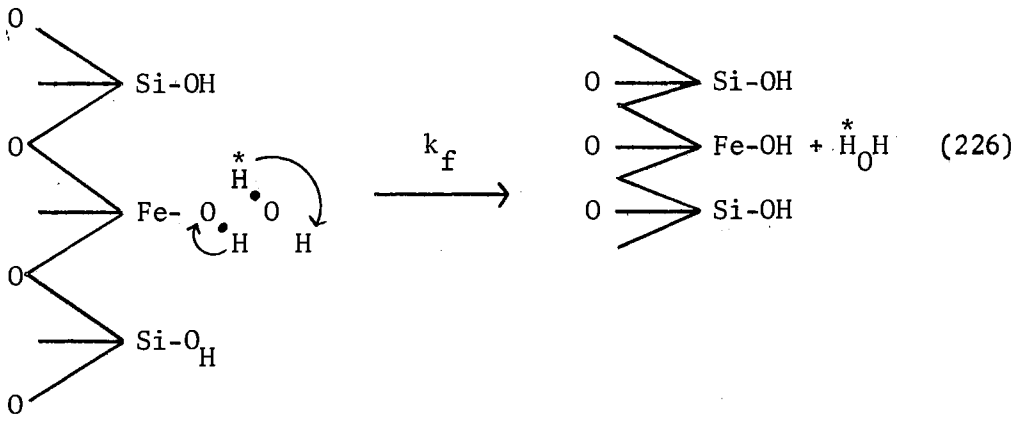

(226)

Such a mechanism is certainly not new, and it could satisfy the high pH requirement with $k_f \gtrsim 10^9$ sec^{-1}.

At this point we must reiterate our previous statements that, in view of the fact that the chemical states accessible to the surface Fe^{3+} are unknown (ESR does not "see" surface ions due to the large crystal field gradients near the surface, and so such measurements do not reveal the nature of the surface) and, moreover, that the kinetics

applicable to aqueous Fe^{3+} are poorly understood, we are left with very few guidelines in selecting our reaction scheme. We are, in fact, subject to the same difficulties which are encountered by catalytic chemists when they attempt to explain surface catalysis by such metal ions; namely, that the nature of these ions and of the local lattice which surrounds them is virtually unknown. The only fact which has been clearly established is that such ions can be involved in chemical reactions which are otherwise impossible. Our viewpoint has therefore been that we can only show that a chemical kinetic expression can in principle predict the appropriate correlation time, and toward that end we have chosen to use the simplest possible reaction scheme, even where it may be in disagreement with the type normally assumed for aqueous iron complexes. At the same time, we have attempted to maintain its reasonableness by seeing to it that it does not disagree with the few data which are available, and this seems to be the most progress we can make at present. Unfortunately, the deuteration data have been of little assistance in this matter, and we consider that question next.

It is obvious from the deuteration data that any kinetic isotope effect which exists is too small to be detected by the procedures we have used. This result is satisfactory in the respect that it is consistent with the D_2O dilution experiment, but it is less than one would hope for. Our results imply either that the force-constants at an exchange site do not change very much with isotope substitution, or that a secondary isotope effect dominates. In view of the fact that, in aqueous solution, the proton which is exchanged is commonly involved in bonding, it seems difficult to support the notion of a secondary isotope effect. It may be noted, however, that in at least one case --

that of aqueous Al^{3+} -- it has been proposed that a transition state involving $Al^{3+}(OH)\cdot(H_3O)$ can exchange whole hydronium ions at a very rapid rate (52). In this situation, the rate of proton transfer is limited by the rate at which H_3O ions are exchanged and one could envision the possibility of a secondary isotope effect.

In developing our scheme, we also take note of the fact that ion-exchange measurements indicate that, where an excess negative charge is "created" in a lattice by the presence of Fe^{3+}, charge-neutrality is maintained by excess H^+ (or H_3O^+) ions. Since the substitution of iron into the SiO_2 lattice produces such an excess negative charge, we take the low pH coordination of a surface iron to involve an H_3O^+ ion. Stepwise dissociation to the OH-ligand then can produce the required 3:2:1 steps in the constant K as obtained by the least-squares procedure. It is recognized that the slightly smaller Na^+-ion could also satisfy this requirement, but in view of the fact that our experimental results have shown that a 100-fold increase in the Na^+-ion concentration has no effect upon τ, it is felt that the Na^+-ion must be ignored as a primary influence upon the interaction mechanism. We therefore take the dominant surface species to be $\equiv Fe\cdot H_3O$, $(\equiv Fe\cdot H_2O)^-$, and $(\equiv Fe\cdot OH)^=$.

In order to arrive at a reaction scheme which is consistent with the experimental data, it is necessary to consider the time scale of the (possible) proton exchange mechanisms. If an Fe^{3+} ion passes through all of the chemical states which are accessible to it in a time which is short compared to the relaxation time of a proton of interest, and if each species has the same scalar interaction constant A/h (which seems to be true for aqueous Fe^{3+} monomers (53)), then the lifetime to insert into the scalar interaction, τ_h, is given by

$$\tau_h^{-1} = \sum_i f_i \, \tau_{hi}^{-1} \tag{227}$$

where the f_i are fractions which express the probability that a given species will be the ith one, and where the τ_{hi} are the associated proton lifetimes.

If each Fe^{3+} species has a lifetime which is long compared to its ability to exchange protons with the solvent water, it will be possible to express the proton T_1 as though each species represented a separate relaxing site, and the observed T_1 would become

$$T_1^{-1} = \sum_i P_i \, T_{1i}^{-1} \tag{228}$$

where the P_i are the time-independent probabilities that a proton will be found on an iron species which can be characterized by the longitudinal relaxation time T_{1i}.

These two cases are distinguishable by means of field-dependence measurements, because the first one will yield a single correlation time, whereas the latter expression will (in some parts of the pH region) yield more than one correlation time. We have examined the reasonableness of assuming that Equation 228 applies (see the following sections) and have concluded that Equation 227 must be chosen instead. Hence, we assume that competitive proton exchange processes are operative, and we use Equation 227, along with the following reaction scheme, to compute τ_h:

$$\text{I.} \quad \equiv Fe(H_3O) + H_2O \underset{k_{-1}}{\overset{k_1}{\rightleftharpoons}} \equiv Fe(H_2O)^- + H_3O^+ \; ; \; K_1$$

$$\text{II.} \quad \equiv Fe(H_2O)^- + H_2O \underset{k_{-2}}{\overset{k_2}{\rightleftharpoons}} \equiv Fe(OH)^= + H_3O^+ \; ; \; K_2 \tag{229}$$

$$\text{III.} \quad \equiv Fe(OH^*)^= + H_2O \overset{k_3}{\rightleftharpoons} \equiv Fe(OH) + \overset{*}{H}OH \; ; \; K_3 = 1 \; .$$

Let reaction I dominate at low pH (i.e., take $k_{-1}[H_3O] >> k_2$) and let reactions II and III dominate in all other regions. If the lifetime τ_{h1} is associated with $\equiv Fe(H_3O)$, τ_{h2} with $\equiv Fe(H_2O)^-$, and τ_{h3} with $\equiv Fe(OH)^=$, one can solve the associated differential equations to obtain

$$\begin{aligned} \tau_{h1} &= 3/k_1 && ; \; k_{-1} >> k_2 \\ \tau_{h2} &= k_3(k_3-k_2/2)^{-1}\,(2k_2^{-1}-K_3^{-1}) \approx 2/k_2 && ; \; k_3 >> k_2 \\ \tau_{h3} &= 1/k_3 \; . \end{aligned} \tag{230}$$

The probability that a proton of hydration is present on the i^{th} species is found from standard chemical kinetics to be $(f_1 + f_2 + f_3 = 1)$.

$$\begin{aligned} f_1 &= 3[H_3O]^2\,\{3[H_3O]^2 + 2K_1[H_3O] + K_1K_2\}^{-1} \\ f_2 &= 2K_1[H_3O]\,\{3[H_3O]^2 + 2K_1[H_3O] + K_1K_2\}^{-1} \\ f_3 &= K_1K_2\{3[H_3O]^2 + 2K_1[H_3O] + K_1K_2\}^{-1} \; . \end{aligned} \tag{231}$$

Hence, the effective lifetime τ_h is given by

$$\tau_h^{-1} = \sum_{i=1}^{3} f_i\,\tau_{hi}^{-1} = \frac{k_1[H_3O]^2 + k_2K_1[H_3O] + k_3K_1K_2}{3[H_3O]^2 + 2K_1[H_3O] + K_1K_2} \tag{232}$$

whereas the total surface occupation probability is obtained from

$$P = \frac{S}{2[H_2O]} \cdot \frac{3[H_3O]^2 + 2K_1[H_3O] + K_1K_2}{[H_3O]^2 + K_1[H_3O] + K_1K_2} \qquad (233)$$

with S = molar concentration of surface Fe^{3+} and $[H_2O]$ = molar concentration of solvent water.

Upon first inspection of the last two expressions, it may appear that the one for τ_h has enough additional constants in it that it is essentially unrestricted by any choice of K_1 and K_2 that would be used to fit the expression for P to the data. However, a more careful analysis of the expression for τ_h shows that the constants K_1 and K_2 are actually the most important ones in determining the shape of the τ_h vs pH curve, so that one does not have nearly as much freedom as might be imagined. Our approach to the problem was therefore to fit the expression for τ_h to the experimental data by means of an iterative least-squares procedure which adjusted all of the constants in Equation 232. The least-squares values of K_1 and K_2 were then inserted into Equation 233, and the constant $s/2[H_2O]$ was set equal to the high pH limit for K as obtained from the field-dependence data. The resulting K vs pH prediction was compared to the actual data and was found to fit the deuterated samples reasonably well whereas it was not in complete accord with the data obtained from undeuterated samples. In view of the fact that the shape of the resulting curve was correct and also that we had used an oversimplified model, the plots were considered to be satisfactory.

We have also attempted the reverse procedure, where the expression for P is adjusted by least-squares methods, the derived constants K_1 and K_2 are inserted into the expression for τ_h, and the constants k_1, k_2 and k_3 are adjusted for a best fit to the τ vs pH data. In either

case, we find that one can always get a "perfect" fit to the first set of data considered, but that the second curve will always be slightly in error. Nevertheless, we feel our contention that the PMR results can in principle be related to chemical kinetic effects has been adequately demonstrated. In light of the previously discussed difficulties in knowing which reactions to apply, a "perfect" fit in each case would probably not be any more convincing, since it is really the shape of the curves which is most important.

Figures 44 through 46 show the curves (and the original data) as obtained by the first method of the preceding paragraph. The least-squares technique discussed by Melton (54) was used in this case (and in those to follow),[5] but before discussing these results further, we wish to consider some alternative possibilities.

Other Data Reduction Schemes

We previously presented arguments to the effect that the stepwise behavior in the constant K (as derived from the field-dependence data) would best be explained on the basis of a surface iron species which undergoes stepwise dissociation as the pH is increased. However, that statement was based upon a rather simple reduction of the field-dependence data and one which is clearly not fully adequate to predict the detailed field-dependence of T_1. Specifically, it can be noted that the predicted T_1 always changes more rapidly with applied magnetic field than the experimental T_1, and it is therefore necessary to ask if

---

[5]We wish to thank Gulf Research and Development Company for the use of their "reactive terminal" time-sharing service (IBM 360/80) when these results were checked.

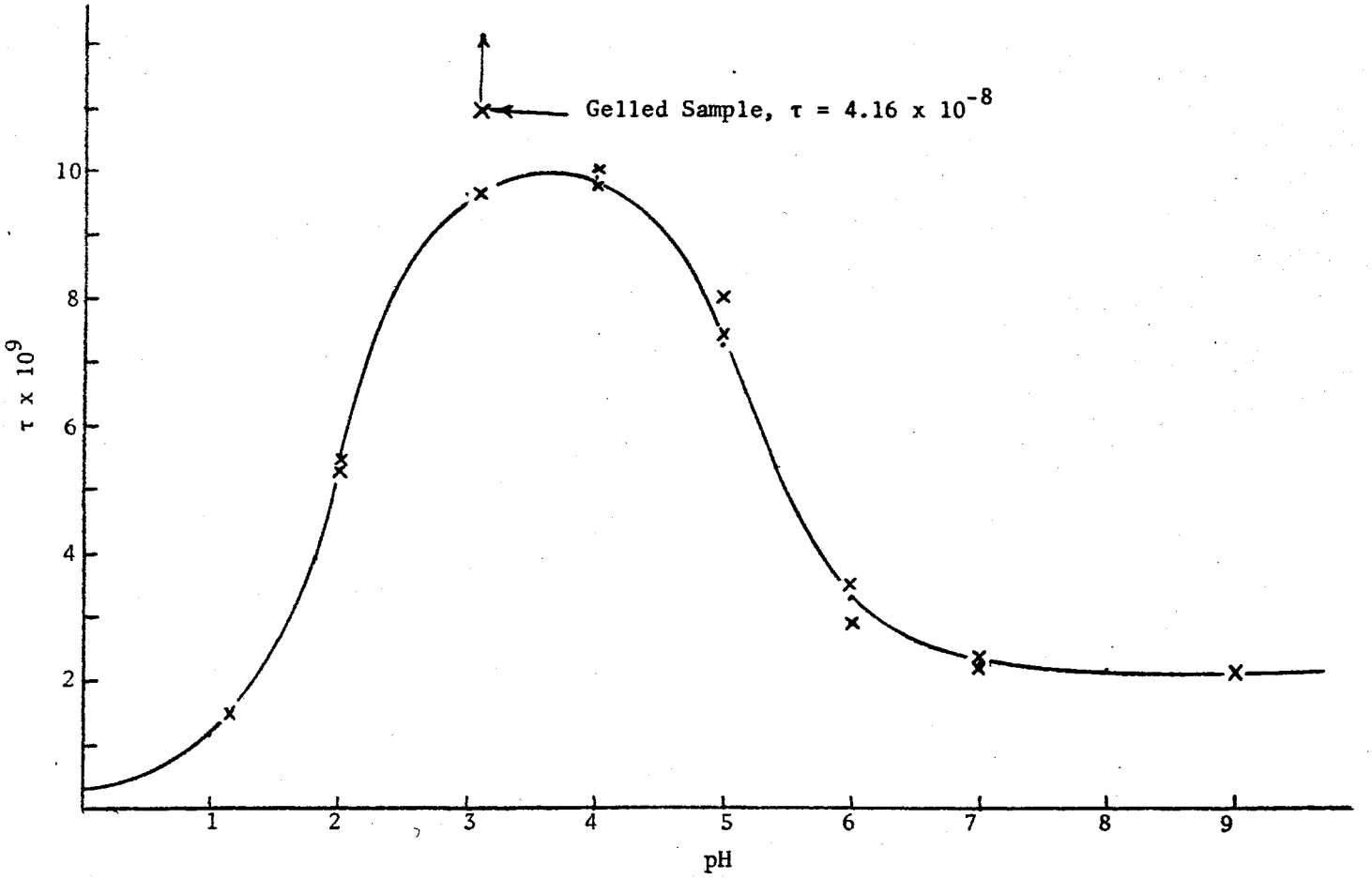

Figure 44. Least-squares Fit to the Data of Figure 37 (τ vs pH) According to Equation 232 With the Result That $K_1 = 7.89 \times 10^{-2}$, $K_2 = 2.86 \times 10^{-6}$, $k_1 = 3.17 \times 10^{9}$, $k_2 = 1.64 \times 10^{8}$, and $k_3 = 4.63 \times 10^{8}$

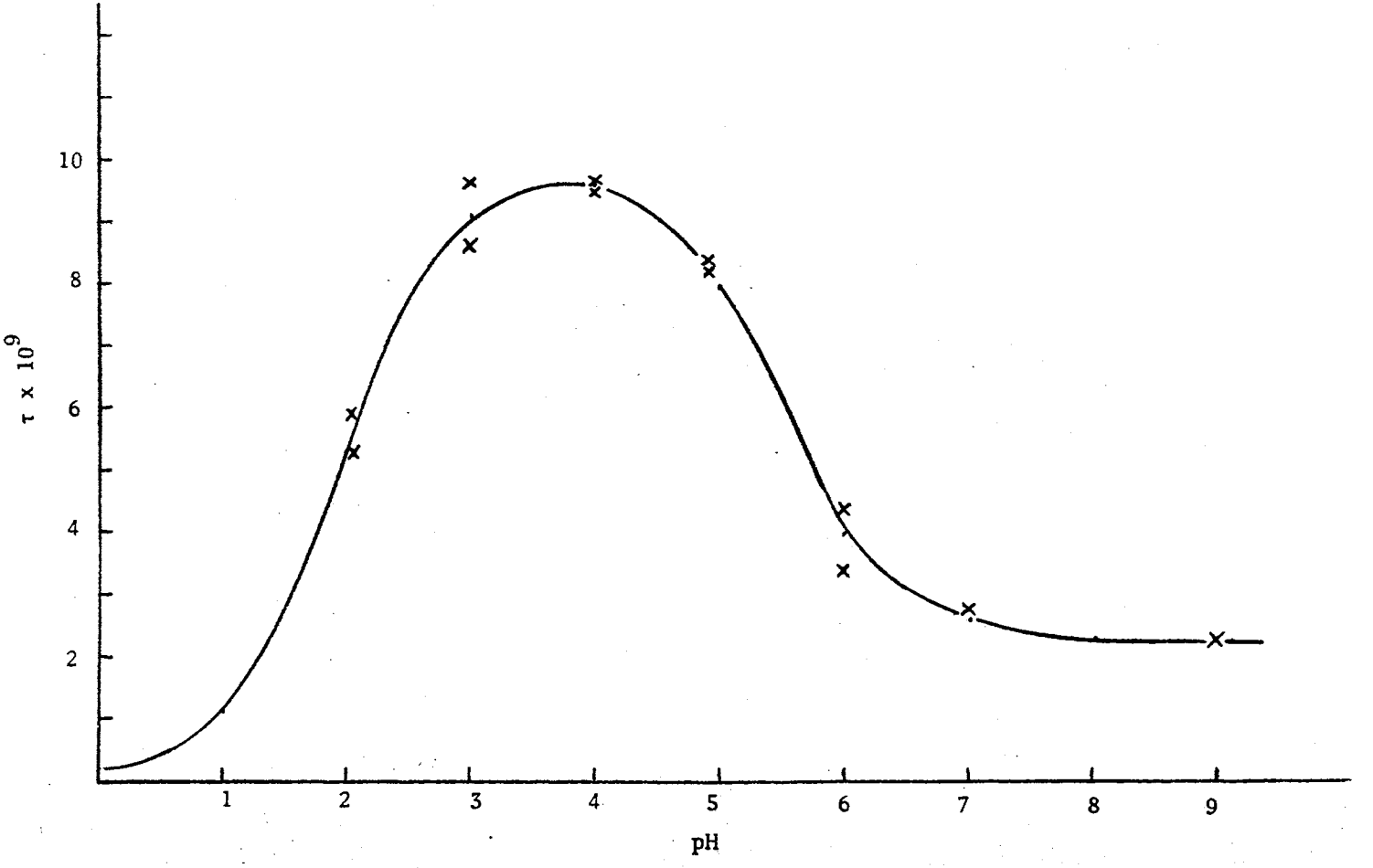

Figure 45. Least-squares Fit to the Data of Figure 38 (τ vs pH for a Deuterated LS Sample) According to Equation 232 With the Result That $K_1 = 8.44 \times 10^{-2}$, $K_2 = 1.96 \times 10^{-6}$, $k_1 = 3.19 \times 10^{9}$, $k_2 = 1.59 \times 10^{8}$, and $k_3 = 4.34 \times 10^{8}$

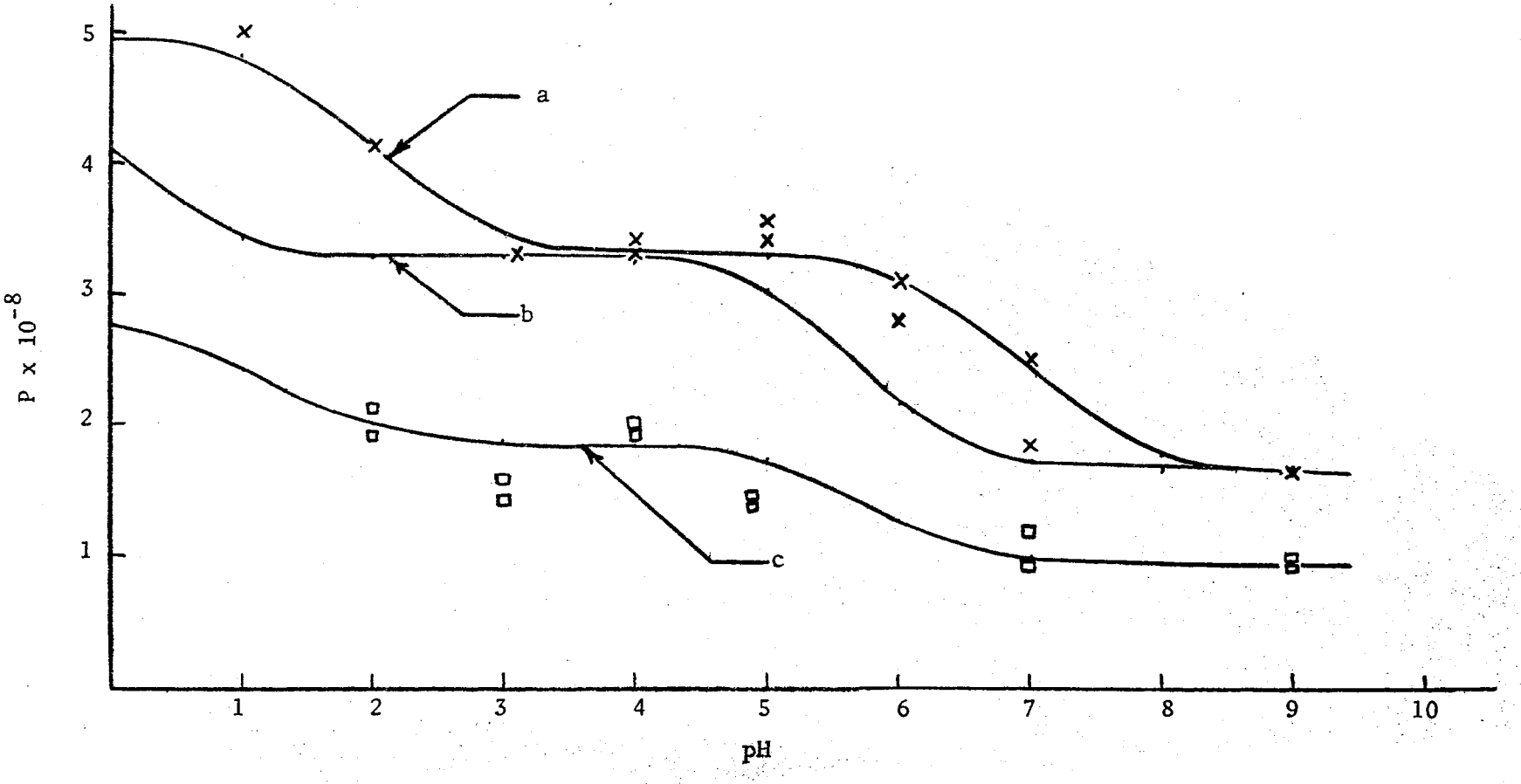

Figure 46. Curve a: Least-squares Fit to K vs pH Data as Shown in Figure 39 for Undeuterated Samples, Yielding $K_1 = 9.81 \times 10^{-3}$ and $K_2 = 1.06 \times 10^{-7}$. Curve b: Result Predicted on the Basis of K_1 and K_2 Derived From the Least-squares Fit of Figure 44. Curve c: Result Predicted on the Basis of K_1 and K_2 Derived From the Least-squares Fit of Figure 45.

some other representation of these data could be more meaningful.

Consider, for example, that (a) different bonding electrons may have different relaxation times, as is often found in a crystalline environment (this is a symmetry effect), or (b) that protons attached to different bonds may exchange at different rates. In either situation, one would be in a position to argue that the data should be represented by more than one field-dependent term, and our earlier statements concerning stepwise dissociation could require complete revision. We, therefore, attempted to interpret the field-dependence data in terms of two other equations, each of which contained two frequency-dependent terms.

In the first case, the least-squares analysis was in the terms of the equation

$$T_{1(obs)}^{-1} - T_{1hf}^{-1} = A\,\tau_1/[1+(\omega_s\tau_1)^2] + B\,\tau_2/[1+(\omega_s\tau_2)^2] \qquad (234)$$

where T_{1hf} is the high-field limit to $T_{1(obs)}$. This expression has the form to be expected in a situation where two scalar terms contribute to the total relaxation and it can represent the field-dependence data extremely well, provided that A, B, τ_1, and τ_2 are taken to be adjustable parameters. Figure 47 shows one typical fitted curve obtained by this means, and the general indication seems to be that this approach will be fruitful. Unfortunately, when all of the field-dependence data have been reduced to the preceding four parameters, one finds that a plot of A, B, τ_1, and τ_2 as a function of indicated pH produces a "shotgun pattern" in the data points and, furthermore, that the plots for deuterated and undeuterated LS are very dissimilar. For these reasons, the plots are not reproduced here, but the derived constants are, and they are

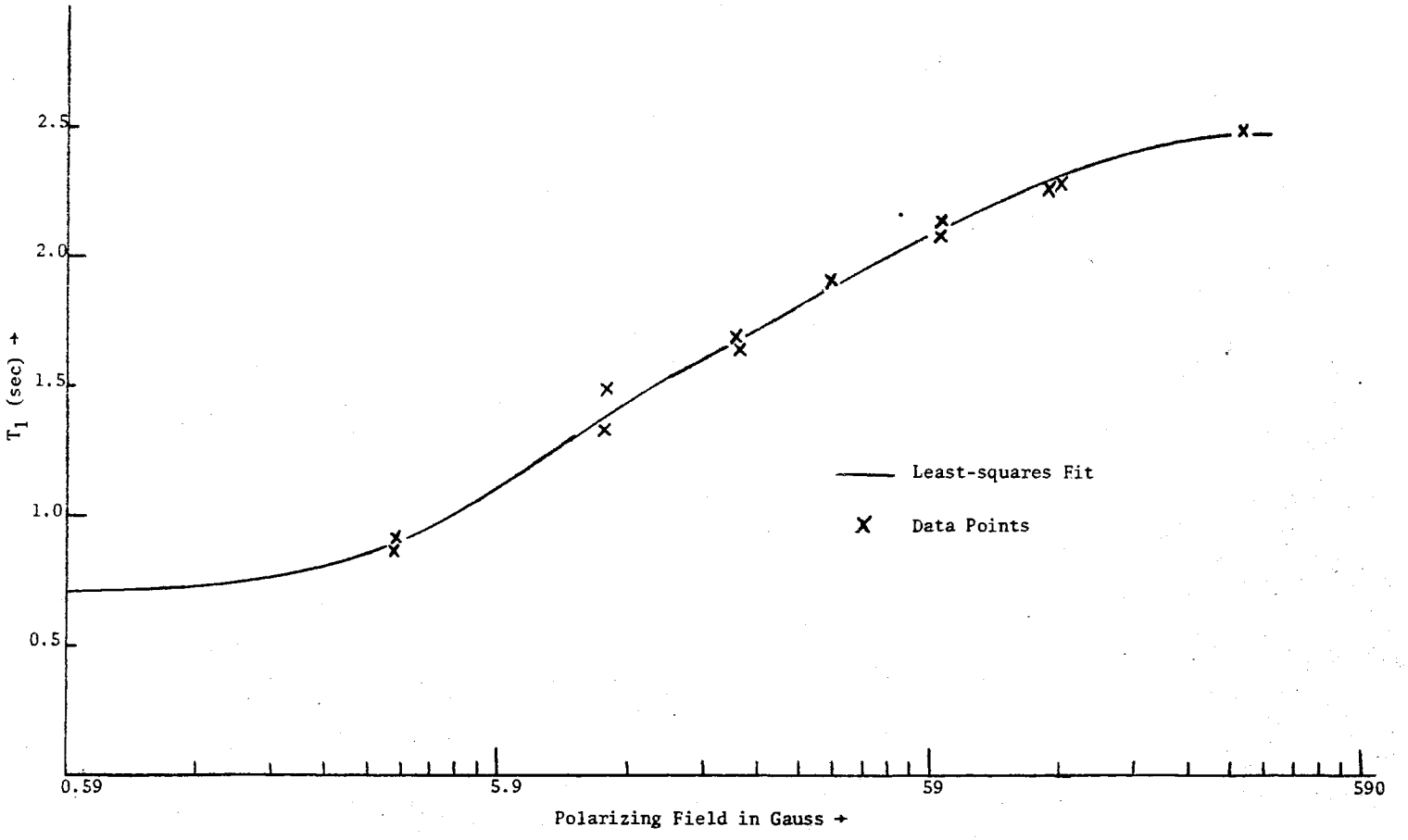

Figure 47. Least-squares Fit to Deuterated 8% by Weight SiO_2 Ludox LS Field-dependence Data by Means of Equation 234. For these pH 4.00 data (regarded as the most difficult to fit by a single expression such as that used to produce Figure 29) one obtains $A = 6.79 \times 10^{7}$, $B = 1.54 \times 10^{8}$, $\tau_1 = 1.24 \times 10^{-8}$ sec, and $\tau_2 = 1.16 \times 10^{-9}$ sec.

shown in Table XVIII.

A second approach which is attractive is one which contains a combination of the proton-proton, dipole-dipole interaction with the previously-used scalar interaction. In this case, one would assume that the field-dependence data are best represented in terms of the equation,

$$T_{1(obs)}^{-1} - T_{1hf}^{-1} = A\,\tau_I/[1+(\omega_I\tau_I)^2] + A\,4\tau_I/[1+4(\omega_I\tau_I)^2] + B\,\tau_s/[1(\omega_s\tau_s)^2] \tag{235}$$

where ω_I is the proton precession frequency in the polarizing field B_p, where $\omega_s = 650\omega_I$, and where A, B, τ_I and τ_s are again taken to be adjustable parameters. As expected, this equation can produce an excellent fit to the field-dependence data, but there are two distinct sets of parameters which will produce a satisfactory fit to a given set of data. One set corresponds to the case where the terms containing ω_I are the first to decrease with increasing field, and the other set corresponds to the opposite situation. In fact, once one solution is known, the other may be calculated with the aid of the formulas

$$\begin{aligned} A &= B^o\ 11.85 \times 10^3 \\ B &= A^o \cdot 1.85 \times 10^3 \\ \tau_I &= 370\ \tau_s^o \\ \tau_s &= \tau_I^o/370 \end{aligned} \tag{236}$$

where the superscript "o" indicates a known parameter.[6]

It was found that the preceding formulas did not completely anticipate the results actually obtained by computer, but since they were

---

[6]These formulas are easily obtained by requiring that the terms in A and B be interchanged in such a way that the new scalar term can replace the old dipolar term and vice-versa. It must also be recalled that the conditions $\omega_s\tau_s = 1$ and $\omega_I\tau_I = 0.5686$ are equivalent.

TABLE XVIII

LEAST-SQUARES CONSTANTS APPROPRIATE TO THE FIELD-DEPENDENCE OF LUDOX LS[1]

Undeuterated Ludox LS						Deuterated Ludox LS					
pH	$Ax10^{-8}$	$Bx10^{-8}$	$\tau_1 x10^{8}$	$\tau_2 x10^{9}$	$1/T_{1hf}(sec^{-1})$	pH	$Ax10^{-8}$	$Bx10^{-8}$	$\tau_1 x10^{8}$	$\tau_2 x10^{9}$	$1/T_{1hf}(sec^{-1})$
2.0	0.864	2.87	1.32	3.65	0.714	2.0	0.540	1.76	2.41	1.95	0.455
3.1	1.71	2.14	1.59	2.85	0.645	3.0	0.674	3.00	1.89	0.624	0.476
4.0	1.36	2.57	2.00	2.90	0.589	4.0	0.679	1.59	1.24	1.16	0.400
5.0	1.33	2.68	1.49	3.04	0.555	4.9	0.554	1.57	1.79	2.00	0.357
6.0	2.02	2.20	0.501	1.17	0.555	6.0	0.479	1.66	0.944	1.34	0.357
7.0	0.330	1.86	0.628	1.45	0.589	7.0	0.139	1.14	1.17	1.87	0.370
						9.0	0.0332	1.47	2.46	1.30	0.357

[1]From the data of the previous chapter, and with the equation discussed in the text.

always able to predict the second solution to within 10%, they were deemed to be satisfactory for the present purposes. Their chief virtue, in our view, lay in the fact that significant computer time was saved by their use.

A plot of the parameters A, B, τ_I and τ_s as a function of pH produces a reasonably smooth set of curves for either deuterated or undeuterated samples. Furthermore, the dipole-dipole relaxation rate appears to have been reduced under deuteration to the correct 20% - 30% of the undeuterated rate, provided that one selects a set of solutions which we shall call group one (see Tables XIX and XX). This set of solutions also appears to verify the D_2O dilution experiment at pH 9 since it predicts that, at low-fields, the dipole-dipole relaxation rate will constitute less than 1/3 of the total surface contribution. Unfortunately, the pH 9 group two solutions also make this prediction, so that it cannot be used as a criterion for selecting the best group of solutions. The greatest difficulty with the group one solutions lies in the values assigned to τ_I, the dipole-dipole correlation time. Because the appropriate times range between 10^{-6} and 10^{-5} seconds, they exceed typical measured values for adsorbed water (10^{-9} to 10^{-7} seconds) by up to four orders of magnitude, and they also exceed the Debye-Stokes correlation time that is calculated for a single colloidal particle (η V/kT = 4×10^{-7} sec at 25°C for a 15 millimicron diameter particle). At pH 4, where the double layer thickness should be negligible, the fact that the required τ_I is two orders of magnitude larger than η V/kT makes the solutions extremely difficult to rationalize, although they are qualitatively attractive because they "predict" that the gelation of a pH 4 sample should produce a much larger decrease in $T_{1(1f)}$ than the situation in

TABLE XIX

LEAST-SQUARES CONSTANTS APPROPRIATE TO THE FIELD-DEPENDENCE OF DEUTERATED LUDOX LS[1]

pH	Group One					Group Two				
	$Ax10^{-4}$	$Bx10^{-8}$	$\tau_I x10^6$	$\tau_s x10^9$	$1/T_{1hf}(sec^{-1})$	$Ax10^{-4}$	$Bx10^{-7}$	$\tau_I x10^6$	$\tau_s x10^8$	[1]
2	3.23	1.36	4.85	2.81	0.555	7.37*	5.97*	1.04*	1.31*	37%
2	2.88	1.38	5.10	3.14	0.555	7.44*	5.34*	1.16*	1.38*	37%
3	3.39*	1.42*	7.46*	1.54*	0.476	7.67	6.26	0.570	2.02	15%
4[3]	2.29*	1.73*	9.33*	1.89*	0.392	9.35	4.24	0.700	2.52	23%
4	3.39*	1.23*	6.42*	1.29*	0.392	6.65	6.26	0.477	1.73	---
4.9	2.48(2.73*)	1.05(1.01*)	7.21(6.98*)	3.39(3.02*)	0.408	5.67*	4.60*	1.25*	1.95*	28%
6	2.09*	1.66*	4.44*	1.63*	0.357	8.96	3.86	0.603	1.20	37%
7	0.696*	1.15*	4.25*	1.76*	0.370	6.22	1.29	0.651	1.15	58%
9	0.185*	1.51*	9.11*	1.26*	0.357	8.16	0.342	0.466	2.46	19%

[1]From the data of the previous chapter, and with the equation discussed in the text.

[2]Dipolar contribution as a percent of the total surface relaxation rate at low fields.

[3]Preferred solution, representing the best pH 4 data set.

*Solutions marked with an asterisk were obtained with the least-squares procedure. Unmarked solutions were obtained with the formulas given in the text.

TABLE XX

LEAST-SQUARES CONSTANTS APPROPRIATE TO THE FIELD-DEPENDENCE OF UNDEUTERATED LUDOX LS[1]

pH	Group One					Group Two			
	$Ax10^{-5}$	$Bx10^{-8}$	$I x10^{6}$	$_{s}x10^{9}$	$1/T_{1hf}(sec^{-1})$	$Ax10^{-4}$	$Bx10^{-9}$	$I x10^{6}$	$_{s}x10^{9}$
1	5.47*	0.476*	0.194*	7.60*	0.675	2.58(2.46*)	1.01(0.992*)	2.82(2.99*)	0.525(0.536*)
2	1.61*	0.636*	1.56*	14.7*	0.714	3.44	0.298	5.45	4.22
3.1	1.03*	1.91*	5.60*	2.45*	0.645	10.6(11.5*)	1.91(1.67*)	0.907(1.13*)	15.1(16.1*)
4	1.14	1.38	1.18	20.8	0.625	7.47*	0.211*	7.72	3.19*
5	1.46*	1.23*	1.25*	15.4*	0.556	6.65	0.271	5.70	3.38
6	1.18*	2.00*	0.453*	5.01*	0.556	10.8	0.218	1.86	1.22
7	1.88*	0.887*	0.200*	3.87*	0.526	4.80	0.348	1.43	0.540
9	---	---	---	---	---	---	---	---	---

[1]From the data of the previous chapter. Note that these data are not as uniform as those obtained from deuterated samples.

*Solutions marked with an asterisk were obtained with the least-squares procedure. Unmarked solutions were obtained with the formulas given in the text.

which a pH 9 sample is gelled. They are qualitatively unattractive because they imply that the rotational correlation time of a surface water molecule is longest at the point of zero electrostatic field.

The group two solutions are marginal in terms of the magnitude of τ_I, which hovers about the value of 10^{-6} seconds. They are, however, untenable in terms of both the gelation and the deuteration experiments because they predict that (1) the dipolar mechanism will dominate at higher magnetic fields than the scalar mechanism, and (2) that gelation of a pH 7 sample should produce the largest change in $T_{1(1f)}$. Since experiment contradicts both conclusions, this set of conclusions must also be rejected.

Finally, one may question the form of the equation used to obtain the least-squares fit, and ask if a different combination with the dipole-dipole interaction would produce more acceptable τ_I values. Since the value of τ_I must be such that the corresponding interaction is reduced to one-half of its value at $\omega = 0$ when $\omega_I\tau_I = 0.5686$, then τ_I is determined by the position of the "step" in the field-dependence data, and it will change only slightly as various other interaction mechanisms are substituted for the scalar term (the constant A, on the other hand, can undergo large changes). Therefore, it is most unlikely that any other treatment of the data would yield a τ_I which is more satisfactory, especially when one recalls that the basic functional form of such interactions is nearly identical in all cases. We therefore can reject the idea of using different paramagnetic interactions, and we can also reject the idea of using more frequency-dependent terms on the grounds that the data are so well represented by a two correlation time expression that the addition of a third term would be

operationally useless.

In final summary, it has been concluded that expressions involving two or more frequency-dependent terms cannot be rationalized in terms of the entire body of data gathered to this point. Although a single frequency-dependent term also has its shortcomings, it is the only method we have found to be satisfactory on the basis of first principles. It cannot account, by itself, for the gel behavior, but then neither can a dipole-dipole interaction which has been adjusted to fit the field-dependence data. For these reasons, we have selected the simplest interpretation as the most tenable; i.e., that the scalar term alone dominates the field-dependence; but that there is an accompanying distribution of correlation times whose form is at present unknown.

The High-field Variation of T_2

It was previously stated that one explanation for the high-field results could be found in the behavior expected for aqueous iron complexes, and in order to support that statement, we wish to present in this section some calculations which show that the so-called $\Delta\omega$ effect can reasonably be expected to influence T_2 at fields exceeding 1000 G. In making these estimates, we are faced with the problem that no NMR studies have yet been made which involve Fe(III) above roughly pH 3, although it is known that, below the mononuclear wall, iron is amphoteric and should form the $Fe(OH)_6^{3-}$ complex at pH 9 (55). Hence in the unmodified samples studied at high-fields (see Table XI of Chapter VI), one should expect this aqueous complex to dominate, and there should be six protons in the first hydration sphere.

The Larmour frequency shift upon entering the hydration sphere is

given by Equation 212; i.e.

$$\frac{\Delta\omega_M}{\omega_M} = \frac{S(S+1)}{3}\left(\frac{A}{h}\right)\frac{g|\beta|}{kT\gamma_I} \tag{237}$$

where β is the Bohr magneton, g is the Lande' g-factor, and all other symbols have their usual meaning. If one takes (after Michel) $A/h \doteq 5\times10^6$ sec^{-1} and S = 5/2, it is found that

$$\frac{\Delta\omega_M}{\omega_M} = 2.42 \times 10^{-4} \tag{238}$$

and at 14.1 kilogauss (60 MHz)

$$\Delta\omega_M = -9.13 \times 10^4 \text{ radian/sec} \quad . \tag{239}$$

Using the iron analysis data previously presented, one finds that the probability of finding a proton in the hydration sphere is on the order of 10^{-4} - 10^{-5} for the extractable iron. Hence, the first result obtained is that the observed shift at 60 MHz should lie between -0.1 and -1.0 cps. This agrees with measurements made on unmodified Ludox LS and HS with a Varian A60 (not previously reported), using a special spherical sample holder containing dioxane as an internal reference. Typical shifts were on the order of 0.9 cps in both cases, and were not due to diamagnetic effects.

To decide if the $\Delta\omega$ effect is important at 60 MHz, one may note that Equation 65 of Chapter II requires that

$$\tau_M(\Delta\omega_M)^2 \gtrsim T_{2M}^{-1} \tag{240}$$

where T_{2M} is the transverse relaxation time in the appropriate hydration sphere, and where τ_M is the proton lifetime. If Michel's and Judkin's (separate) results are adopted, T_{2M}^{-1} ought to be given by

$$T_{2M}^{-1} \doteq \frac{2S(S+1)}{3} \frac{A}{h} T_{1e} \tag{241}$$

where T_{1e} is the electron relaxation time for aqueous Fe^{3+} (5.8×10^{-11} sec). Insertion of the previous values for S and A/h, along with the appropriate T_{1e}, gives

$$T_{2M}^{-1} \doteq 8.46 \times 10^{3} \text{ sec}^{-1} \quad .$$

If τ_M^{-1} is of roughly the same order of magnitude as the acid dissociation rate for $Fe(H_2O)^{3+} \gtrsim 10^7$ sec^{-1}, then $\tau_M(\Delta\omega_M)^2$ is roughly 10^3 sec^{-1}. Allowing for the uncertainties in both A and τ_M this result predicts that the $\Delta\omega$ effect is important for protons (Judkins found that it was very important for O^{17}). Furthermore, it gives an observed T_2 lying between 0.1 and 1.0 second (depending upon the way in which a particular sample gels). If the observation of Stumm is correct that the dissolved iron becomes incorporated into the gel network (and this does not always occur), then one might reasonably expect T_{1e} to increase to the point where $\tau_M(\Delta\omega_M)^2 \ll T_{2M}^{-1}$ so that the $\Delta\omega$ effect would disappear as, indeed, some of the data indicate.[7]

Finally, we note that a similar calculation for 1010 G indicates that the $\Delta\omega$ effect should be unimportant, again in rough agreement with the data.

The Gel Behavior

We have reserved this discussion for last because the observed gel behavior has been one of the most puzzling aspects of the study, and it

---

[7] Because some of these samples had a reduced pH, it is also possible that τ_M had simply decreased.

is in fact an area for which we have been at a loss to offer any explanation. Part of the difficulty undoubtedly lies with insufficient data, and it is the author's opinion that future studies of colloid PMR should include a careful examination of gel behavior. Nevertheless, the data which are available do show that the PMR in gelled samples is somehow a joint property of the pH and the rigidity of the gel, with the greatest effect being noted when an initially liquid sample is gelled at pH 4. This effect is apparently a chemical one, since the mean proton lifetime on a surface Fe^{3+} ion appears to increase quite markedly at pH 4, whereas the effect is very slight at pH 9. We can only speculate that our results reflect the very recent observations of Matijeveck and his school to the effect that the Ludox colloids have some very unusual (but unknown) surface properties which are profoundly influenced by pH changes (56), but it would appear that the present state of knowledge is such that we cannot go beyond this point.

Concluding Remarks

In view of the unsatisfactory state of current knowledge about the surface properties of the colloid we have studied, and further, considering the fact that the properties of aqueous and lattice iron have only recently been of general interest, it has been impossible to do more than to give a series of phenomenological and semi-quantitative arguments in support of our thesis. Neverthess, it is felt that the proposed mechanism is basically correct and that the data we have presented will eventually be interpretable in terms of the detailed chemical studies which are now beginning to appear in the literature. We are in agreement with several other authors as to the basic interaction

mechanism which is operative in these colloids, and we also agree with Hair that the pKa of a surface ion on silica can decrease by up to three units (57). It is gratifying that, in every case where we have been able to compare our work to that of others, the agreement has been satisfactory, especially since that comparison was always made after our work had been completed.

It should probably be mentioned that the instrument used for this study was constructed by the writer -- an enterprise which required considerable time and effort -- but that since its details have been reported elsewhere,[8] he elected not to describe it at length here. Because it was capable of directly measuring the dominant correlation time, his work has considerably eased, and as far as is known, it was the only such instrument in use in the United States. Unfortunately, it has now been dismantled and only one or two other instruments now exist which can make similar, very low-field measurements. Since in NMR the tendency has been to use the largest available magnetic field, it will probably remain true that the interactions of the type studied here (ones which largely disappear above 1000 gauss) will continue to be overlooked. Although it is often argued that high sensitivity necessitates a large magnetic field, the discussion of the second chapter should demonstrate that this is not the only consideration, and that the problems can be overcome.

---

[8]See references 54 and 58 for a complete schematic diagram of the instrument, as well as performance considerations.

BIBLIOGRAPHY

1. Abragam, A. The Principles of Nuclear Magnetism. London: Oxford University Press, 1961.

2. Bloch, F. Phys. Rev. 83, 1062 (1951).

3. McConnell, H. M. J. Chem. Phys. 28, 430 (1958).

4. (a) Anderson, P. W. J. Phys. Soc. Japan 9, 316 (1954).
   (b) Kubo, R. and K. Tomita. J. Phys. Soc. Japan 9, 888 (1954).

5. Zimmerman, J. R. and W. E. Brittin. J. Phys. Chem. 61, 1328 (1957).

6. Lumry, A. J. Phys. Chem. 65, 837 (1961).

7. Swift, T. J. and R. E. Connick. J. Chem. Phys. 37, 307 (1962).

8. Swift, T. J. and R. E. Connick. J. Chem. Phys. 37, 307 (1962).

9. Luz, Z. and R. G. Shulman. J. Chem. Phys. 43 (10), 3750 (1965).

10. van der Ziel, A. Noise. New York: Prenctice-Hall, Inc., 1954.

11. Pollak, V. L. and R. R. Slater. Rev. Sci. Instrum. 37 (3), 268 (1966).

12. Iler, R. K. The Colloid Chemistry of Silica and Silicates. Ithaca, New York: Cornell University Press, 1955.

13. Rule, J. M. U. S. Pat. No. 2,577,485 (1951).

14. Verwey, E. J. W. and J. T. G. Overbeek. Theory of the Stability of Lyophobic Colloids. New York: Elsevier Pub., 1948.

15. Derjaguin, S. V. and L. Landau. Acta. Physiochim. URSS, 14, 633 (1941).

16. Levine, S. and G. M. Bell. J. Coll. Sci. 17, 838 (1962).

17. Vold, M. J. J. Coll. Sci. 16, 1 (1961).

18. Grahame, D. C. Chem. Revs. 41, 441 (1947).

19. (a) Matijevic, E. and L. H. Allen. Environ. Sci. Technol. 3 (3), 264 (1969).
(b) Allen, L. H. and E. Matijevic. J. Colloid Inter. Sci. 31 (3), 287 (1969).
(c) Allen, L. H. and E. Matijevic. J. Colloid Inter. Sci. 33 (3), 420 (1970).
(d) Depasse, J. D. and A. Watillion. J. Colloid Inter. Sci. 33 (3), 430 (1970).

20. Li, H. Y. M. S. Thesis. Oklahoma State University (1966).

21. Product Data Sheet No. A-37879. E. I. DuPont de Nemours and Company, Wilmington, Delaware.

22. (a) Peri, J. B. J. Phys. Chem. 70, 2937 (1966).
(b) Peri, J. B. and A. L. Hensley, Jr. J. Phys. Chem. 72 (8), 2926 (1968).

23. Iler, R. K. The Colloid Chemistry of Silica and Silicates. Ithaca, New York: Cornell University Press, 1955, pp. 242-247.

24. Fripiat, J. J. and J. Uytterhoeven. J. Phys. Chem. 66, 800 (1962).

25. (a) Hockey, J. A. Chem. Ind. (London). 57 (1965).
(b) Boehm, H. P. Angew. Chem. Int. Ed. 5, 533 (1966).

26. Heston, W. M., Jr. J. Phys. Chem. 64, 147 (1960).

27. Bolt, G. H. J. Phys. Chem. 61, 1166 (1957).

28. (a) Stumm, W. and C. R. O'Melia. J. Am. Water Works Assoc. 60, 514 (1968).
(b) O'Melia, C. R. and W. Stumm. J. Coll. Inter. Sci. 23, 437 (1967).
(c) Stumm, W. and J. J. Morgan. J. Am. Water Works Assoc. 54, 971 (1962).

29. Biedermann, G. and P. Schendler. Acta Chem. Scand. 11, 731 (1957).

30. Stumm, W. and C. R. O'Melia. J. Am. Water Works Assoc. 60, 514 (1968).

31. Hazel, F. J. Am. Chem. Soc. 71, 2256 (1949).

32. Fripiat, J. J. and R. Touillaux. Trans. Faraday Soc. 65 (5), 1236 (1969).

33. Pollak, V. L. Private Communication.

34. Crank, J. The Mathematics of Diffusion. Oxford: Clarendon Press, 1956.

35. Hausser, R. and G. Laukien. Zeit. Physik. 153, 394 (1959).

36. Castner, T., Jr. J. Chem. Phys. 32 (3), 668 (1960).

37. Geschke, D. Z. Naturforsch. A. 23 (5), 689 (1968).

38. (a) Woessner, D. E. J. Chem. Phys. 36 (1), 1 (1962).
(b) Woessner, D. E. and J. R. Zimmerman. J. Phys. Chem. 67, 1590 (1963).

39. Michel, D. Z. Naturforsch. 21a (3), 366 (1966).

40. O'Reilly, D. E. Advances in Catalysis XII, 31 (1960).

41. Wolfsberg, M. Annual Review of Physical Chemistry XX, Annual Reviews, Inc. (1969).

42. Resing, H. A. Adv. Mol. Relaxation Proc. 1, 109 (1967-68).

43. Benson, S. W. The Foundations of Chemical Kinetics. New York: McGraw-Hill, 1960.

44. Cohen, M. H. and D. Turnbill. J. Chem. Phys. 31, 1164 (1959).

45. Bloembergen, N. J. Chem. Phys. 27, 595 (1957).

46. Koegeboehn, L. P. M. S. Thesis, Oklahoma State University (1963).

47. Li, H. Y. M. S. Thesis, Oklahoma State University (1966).

48. Poole, C. P., Jr. and H. A. Farach. J. Mag. Resonance. 1, 551 (1969).

49. Gibson, J. F. Disc. Faraday Soc. No. 26, 72 (1958).

50. French, C. M. and J. P. Howard. Trans. Faraday Soc. 52, 712 (1956).

51. Judkins, M. R. Ph.D. Thesis, University of California (1967).

52. Fong, D. W. and E. Grunwald. J. Am. Chem. Soc. 91 (10), 2413 (1969).

53. Broersma, S. J. Chem. Phys. 26 (6), 1405 (1957).

54. Melton, B. F. Ph.D. Thesis, Oklahoma State University (1970).

55. Singley, J. E. and J. H. Sullivan, Jr. J. Am. Water Works Assoc. 61 (4), 190 (1969).

56. Matijevic, E. and L. H. Allen. Environ. Sci. Technol. 3 (3), 264 (1969).

57. Hair, M. L. and W. Hertl. J. Phys. Chem. 73 (12), 4269 (1969).

58. Mitchell, D. E. M. S. Thesis, Oklahoma State University (1963).

APPENDIX A

A FORTRAN PROGRAM TO YIELD A WEIGHTED LEAST-SQUARES FIT TO FIELD-DEPENDENCE DATA

The equations which lead to the program shown in Table XXI have been previously presented in the main text (Equations 79 through 81). Because it is doubtful that a potential user would find the specific embodiment of the program to be of direct use (it is taylored to the measurements produced by an EFFP apparatus), only its general features will be discussed. It should be noted, however, that the program can fit general field-dependence data, provided that the statements preceding the "CALL SUM(A,T)" command are suitably altered.

FORTRAN Language Used

The listed program can be handled by a compiler capable of manipulating FORTRAN II or any higher-level version. It is not compatible with FORTRAN I, but this version is nearly obsolete, and the program should therefore be usable on a wide variety of machines.

In its most recent application, the program was run on a time-sharing system, and the options which were originally used to enable an IBM 650 computer to handle it are not shown. It is compatible with such a computer, provided that auxiliary disc storage is available.

The only statements which may be unfamiliar to the general FORTRAN user are the READ and WRITE, statements as used in this program. They

TABLE XXI

PROGRAM LISTING

```
C       MAIN PROGRAM
        DIMENSION A(20),T(20)
        COMMON SUMY,SUMYX,SUMX4,SUMX2,NDATA,ADATA,TLOW
1       N=0
        IT=0
        READ(5,2)TLOW,B,NDATA
2       FORMAT(2E10.3,13)
        READ(5,3)(A(J),T(J),J=1,NDATA)
3       FORMAT(6E10.3)
        WRITE(6,101)
101     FORMAT('INITIAL GUESS AT TAU? E10.3')
        READ(9,3)TAU1
C
C       TRANSFORM COORDINATES
C
        DO 4 I=1,NDATA
        A(I)=(4.26E+03)*A(I)*(6.28)*B*(650.)
        T(I)=(T(I)*TLOW)/(T(I)-TLOW)
4       CONTINUE
C
C       COMPUTE ALL APPROPRIATE SUMS
C
        CALL SUM(A,T)
C
C       COMPUTE NEW TAU BY NEWTON'S METHOD.
C
10      TAU2=TAU1-(SQL(TAU1)/SQDRL(TAU1))
C
C       COMPUTE PERCENTAGE CHANGE IN TAU SINCE LAST ITERATION.
C       IF IT IS SMALLER THAN 1%, TERMINATE THE LOOP.
C
        DUM=ABSF((TAU2-TAU1)/TAU2)
        IF(DUM-.01)5,5,7
5       TB=1.0/CON(TAU2)
        TBULK=TLOW/(1.-(TB*TAU2*TLOW))
        WRITE(6,6)TAU2,TB,TLOW,TBULK
6       FORMAT(4HTAU=,E10.3,3H K=,E10.3,6H TLOW=,E10.3,7H TBULK=,E10.3)
        GO TO 1
7       N=N+1
C
C       REPLACE OLD TAU WITH NEW TAU
C
        TAU1=TAU2
C
C       IF FLAG IS SET, WRITE TAU2
C
```

TABLE XXI (Continued)

```
      IF(IT)8,9,8
8     WRITE(6,3)TAU2
9     CONTINUE
C
C     CHECK TO SEE IF 50 ITERATIONS ARE COMPLETED
C
      IF(N-50)13,11,11
11    WRITE(6,12)
12    FORMAT(17HCONVERGENCE CHECK)
C
C     SET FLAG (CALLED "IT") TO UNITY
C
      IT=1
      N=0
13    CONTINUE
      GO TO 10
      END

      SUBROUTINE SUM(X,Y)
      DIMENSION X(20),Y(20)
      COMMON SUMY,SUMYX,SUMX4,SUMX2,NDATA,ADATA,TLOW
      ADATA=0.
      SUMY=0.
      SUMYX=0.
      SUMX4=0.
      SUMX2=0.
      DO 1 I=1,NDATA
      TEMP=1./(((Y(I)/TLOW)-1.)**2)
      SUMY=SUMY+(Y(I)*TEMP)
      SUMYX=SUMYX+((Y(I)/(X(I)**2))*TEMP)
      SUMX4=SUMX4+((1./(X(I)**4))*TEMP)
      SUMX2=SUMX2+((1./(X(I)**2))*TEMP)
      ADATA=ADATA+TEMP
1     CONTINUE
      RETURN
      END

      FUNCTION SQL(TAU)
      COMMON SUMY,SUMYX,SUMX4,SUMX2,NDATA,ADATA,TLOW
      TEMP=(SUMY*(TAU**5))-(ADATA*CON(TAU)*(TAU**4))
      TEMP=TEMP+(3.*SUMYX*(TAU**3))-(4.*CON(TAU)*SUMX2*(TAU**2))
      SQL=TEMP-(3.*SUMX4*CON(TAU))
      RETURN
      END

      FUNCTION SQDRL(TAU)
      COMMON SUMY,SUMYX,SUMX4,SUMX2,NDATA,ADATA,TLOW
      TEMP=(5.*SUMY*(TAU**4))-(4.*CON(TAU)*ADATA*(TAU**3))
```

TABLE XXI (Continued)

```
      TEMP=TEMP-(CONDR(TAU)*ADATA*(TAU**4))
      TEMP=TEMP+(9.*SUMYX*(TAU**2))-(8.*CON(TAU)*TAU*SUMX2)
      TEMP=TEMP-(4.(CONDR(TAU)*SUMX2*(TAU**2))
      SQDRL=TEMP-(3.*CONDR(TAU)*SUMX4)
      RETURN
      END

      FUNCTION CON(TAU)
      COMMON SUMY,SUMYX,SUMX4,SUMX2,NDATA,ADATA,TLOW
      TEMP=(SUMYX*(TAU**3))+(SUMY*(TAU**5))
      CON=TEMP/(SUMX4+(2.*SUMX2*(TAU**2))+(ADATA*(TAU**4)))
      RETURN
      END

      FUNCTION CONDR(TAU)
      COMMON SUMY,SUMYX,SUMX4,SUMX2,NDATA,ADATA,TLOW
      TEMP=(3.*(TAU**2)*SUMYX)+(5.*(TAU**4)*SUMY)
      TEMP=TEMP/(SUMX4+(2.*SUMX2*(TAU**2))+(ADATA*(TAU**4)))
      TEMP2=(SUMYX*(TAU**3))+(SUMY*(TAU**5))
      TEMP2=TEMP2*((4.*TAU*SUMX2)+(4.*ADATA*(TAU**3)))
      TEMP2=TEMP2/((SUMX4+(2.*SUMX2*(TAU**2))+(ADATA*(TAU**4)))**2)
      CONDR=TEMP-TEMP2
      RETURN
      END
```

are peculiar to the particular system used and take the form: READ/WRITE (N_1,N_2) ..., where N_1 is a device number and N_2 is the FORMAT statement number which applies to the READ/WRITE command. In this program, N_1=5 signifies that the data have been entered into storage prior to program execution, and the system behaves as though it were operating a card reader. N_1=6 signifies that output data are to appear at the remote terminal, and N_1=9 signifies that program execution is to halt while input data are entered at execute time via the remote terminal.[1] By this means, the operator can modify the execution of subsequent steps (hence the name "reactive terminal system"). Obviously, statements with N_1=9 are not compatible with "hands off" batch processing systems.

General Operating Description

The first READ statement calls for the low-field value of T_1 (TLOW), the field to current ratio in Gauss/ampere for the sample coil (B), and the number of data points to be entered (NDATA). The second READ statement calls for the polarizing current in amperes (A) and the associated value of T_1 (T); these are the data points, and the program will accept up to twenty of them at three points per input card. The next READ statement calls for the operator to make an initial guess at the proper value for tau (called TAU1), and once this guess has been entered a coordinate transformation is made on the data points. Specifically, all of the A_i are replaced with the Larmour frequency which

---

[1]The disadvantage of this option lies in the fact that a time-sharing system will "dump" the program into auxiliary storage while it is awaiting the completion of input. Once input is completed, the user must wait for the system to find room for his program again, and if general usage is heavy, this may involve a three to ten minute pause.

corresponds to the current values entered in amperes, and the T_i are replaced with the coordinates given by Equation 77 in the main text.

The "SUM" subroutine is called next, and it computes all of the sums which are necessary to Equations 80 and 81. These sums are transmitted to the remainder of the program through COMMON storage. The weighting function given by Equation 79 is also included in this subroutine, and it may be modified at will by changing the "TEMP=..." statement. For example, if TEMP=1.0 is inserted in place of the listed statement, one obtains an unweighted least-squares fit, since this sets the weighting function equal to unity.

The remainder of the program attempts to solve Equation 81 by Newton's method which then yields a modified value for tau (TAU2) by the use of two functions called SQL and SQDRL. SQL yields the left side value of Equation 81 and SQDRL yields its derivative. The reason for the utility of the "new" guess is well-known and will not be discussed here. This modification process continues repeatedly until tau changes by less than one percent during any iteration. The current value is then considered to be satisfactory and is printed as the desired answer.

As a built-in "monitor", the program keeps track of the number of iterations (N) which have been completed. Once 50 iterations have been reached (and this rarely occurs), a flag is set which causes the result of each iteration to be printed after a warning message has been issued. The operator may then terminate the calculation if he so desires by means of an available console switch, or alternatively, the program may be modified (a) so as to cause it to proceed to the next data set (this would be necessary in a batch-processing system) or (b) to accept a new guess at tau. In any case, this program -- like all programs which

involve indefinitely prolonged loops -- must have a built-in means of avoiding a costly run-away. Without this precaution, one has to await the intervention of the system monitor program. On larger systems, this intervention occurs only after an excessive waste of computer time.

APPENDIX B

RELAXATION IN H_2O-D_2O MIXTURES[1]

Consider an oxygen atom which may bind protons and/or deuterons in the three forms H_2O, HDO, and D_2O (the PMR signal will be due to the first two forms listed). Label the positions which may be occupied by either a proton or a deuteron as positions A and B, respectively. If the probability that a given position is occupied by a proton is α, then the probability that a given position is occupied by a deuteron is $1 - \alpha$. Therefore, the joint probability that A is occupied by a proton at the same time B is occupied by a deuteron is given by $\alpha(1 - \alpha)$. Since the reversed situation is physically indistinguishable from the one just given, the probability that a randomly chosen molecule is HDO is given by

$$P'_{HDO} = 2\alpha(1 - \alpha) \quad . \tag{B.1}$$

By a similar set of arguments, one finds

$$P'_{H_2O} = \alpha^2 \tag{B.2}$$

$$P'_{D_2O} = (1 - \alpha^2) \tag{B.3}$$

The probability of finding a particular proton on H_2O (called P_{H_2O}) is given by

---

[1]Derivation due to V.L. Pollak, private communication, March, 1967.

$$P_{H_2O} = \frac{2P'_{H_2O}}{(2P'_{H_2O} + P'_{HDO})} = \frac{2\alpha^2}{[2\alpha^2 + 2\alpha(1 - \alpha)]}$$

or

$$P_{H_2O} = \alpha \quad . \tag{B.4}$$

Similarly, the probability of finding a particular proton on an HDO molecule is given by

$$P_{HDO} = 1 - \alpha \quad . \tag{B.5}$$

Therefore, the fraction of time spent by a proton in H_2O is α and the fraction of time spent in HDO is $(1 - \alpha)$. The proton in an H_2O molecule has a different intramolecular dipole-dipole coupling with its neighbor than the proton in an HDO molecule. There are, therefore, two values of T_1 associated with the protons under observation, and, since the condition of rapid exchange is assumed, one may use the results of Chapter II. These lead to a net relaxation rate (called T_{obs}^{-1}) given by

$$T_{obs}^{-1} = T_{H_2O}^{-1} + (1 - \alpha)\, T_{HDO}^{-1} \quad . \tag{B.6}$$

In general, there are two contributions to T_1 in pure water -- the intra- and the inter-molecular dipole-dipole interaction. Neglecting for the moment any H-D coupling, one has for H-H coupling

$$T_{H_2O}^{-1} = T_{(tra)}^{-1} + T_{(ter)}^{-1} \tag{B.7a}$$

and

$$T_{HDO}^{-1} = T_{(ter)}^{-1} \tag{B.7b}$$

where

$T_{(ter)}$ = intermolecular contribution to T_1;

$T_{(tra)}$ = intramolecular contribution to T_1.

Substitution of B.7 into B.6 leads to

$$T_{obs}^{-1} = \alpha T_{(tra)}^{-1} + T_{(ter)}^{-1} \quad . \tag{B.8}$$

One also has

$$T_{(tra)}^{-1} = (1 - \beta)\, T_{1p}^{-1} \tag{B.9a}$$

$$T_{(ter)}^{-1} = \alpha\beta T_{1p}^{-1} \tag{B.9b}$$

where

T_{1p} = relaxation rate observed in pure water;

β = fractional contribution of the inter-molecular dipole-dipole coupling to the total relaxation rate observed in pure water.

If β is expressed in explicit terms, one has

$$\beta = (1/T_{(ter)})/(1/T_{H_2O}) \quad . \tag{B.9c}$$

The preceding equations lead to the result that

$$T_{obs}^{-1} = \frac{\alpha}{T_{1p}} \quad . \tag{B.10}$$

Where H-D coupling is still not included. One can include such couplings by taking

$$T_{HDO}^{-1} = R\, T_{H_2O}^{-1} \tag{B.11}$$

where R is a constant. The inclusion of Equation B.11 in the derivation leads to

$$T_{obs}^{-1} = \frac{[\alpha + (1 - \alpha) R]}{T_{1p}} \qquad (B.12)$$

in agreement with the published formula.

Thus, where only the dipole-dipole interaction is present, T_1^{-1} is expected to be a linear function of α.

VITA

Richard Raymond Slater, Jr.

Candidate for the Degree of

Doctor of Philosophy

Thesis: PROTON MAGNETIC RELAXATION IN AQUEOUS COLLOIDAL SILICA

Major Field: Physics

Biographical:

Personal Data: Born in Wyandotte, Michigan, the son of Richard R. and Patria L. Slater.

Education: Bachelor of Science, Electrical Engineering, from Rose Polytechnic Institute, Terre Haute, Indiana, June, 1960. Completed the requirements for the degree of Doctor of Philosophy in May, 1972.

Professional Experience: API-PRF Predoctoral Fellow, 1964-67; outstanding student research paper, Southwestern Research Conference, 1966. Five professional publications; member of Sigma Pi Sigma; National Guest Lecturer on electron spectroscopy, Society for Applied Spectroscopy, 1971; Research Management as Section Supervisor, Chemical Physics Section, Gulf Research and Development Company, directing 12 Ph.D., 4 M.S., 1 B.S. holders, and two technicians; invited Lecturer at the University of Pittsburgh, Carnegie-Mellon University, the Pittsburgh Catalysis Society and Mellon Institute.